THESIS FOR THE DEGREE OF LICENTIATE OF ENGINEERING

Generation of Fines in Bench Blasting

VICTORIA SVAHN

Department of Geology
CHALMERS UNIVERSITY OF TECHNOLOGY
Göteborg, Sweden, 2003

Generation of Fines in Bench Blasting
VICTORIA SVAHN

Chalmers tekniska högskola
Geologiska institutionen
Publ A 104
ISSN 1104-9839

Chalmers reproservice
Göteborg, Sweden, 2003

Generation of Fines in Bench Blasting
VICTORIA SVAHN
Department of Geology
Chalmers University of Technology

ABSTRACT

Fines are the finest rock fraction generated in quarries, a material for which there is very little use today unless there is an asphalt or concrete plant nearby. This fraction thereby becomes both an environmental issue and an economic loss for the producers. There are a number of likely sources contributing to the generation of fines, even though it is hard to specify the extent. This thesis presents model-scale tests in a study of the crushing around a borehole. Crushing of the near vicinity of the borehole arises due to the enormous pressure caused by the detonation of the explosive. While this has been generally believed to be the major source, no one has so far been able to prove it, as it is impossible to say from where inside the bench fines originate. The thesis also includes the results from some fieldwork that aimed to investigate how the diameter of the borehole affects the fragmentation.

The model-scale tests were made with mortar cylinders, as the blasts needed to be repeatable and the material possible to colour. The colours were necessary so that each fraction could be traced to a part of the original test specimen. The results show that the crushing of the material close to the borehole is a major source of fines. Even though mortar seems to be a suitable model material, the absolute values of the amount of fines are not likely to be reliable. However, the conslusions should be applicable to rock. Not only was the crushing mechanism found, but there was also another general fragmentation, which can occur anywhere in the material. The amount of fines seems to be related to a constant, the distance to a free face and the borehole radius.

The half-scale field tests were carried out in two stages, in the first of which two borehole diameters and one decoupled borehole were tested. In the second stage, three other borehole diameters were investigated. All of the rounds had the same specific charge. The last three rounds showed a very similar fragmentation, however the first three were slightly different. The largest borehole, of all six rounds, and the decoupled one gave the coarsest fragmentation.

Using the equation, derived from the model-scale tests, for the Bårarp blasts, indicates that no difference in fines generation is to be expected. The last three blasts, but not the first three rounds, support this.

The newly generated specific surface was calculated for the Bårarp rounds. When comparing these to the explosive energy per volume of rock, it is shown that the greater the specific energy (MJ/m^3) is, the finer the fragmentation (larger specific surface). The correct relationship is difficult to define because there are only two clusters of points to evaluate and the range of the specific energies is small. However, the borehole diameter does not affect the final fragmentation result when the specific energy, and the relation between the distance to a free face and the borehole radius are the same, provided, the blasting conditions are unchanged.

Keywords: fines, rock fragmentation, bench blasting, quarry, aggregates

PREFACE

The work presented in this thesis was conducted at both the Department of Geology, Chalmers University of Technology, and Swedish Rock Engineering Research (SveBeFo). Mats Olsson at SveBeFo was in charge of the design and performance of the half-scale blasts at Bårarp. The financial contributors to this project are Swedish Rock Engineering Research (SveBeFo), the Development Fund of the Swedish Construction Industry (SBUF), the Swedish Aggregates Producers Association (SBMI), the Swedish National Road Administration and the Swedish National Railway Administration. They are all gratefully acknowledged for their support.

Throughout this research project I have met a lot of enthusiastic, inspiring and knowledgeable people. Although I do not name them all, I hope that I have succeded in expressing my gratitude to them all along the way.

My supervisor, Professor Gunnar Gustafson, is sincerely thanked for constructive comments on the thesis, and my assistant supervisor, Patrik Alm, Ph.D., for valuable guidance in the academic work. Lecturer and former assistant supervisor, Bo Ronge, is acknowledged for initiating the project as well as being an outstanding guide to the field of geology. Mats Olsson at SveBeFo is thanked for support, advice and discussions during the project. Finn Ouchterlony (SveBeFo) is appreciated for taking the time to discuss confusing matters within the field of rock blasting.

A project reference group with representatives from the industry has been active thoughout these years; they are all acknowledged for their commitment and valuable discussions.

During the production and blasting of the model-scale mortar cylinders, Tommy Johansson (Sabema), Lars Palmgren (Chalmers) and Aaro Pirhonen (Chalmers) contributed their expertise and help. I thank them for always finding the time.

For the half-scale tests, Emmaboda Granit AB is acknowledged for letting us work in their quarry. Both NCC Ballast Syd and Dyno Nobel are thanked for assistance in the blasting and sieving processes. Linda Olsson is appreciated for helping out with the evaluation of the rock properties. I would also like to thank Peter Starzec (Swedish Geotechnical Institute) for the modeling of an *in situ* block size distribution curve. Also, Mats Olsson (SveBeFo) is appreciated as the great project manager that he is.

I would also like to take this opportunity to acknowledge those who have helped out during the writing process of this thesis. Karin Holmgren is greatly appreciated for the illustrations in this thesis and Marie Henriksson for always helping out with problems that have arisen. Lora Sharp-McQueen is thanked for the language editing and, perhaps the most, for her enthusiastic interest in my work.

Friends and colleagues at the department have given me many wonderful times to remember. Special thanks go to the members of the aggregate research group, Jan Hansson, Balasan Khachadoorian and Mathias Jern, for the support and interesting discussions we have had.

Finally, great gratitude goes to my parents for their never-ending support and encouragement. For love, patience and the best medicine – laughter, I am grafteful to you, Martin.

Göteborg, February, 2003

Victoria Svahn

LIST OF PUBLICATIONS

This thesis is based on the work contained in the following publications:

I. Svahn, V., 2002: Generation of Fines around a Borehole: a Laboratory Study. Proceedings of the 7th International Symposium on Rock Fragmentation by Blasting, Beijing, China, August 11 – 15, pp 122 - 127.

II. Olsson, M. & Svahn, V., 2003: Fragmentering i bergtäkter (in Swedish). Swedish Rock Engineering Research (SveBeFo), Report 60, Stockholm, Sweden. (To be published in spring 2003.)

TABLE OF CONTENTS

LIST OF NOTATIONS

Roman letters

A	rock factor (Kuznetsov equation) [-], new specific surface of a fraction (Kristiansen) [cm^2]
A_{cube}	surface area of a cubical particle [m^2]
$A_{particle}$	surface area of a particle [m^2]
A_{sample}	surface area of a sample/fraction [m^2]
B	burden [m], variable depending on type of explosive (Kristiansen) [cm^{-1}]
B_{max}	maximum burden [m]
BCL	bottom charge length (Kuz-Ram model) [m]
b	specific drilling [m/m^3]
b_{rock}	rock constant (Kristiansen) [-]
$b_{explosive}$	explosive constant (Kristiansen) [-]
C	proportion of the hole loaded vertically (JKRMC) [-]
C.R.	coupling ratio (JKRMC) [-]
CCL	column charge length (Kuz-Ram model) [m]
c	rock constant (Langefors *et al.*) [kg/m^3], constant [m^2]
$\underline{c}$	c + 0.005 for B_{max} = 1.4 - 15.0 m (Langefors *et al.*) [kg/m^3]
c_{1-5}	constants
d	diameter
E	relative weight strength of the explosive (Kuz-Ram model) [-]
E_0	energy from the explosive [J]
E_d	Young's dynamic modulus [MPa]
f	degree of confinement (Langefors *et al.*) [-]
H	depth of the boreholes [m], height of the bench (Kuz-Ram model) [m]
h_0	length of stemming [m]
h_b	length of the bottom charge [m]
h_c	length of the column charge [m]
K	height of the bench [m]
k	constant (Kristiansen) [cm^{-2}]
k_{50}	mean fragmentation size
L	total charge length (Kuz-Ram model) [m], the side length of a cube (Kristiansen) [cm]
l	side length of a cubical particle [m]
l_b	bottom charge concentration [kg/m]
l_f	length in full scale (Naarttijärvi *et al.*)
l_m	length in model scale (Naarttijärvi *et al.*)
M	mass of a sample [kg]
M_0	amount of fines from a "general" fragmentation [%]
M_f	amount of fines from the area surrounding a borehole [%]
m_{ex}	mass of explosive [kg]
m_{fines}	mass of fines [kg]
m_{rock}	mass of the rock mass [kg]
N	conversion constant (JKRMC), number of particles
n	number of boreholes, index of uniformity (Kuz-Ram model) [-], number of samples
P_b	blast hole pressure (JKRMC) [Pa]
p	degree of compactation (Langefors *et al.*) [kg/m]

Q	amount of explosive (Hopkinson), mass of TNT (trinitrotoluene), which is equivalent in energy to that of the explosive charge (Kuznetsov equation) [kg]
Q_{tot}	amount of explosive in each borehole [kg]
q	specific charge [kg/m^3]
R	distance (Naarttijärvi)
R_0	the distance from the borehole (to be fragmented) [m]
r_b	radius of borehole [m]
r_c	radius of charge (JKRMC) [mm]
r_h	radius of borehole (JKMRC) [mm]
S	spacing between boreholes [m]
S_{spec}	specific surface for a particle [m^2/m^3]
$S_{spec,cube}$	specific surface for a particle of cubical shape [m^2/m^3]
$S_{spec,sphere}$	specific surface for a particle of spherical shape [m^2/m^3]
$S_{spec,sample}$	specific surface of the sample [m^2/m^3]
s	weight strength of the explosive (Langefors *et al.*) [-]
u	subdrilling [m]
V	weight of a fraction (Kristiansen) [g]
V_0	rock volume broken per blast hole (Kuznetsov equation) [m^3]
V_{ex}	volume of explosive [m^3]
V_p	compressional wave velocity [m/s]
$V_{particle}$	volume of a particle [m^3]
V_{cube}	volume of cubical particles [m^3]
V_{rock}	volume of rock [m^3]
V_{sphere}	volume of spherical particles [m^3]
VOD	velocity of detonation [m/s]
W	standard deviation of drilling accuracy (Kuz-Ram model) [m]
x	screen size [mm], explosive per cm^2 of borehole (Kristiansen) [g/cm^2], side length of a cubical model (Kristiansen) [cm], distance from the centre of the borehole [m]
x_c	characteristic screen size corresponding to the 73.2 % passage (JKMRC) [mm]
$\bar{x}$	mean fragment size (Kuznetsov equation) [cm], mean value for sample series x
Y	proportion of material retained on screen (JKMRC) [-], surface area/volume of the cubical models (Kristiansen) [cm^{-1}]
$\underline{y}$	percentage of fines (0 - 4 mm) generated in the blast (Kristiansen) [-]
$\bar{y}$	mean value for sample series y
z	scale distance (Hopkinson)

Greek letters

α	particle shape factor [-]
λ	scale factor (Naarttijärvi *et al.*) [-]
ρ	density [kg/m^3]
ρ_{ex}	density of explosive [kg/m^3]
ρ_f	density of full scale material (Naarttijärvi *et al.*)
ρ_m	density of model material (Naarttijärvi *et al.*)
ρ_{rock}	density of rock [kg/m^3]
$\rho_{x,y}$	correlation coefficient
σ_c	compressive strength [MPa]

$\sigma_{c,\ Point\ load}$	compressive strength (determined by Point Load Testing) [MPa]
σ_s	shear strength [MPa]
σ_t	tensile strength [MPa]
$\sigma_{t,\ Brazilian}$	tensile strength (determined by Brazilian test) [MPa]
σ_x	standard deviation for sample series x
σ_y	standard deviation for sample series y

Abbreviations

ANFO	Ammonium Nitrate and Fuel Oil
CZM	Crushed Zone Model
JKMRC	Julius Kruttschnitt Mineral Research Centre
NBC	Natural Breakage Characteristic
RMR	Rock Mass Rating
TCM	Two Component Model
TNT	Trinitrotoluene
VOD	Velocity of Detonation

1 INTRODUCTION

Seventy million tons of aggregates for construction purposes are produced in Sweden annually (2000). For every year, the part consisting of crushed rock increases, as it is important to preserve our natural gravel and, thereby, future water resources. The aggregate production process consists of blasting, crushing and screening. In an open pit quarry, the blasting procedure is called bench blasting, since the rock is charged at the top of the rock mass, the bench, and fired towards one or two free faces.

The nature of research concerning blasting in rock is complex. There are a lot of parameters that can vary, and learning how each and every one of them affects the fragmentation is a difficult task. Moreover, each quarry is unique: differences in geology and equipment always require variations in the blasting design. What might be under-blasting in one quarry could mean overblasting with generation of fines in another. The site-specific interaction between geology and the confined explosive must always be kept in mind.

1.1 BACKGROUND

Fines are the finest fraction generated in quarries, a material for which there is very little use today unless there is an asphalt or concrete plant nearby. This fraction thereby becomes both an environmental issue and an economic loss for the producers.

The extent to which this is a problem for the producers varies with the quality of the geological material. Generally, the problem is significant for many aggregate producers in western Sweden; more knowledge about different generating processes is desirable. However, it is important to remember that it is not only the blasting process that causes fines, but also the following crushing and screening procedures. It has been shown that small cost increases of drilling and blasting do not make much difference compared with the benefits of improved fragmentation, and that the greatest impacts come from excavation and crushing costs (Kojovic *et al.* 1995). It is vital to consider the overall production cost, rather than simply examining parts of the aggregate producing process separately, when optimising. Apart from the mechanical processing of the material, the natural state of the rock plays a critical role.

1.2 OBJECTIVES

The project “Fragmentation in Quarries” was initiated by Swedish Rock Engineering Research (SveBeFo) and the Department of Geology at Chalmers in 2000. The objectives of the project are to contribute to better understanding of the fragmentation process when blasting in open pit quarries and to investigate specifically different sources of fines in the blasting process. During these three years, the generation of fines around a charged borehole and the effect of different borehole diameters have been studied.

1.3 HYPOTHESES

Four hypotheses about how fines may be generated in the blasting process were initially formulated. These are:

1) crushing near the borehole,
2) abrasion between weakness planes,
3) colliding pieces of rock, and
4) blast damage from a previous round.

Crushing of the near vicinity of the borehole arises due to the enormous pressure caused by the detonation of the explosive. Although this has been generally believed to be the major source, no one has so far been able to prove it, as it was not known where inside the bench such material originates. The abrasion between weakness planes is also a likely source of fines as the surfaces of joints and cracks, newly formed as well as *in situ*, slide against each other once the rock mass starts to move. Once the rock is set in motion and the pieces are liberated, they collide with each other and secondary fragmentation takes place. This type of fragmentation causes a finer fragmentation, and one can imagine that the amount of fines will increase. The rock mass is liberated and the muckpile ends up in front of the bench to be blasted next. In this bench there will be evidence left of the former blast, i.e. damage in the form of microcracks. These microcracks have the effect of reducing the resistance of the rock to fragmentation. This is very seldom, or almost never, taken into account when the second blast is designed. Hence, the fragmentation could become unnecessarily severe, and produce excess fines.

1.4 THE SCOPE OF THE STUDY

This work includes a study of the first hypothesis, crushing near the borehole. To study this rather complex process, it was decided to do so in a material other than rock. The chosen material is mortar, since it is possible to control many parameters, repeat the tests and also find a way to trace the origin of the final sieved fractions. Using mortar instead of rock can be highly questionable, but as the objective was to look at trends in the fragmentation, and not to investigate how much fines, in absolute numbers, were generated, it was an acceptable solution. An analysis of this can be found in the discussion part of the thesis.

The study also includes some fieldwork, the aim of which was to study the effect of different borehole diameters on the fragmentation. This can be done in a production quarry. The quarry chosen, located in western Sweden, consists of granitic gneiss. This quarry can be considered quite homogenous; the joint frequency is very low. The aim was to keep as many geological parameters as constant as possible.

Both the laboratory and field tests aim at studying the fragmentation process in bench blasting and the goal was to study the outcome and contribute to a better understanding of rock fragmentation. As many researchers have shown before, this is a very difficult task. In large-scale blasts the geological material is very unpredictable, which makes it hard to interpret the results. In small-scale blasts where the rock is more easily defined, the question is how reliable the results are for full-size production blasts.

2 LITERATURE REVIEW

Typical ongoing operations in a quarry are drilling and blasting, loading and hauling, crushing and screening. Since they are all interdependent, it is important to consider the entire process as a whole to optimize quarries. This literature review, however, summarizes only the blasting operation and the factors influencing the fragmentation outcome. This review aims to provide an introduction to bench blasting and the terminology that is extensively used in this thesis. Then follows an overview of how key factors influence the fragmentation, both overall and in the generation of finer fractions. The review covers existing hypotheses and seeks to identify others not yet considered in bench blasting.

2.1 BENCH BLASTING

Geological material is excavated in mines and quarries all around the world. The blasting technique used in open pit quarries is called bench blasting, for which vertical, or almost vertical, boreholes are drilled in rows at the top of the the rock mass to be blasted, known as the bench. Then the boreholes are filled with explosives that are fired against the free face. Bench blasting means turning the *in situ* rock mass into a muckpile of appropriate size distribution for excavation equipment and further use of the material (Figure 2.1). This task must be carried out without causing any damage to the surrounding rock or endangering and disturbing the nearby environment. There is increasing pressure to take into account the effect blasting has on the recovery and value of the final mineral products, such as excessive fines or oversized fragments (JKMRC 1996). To deal with problems such as these, it is necessary that operators have a clear understanding of the objectives of their blasting operations. With understanding, measurements, comparison and an iterative feedback cycle, the quarry stands a better chance of controlling the blast outcome and increasing the value of the end products.

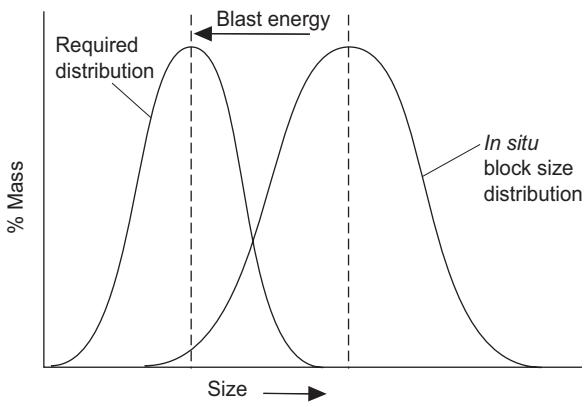

Figure 2.1 The fragmentation process (after JKMRC 1996).

2.1.1 Bench blasting design

When designing the bench blast, it is important to decide which geometries to use so that the boreholes are placed at the right distance from each other, the free face and the theoretical bottom of the bench. Figure 2.2 gives an overview of the bench geometries; this section briefly summarizes bench blasting design.

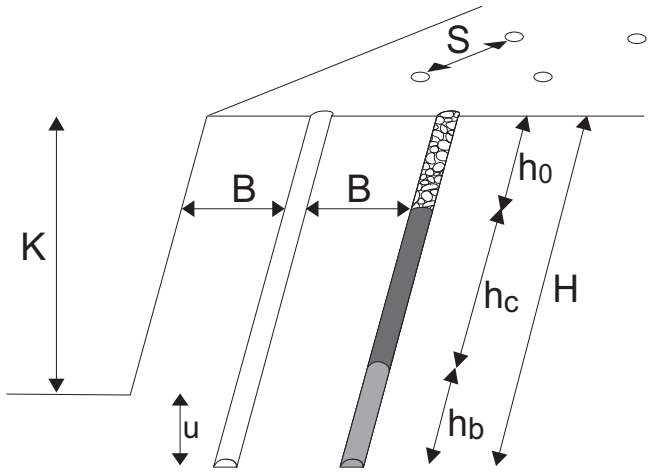

Figure 2.2. Geometries and notations in bench blasting.

The height of the bench, from the floor to the top, K [m], is not to be confused with the depth of the boreholes, H [m], which is often longer, as the boreholes are inclined; S [m] is the distance between the boreholes, and the distance between each row of boreholes is the burden, B [m]. The burden is the distance between a charge and the free face; in addition to the face of the bench, every row of boreholes becomes a new free face when the rock in front of it is liberated. The boreholes are charged in three steps. First, the bottom charge, h_b [m], is placed at the bottom of the hole. The borehole is usually drilled to a depth a bit below the intended floor of the bench, and this part of the hole is called the subdrilling, u [m]. This is done because this part of the hole is more confined and a stronger explosive is needed to fragment it enough. On top of the bottom charge, most of the borehole is filled with the explosive chosen, i.e. the column charge, h_c [m]. To use the gases produced during the detonation of the explosive more efficiently, a stemming material is put on top of the charge, h_0 [m], to keep them from escaping.

The specific charge, q [kg/m^3], is the amount of explosive needed to liberate one cubic meter of rock.

$$q = \frac{n \cdot Q_{tot}}{n \cdot B \cdot S \cdot K} \tag{2.1}$$

where n = number of boreholes
Q_{tot} = amount of explosive in each hole [kg]

The specific drilling, b [m/m^3], is the total of metres drilled needed to liberate one cubic meter of rock.

$$b = \frac{n \cdot H}{n \cdot B \cdot S \cdot K} \tag{2.2}$$

The burden, B [m], is the distance between the first row of boreholes and the free face at the time of detonation. When calculating the practical burden, the drilling precision must be taken into account. A rule of thumb is that the burden, in metres, should be the same as the diameter of the borehole, in inches, (Olofsson 1999).

The maximum burden, B_{max} [m], is calculated by Langefors formulae (Langefors *et al.* 1963).

$$B_{\max} = \frac{d}{33}\sqrt{\frac{p \cdot s}{\underline{c} \cdot f \cdot (S/B)}} \tag{2.3}$$

where d = borehole diameter at the bottom of the hole [mm]
p = degree of compactation of the explosive [kg/m]
s = weight strength of the explosive [-]
c = rock constant [kg/m^3]
$\underline{c}$ = c + 0.005 for B_{max} 1.4 - 15.0 m
f = degree of confinement, 1.0 for vertical boreholes, 0.95 for boreholes with an angle of 3:1
S/B = ratio of distance between boreholes to the burden, usually 1.25

The equation above has been simplified by Dyno Nobel, and to obtain the maximum burden from the specific charge.

$$q = \frac{l_b}{S \cdot B} = \frac{l_b}{S/B \cdot B^2} \tag{2.4}$$

where l_b = bottom charge concentration [kg/m]

$$B^2 = \frac{l_b}{(S/B) \cdot q} \qquad B = \sqrt{\frac{l_b}{(S/B) \cdot q}}$$

S [m] is the distance between boreholes within the same row; in practice, this is calculated as:

$$S = 1.25 \cdot B \tag{2.5}$$

The fragmentation is, for example, controlled by changing the ratio S/B. A rule of thumb is that S/B < 1.25 gives a coarser fragmentation.

Loading of the boreholes is done in three stages. Since the confinement of the hole is much greater at the bottom, it takes more explosives to liberate it. For this reason the borehole is almost always drilled a certain distance, u [m], below the intended bottom of the bench, i.e. subdrilling. The height, h_b [m], of the bottom charge is approximated by means of the maximum burden.

$$h_b = 1.3 \cdot B_{\max} \tag{2.6}$$

The concentration of the bottom charge is the same as in the calculation for maximum burden.

The upper, unloaded part, of the borehole, h_0 [m], is filled with sand or crushed rock (stemming), preferably with a size of 4 - 9 mm (Olofsson 1999). The function of this part of the hole is to enclose the explosion gases and, thereby, to ensure that the gases contribute to fragmentation work, rather than just being vented out in open air. The length of this unloaded part is generally the same as that of the burden; if the length is greater

there is a risk of boulders, and if it is less, risk of severe throw. For small holes it is sufficient to use a stemming height equal to the burden, but for larger holes, the stemming in general has to be less than the burden (Persson *et al.* 1994).

The column charge, h_c [m], is placed between the bottom charge and the unloaded upper part. The concentration of the explosive is less than in the bottom charge, as there is less confinement. A rule of thumb is 40 - 60 % of the bottom charge.

2.1.2 Rock breakage

The rock breaking process, the fragmentation, in blasting of rock material is very complicated due to the large number of factors that influence the outcome. When Rustan (1981) tried, through a literary review, to summarize these, he came up with almost 30 factors, as well as even more indirect ones which could be divided into 3 groups: geological, geometrical and explosive factors. Moreover, as rock material is highly heterogenous, fragmentation in bench blasting differs for each quarry. Rock properties, such as tension, compressive and shear strength, differ not only between rock types but also within them. However, by studying the outcome from numerous blasts, indications for some trends have been found. These will be introduced in Sections 2.2 and 2.3.

Generally, the geology has a greater impact on the fragmentation than the explosives (Olofsson 1999). Since it is hard to say for each quarry how the explosive will work, it is always recommended to blast a smaller rock mass before using the explosive in a production-size blast. The structure, fractures, cracks and distances should also be thoroughly mapped and documented before each new blast (Olofsson 1999). In this way, drilling patterns and firing sequences can be designed according to a given site. For example, if the structure angles outward from the bench (Figure 2.5d) the heave will improve, the explosive energy will be more effectivly used, and toes are seldom a problem. On the other hand, the backbreak will most likely be severe. If the borehole intersects cracks, filled with sand and dirt for example, the fragmentation becomes poor due to energy loss. The column charge should then be divided into smaller sections with unloaded parts between them (where the intersections are). To avoid this, special drilling patterns should be made, fractures identified and the boreholes placed in more intact parts of the bench; these parts require more fragmentation than the ones already fractured.

Rock of higher density has proven to be more difficult to blast than rock of lower density. This is most likely because heavier rock masses require more energy to obtain the same heave (Olofsson 1999). Field measurements also show that a hard rock mass, with high P-wave velocity, is more easily fragmented by explosives of high velocity of detonation (VOD) and vice versa (Olofsson 1999). On the other hand, softer rock masses are more forgiving in case of overcharging: they seldom cause throw, and the muckpile is still easy to load (Olofsson 1999). Naturally, an increase in specific charge produces a better fragmentation, but the increase should be placed in the column charge, since the bottom charge is much higher in concentration. The risk of throw always increases with increased specific charge, and so does the heave (Olofsson 1999).

Another important factor, studied by Nitro Nobel, is the timing of the initiation system (Olofsson 1999). The study shows that the first row of boreholes must be moved forward by one third of the burden before the next row is detonated. To achieve this, the delay must be somewhere between 10 - 30 ms per metre of burden. Most boreholes are almost vertical, however even a small angle of inclination has been proven to offer better fragmentation. The shock energy, is also better distributed within the rock mass, instead of losing energy to the bottom of the bench.

Although the short summary above deals with the desire to improve the fragmentation, the objective is often to get coarser fragments. To achieve coarser fragmentation, the rock mass should be more homogenous and have as few fractures as possible. Then, the specific charge should be kept low, the ratio S/B around 1.0, and the rows blasted simultaneously (Olofsson 1999). This blasting technique has some negative effects not discussed here, however, it is a demonstration of how complex the blasting design can be in bench blasting.

2.1.3 Size distributions

After the fragmentation, the rock mass becomes a muckpile in front of the bench. This pile consists of fragments of various sizes. Counting all of them to get a size distribution curve, which would be desirable, is an impossible job. Kuznetsov (1973), as many other researchers around the world have done, did research that made it possible to predict the mean fragmentation size, also known as the k_{50} value. This gave one point on the size distribution curve; however, it did not give any information about the amount of fines or boulders.

$$\bar{x} = A \cdot (V_0 / Q)^{0.8} \cdot Q^{0.167} \tag{2.7}$$

where $\bar{x}$ = mean fragment size [cm]
A = rock factor (1 for extremely weak rock, 7 for medium rock, 10 for hard, highly fissured rock, 13 for hard, weakly fissured rock)
V_0 = rock volume [m^3] broken per blast hole
Q = mass [kg] of TNT (trinitrotoluene) which is equivalent in energy to that of the explosive charge in each blast hole

During the evaluation of some test blasts for highway construction, it was found that Kuznetsov's equation provided a more realistic tool for rocks classified as very good by the RMR rock mass scheme (Bieniawski 1989) than for poor quality rock masses (Senyur 1998). However, Cunningham (1983) modified the original Kuznetsov equation, which made it possible to determine the mean fragmentation size for any explosive and the index of uniformity. With this information, a Rosin-Rammler projection of size distribution can be made. Today, it is widely accepted that the mass percent of fragments smaller than any given size varies linearly with fragment size, when plotted in the Rosin-Rammler domain (JKMRC 1996). The Rosin-Rammler projection (Figure 2.3) involves a characteristic screen size, x_c, corresponding to 73.2 % passage, and a uniformity coefficient, n, which indicates the spread of the distribution. This way, one needs to measure only enough fragments to confidently define the slope and intercept of the Rosin-Rammler line.

$$Y = e^{-\left(\frac{x}{x_c}\right)^n} \tag{2.8}$$

where Y = proportion of material retained on screen
x = screen size
n = index of uniformity (defines the spread of the distrubution)
$x_c = \bar{x} / (0.693)^{(1/n)}$

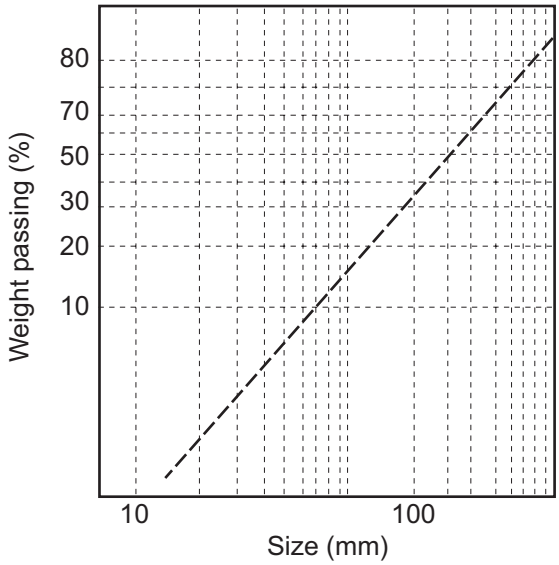

Figure 2.3 Rosin-Rammler size distribution plotted on Rosin-Rammler axes (after JKMRC 1996).

To obtain the value for *n*, Cunningham (1987) used field data and regression analysis of the field parameters to obtain a value of *n* in terms of: drilling accuracy, ratio of burden to blasthole diameter, staggered or square drilling pattern (if staggered, *n* is increased by 10 %), spacing/burden ratio, and ratio of charge length to bench height. It is desireable to have uniform fragmentation, while avoiding excess of both fines and boulders. To achieve this high values for *n* are preferred. The resulting model became known as the Kuz-Ram model.

$$n = (2.2 - 14\frac{d}{B}) \cdot (\frac{1+\frac{S}{B}}{2})^{0.5} \cdot (1 - \frac{W}{B}) \cdot (abs\frac{BCL - CCL}{L} + 0.1)^{0.1} \cdot \frac{L}{H} \qquad (2.9)$$

where d = borehole diameter [mm]
B = burden [m]
S = spacing [m]
W = standard deviation of drilling accuracy [m]
BCL = bottom charge length [m]
CCL = column charge length [m]
L = total charge length [m]
H = bench height [m]

Cunningham (1983) also developed this model by incorporating the use of explosives other than TNT. The final equation to determine average fragmentation size is

$$\bar{x} = A(V_0 / Q)^{0.8} \cdot Q^{0.17} \cdot (E/115)^{-0.63} \qquad (2.10)$$

where E is the relative weight strength of the explosive (ANFO=100), while the relative weight strength of TNT is 115. The use of the Kuz-Ram, or similar models, requires caution: factors such as structures of the rock mass, timing and the spacing/burden ratio should be fully understood (Konya *et al.* 1990). The Rosin-Rammler distribution has been

found to be very useful for modelling most blast fragment distributions with one exception: muckpiles of considerable oversize (Lizotte *et al.* 1994). Experience also shows that the model predicts the coarser part of the distribution curve with good accuracy (Cunningham 1987).

Two other concepts suggested by the Julius Kruttschnitt Mineral Research Centre in Australia are based on rock parameter measurements, model-scale blast fragmentation tests and the measurement of fragmentation after blasting (Moser *et al.* 2000). The two methods are called the Two Component Model (TCM) (Djordjevic 1999) and the Crushed Zone Model (CZM)(Hall *et al.* 2001). The main idea is that it is impossible to describe, with one uniform curve, a fragmentation process that takes place in two stages. On the contrary, there should be two curves, one for the finer part and one for the coarser. Both models calculate the coarse end of the distribution by using a modified Kuz-Ram approach. The TCM uses experimental data from a blast chamber to estimate the fines end, while the CZM is a semi-mechanistic approach. In a critical comparison of the models and an optimum run of mine size distribution, the two models were found to give a coarser fragmentation estimation than the optimum, although the CZM varied less in the fine to intermediate size distributions. Also, the CZM requires less and more easily obtained input parameters than the TCM (Hall *et al*. 2001). Another recent approach is a method proposed by the working group Paris-Leoben Rock Blasting (Moser *et al.* 2000). The fragmentation predicition is based on a Natural Breakage Characteristic (NBC) which is described as the relation between the specific energy and the specific surface. The application of the NBC concept makes it possible to predict the optimum fragmentation size distribution, from lab-scale crushing and grinding tests, which is determined by the natural breakage characteristic of the rock. The first advantage of this method is that it enables one to establish the maximum uniformity that can be achieved. This, in turn, makes it possible to predict the unavoidable minimum fines precentage, as a function of the maximum fragment size. Another advantage is the chance to see whether the actual blast fragmentation is already close to the NBC; if so, little can be done to increase the uniformity of the blasted material.

The actual measurement of fragmentation from large-scale blasts is extremely difficult, which is why there are only a few measurements in use. One way to generate distribution curves is to photograph the muckpile and, by image analysis, try to count the fragments. Statistically, about 5000 fragments need to be counted per analysis: the amount of rocks should represent 10 % of the muckpile to minimize errors arising from segregation. This process will not be dealt with here; however, it is worth mentioning that these photograph analysis methods do not detect fines well, and are in need of further development. Fines are seldom visible in the photographs, as they are hidden in voids between larger fragments or removed by the blasting process in the form of dust. To conclude, by far the best way to determine how a rock mass will behave and what the final fragmentation distribution will be is to make estimations based on some test blasts at the excavation site (Senyur 1998).

2.2 FRAGMENTATION BY BLASTING

The two outcomes of blasting are fragmentation and muckpile formation. Approximately 30 % of the explosive energy contributes to breakage and 70 % to heave (JKMRC 1996). The fragments in a muckpile have three sources: fragments formed by new fractures, *in situ* blocks that just have been liberated and fragments generated by a combination of the former two. This section discusses only the fragmentation part, even though the shape of the muckpile for example, is of interest to the producers as well.

2.2.1 General fragmentation theories

The relationship between rock breakage and energy has been studied since the 19th century. In 1867 and 1885, Rittinger and Kick proposed theories of comminution with ideas such as the energy spent to fragment a solid is proportional to the new area produced by the process as well as proportional to the reduction of volume suffered by the crushed particles (Bond 1952). In the mid 20th century Bond (1952, 1959) presented a third theory which was considered a compromise between the two. He said that the energy to break a particle of a given size is initially proportional to its volume, but that after the first new surface areas are formed, energy flows to these and becomes proportional to area (size squared). He also believed that the work spent to fragment rock is proportional to the length of the new cracks formed. Bond devised a work index which was defined as the energy required to crush a solid of infinite size to a product 80 % of which is smaller than 100 micrometres. This represented the rock's resistance to crushing and grinding, and the index increased as the rate of energy application rose, however this approach does not take into account aspects such as a solid that is not intact.

After performing laboratory experiments in the form of crater and bench blasting, Da Gama (1971) proposed that the size distribution of fragments can be obtained by an empirical formula which consists of empirical factors some of which are dependent on explosive type, rock properties and blasting patterns. Even if it were not clear how these factors worked, they were to be established by a series of field tests conducted under the same conditions as the estimations of fragmentation. This approach comes close to representing the fragmentation mechanisms in bench blasting.

2.2.2 Fragmentation from the borehole to the free face

As an explosive detonates in a borehole, the detonation front has a speed of 3000 - 6000 m/s depending on type of explosive and the diameter of the hole (Persson *et al.* 1994). The chemical energy in the explosive is released, and the compacted explosive is turned into gaseous products, which leads to a dramatic increase of the pressure acting on the wall of the borehole. The gases generated are compressed into a volume of the order of 1000 times less than the volume occupied by these gases at normal temperature and pressure. The rise in temperature of the gases then results in another 100-fold increase in volume. The final pressure is of the order of 10^{10} Pa (Armstrong *et al.* 1993). An unconfined charge that detonates gives rise to a discontinous pressure front propagation at supersonic speed (Johansson *et al.* 1970). A confined charge, for example in a borehole, generates a dynamic stress situation that fragments the surrounding medium.

When blasting rock, the explosive is placed in drilled boreholes. Most of the energy released from the explosive becomes fragmentation work, as the borehole, and thereby the charge, is highly confined (Johansson *et al.* 1970). When the explosive detonates in a fully charged borehole, the walls of the hole are exposed to radial compression acceleration. This acceleration generates a shock wave which propagates radially away from the borehole and the charge. The rock closest to the borehole is exposed to such great dynamic compression that it collapses under the pressure, both between and inside the mineral grains (Jern 2001). As the rock is compressed and crushed, the volume of the borehole expands until it reaches a quasi-static equilibrium state. This state means that the gas pressure inside the hole is matched by the stress induced in the borehole wall. The magnitude of the quasi-static stress is less than the peak stress amplitude caused by the dynamic blast wave. Accordingly, the static strength of the rock material should be the appropriate failure threshold (JKMRC 1996). The pulverisation and the very large increase in surface area of the crushed zone cause a very rapid decrease in the peak stress; the rate

of decay is lower beyond this zone boundary due to the rock's elastic behaviour (Hagan 1973). According to Langefors *et al.* (1963), the maximum size of this crushed zone is approximately half of the borehole diameter. This assumption is based on hard competent rock. For a softer, more porous rock such as sandstone the crushed zone can be much larger. Theoretical approaches have also been suggested, and a model made by Liu *et al.* (1993) found that the crushed zone was 2 - 4 times the borehole radius when common mining explosives where used. This zone could be reduced by three quarters or more in a typical sulphide ore, if the explosive density were reduced by one third.

Besides the dynamic compression acting on the walls of the borehole, they are also subjected to tangential tension stress. This stress gives rise to radial cracks as the stress exceeds the relative low tension strength in the rock material (Figure 2.4). The cracks extend even further as they are filled with explosion gases and secondary crushing takes place (Hagan 1979). The length of these radial cracks is somewhere between 8 and 20 borehole diameters (Persson *et al.* 1994); they tend to branch as the velocity becomes high (Hagan 1973). Although this is the most common way to look at the crack propagation process, another theory has been presented (Brinkmann 1987, 1990), according to which the back damage is primarily controlled by the shock wave and the gases control the breakout of the burden. Swedish Rock Engineering Research (SveBeFo) investigated this further (Olsson *et al.* 2001), and the conclusion was that the shock wave seemed to be responsible for crack lengths in the remaining wall. Another investigation conducted by Daehnke *et al.* (1996) reports that the majority of fracturing occurs due to pressurisation by the detonation gases. However, these tests were performed in transparent PMMA (polymethylmethacrylate), not rock material, to demonstrate the effect of stemming when blasting a borehole.

Even if it looks as if the radial cracking begins at the borehole and extends continuously, small-scale tests have suggested that this is really locally isolated cracks that are formed and later connected with each other as the pressure increases at the crack tips (Hagan 1973). The rising pressure at the crack tips is caused by the increasing crack length. The longest crack is the most unstable and requires the lowest critical pressure, particularly near the blasthole where a small increase in length causes a large decrease in critical pressure. As a result, longer cracks extend first and propagate at higher velocities than shorter ones. When a long crack starts to extend, so does the crack diametrically opposed to it (Hagan 1973). The length of these cracks is influenced by the maximum pressure in the borehole as well as the tension strength of the rock and its ability to absorb energy. Few radial cracks, approximately five to twelve (Langefors *et al.* 1963, Persson *et al.* 1970, Johansson *et al.* 1970, Fourney *et al.* 1983), extend to any significant length. Shear cracks are formed if the pressure is high enough to compress the rock material between the cracks. These are initiated at the point along the tension crack where the stress concentration is maximum (Hagan 1979).

The compressional wave propagates away from the borehole if there is no free face in the vicinity. The result will be a borehole with a diameter of less than double the original size, the crushed zone and the radial cracks that have not reclosed after the compressional wave has passed (Langefors *et al.* 1963). However, this is hardly a desirable result, since the rock mass has not been fragmented enough. It also points out the importance of a free face. When the compressional wave meets the free face, it is reflected as a tension wave and a shear wave (Hagan 1973) returning towards the borehole. The tension wave can exceed, as previously mentioned, the tension strength of the rock material, and the intact rock mass is fragmented; spalling occurs. In bench blasting, where normal burdens are used, the spalling phenomenon does not usually occur. The time interval between detonation and the beginning of movement of the face is close to ten times that needed for the compressional

wave to reach the free face and return (Hagan 1973). However, even if the tensile wave is not strong enough to start a fracture, it can still cause considerable extension of existing cracks. The free face does not necessarily mean the front of the bench: it can just as well be a large open crack or fracture filled with air or softer material (Hagan 1973). It is difficult for the compressional wave to pass this opening, hence some of the energy will be reflected or lost (Hagan 1979). This means that a rock mass with a higher frequency of cracks would absorb more energy than a rock mass with a lower frequency. A negative effect of the free face (here, the face of the bench) is the interaction of radial cracks, propagating towards the free face at an angle of approximately 45°, with the returning tensional wave (Figure 2.4). This could cause the rock mass within this triangular area (between the borehole and face of the bench) to fall out without being fragmented.

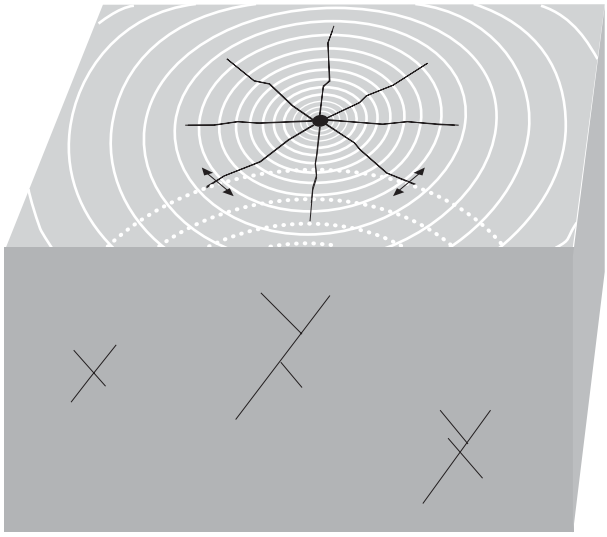

Figure 2.4 Radial cracks and the reflected compressional wave.

The first two stages, the radial cracking and the fragmentation of the rock mass, are the result of the propagating shock wave, and they take place within a few milliseconds. The third stage is a much slower process. The explosion gases, causing enormous pressure on the borehole walls, enter the cracks and dilate them, which leads to an overall swelling of the rock in front of the row of boreholes (JKMRC 1996), and the material is set in motion. As the movement starts, the radial crack network is subjected to a state of tension which promotes further crack propagation. It has also been found that breakage occurs in fragments liberated from the rock mass. This could be either a result of blast waves being trapped inside the fragments (Winzer *et al.* 1980) or that the sudden release from the confined state causes the rock to fall apart (Hagan 1973). As the boreholes detonate according to the firing sequence, the rock is transformed from an intact confined bench to a loose and fragmented muckpile.

2.2.3 Explosive - rock interaction

Rock is a complex engineering material, as it is highly variable in composition, structure and history. Moreover, the action of every explosive is strongly dependent on the surrounding environment, in this case the rock mass. A major problem when optimising rock blasting lies in the uncertainty of the properties and behaviour of rocks under extremely high loading conditions (Hagan 1973). Small-scale investigations of different rock types indicate that there must be a connection between the explosive and the surrounding material to be able to explain the results. They also suggest that the

performance of heterogenous explosives is very much affected by the properties of the surrounding material (Kristiansen *et al.* 1990). Hence, it is important to thouroughly investigate the rock before any blasting operation takes place. The investigation should include rock mass properties, structures and confinement. If possible, every explosive should be assesed in the environment where it is intended to be used (JKMRC 1996). Blasting requirements are strongly influenced by: the amount of existing fractures (the *in situ* block size distribution); the material strength and breakage characteristics; the dynamic properties of the rock mass; the stiffness or degree of brittleness, which influence the fracture and displacement behaviour; and the porosity and density of the rockmass (JKMRC 1996).

2.2.4 Geological properties

In 1963, Langefors and Kihlström published their first version of "The Modern Technique of Rock Blasting" a book that came to mark the begining of a modern era of blasting engineering. They dealt with rock properties by using a rock constant (see equation for maximum burden) which was to represent a charge for satisfactory blasting performance. This constant was developed further by Persson *et al.* (1994) who defined it as the charge needed to liberate and displace one cubic meter of rock. Nowadays, several rock mass properties are identified as being of importance to the blasting performance. For example, the rock mass stiffness determines the distortion of the blasthole wall. The dynamic compressive strength has a major influence on the crushing near a borehole. The attenuation properties affect how far the stress waves travel before their energy falls below what is needed to break the rock. The dynamic tensile strength controls the formation and extension of cracks. The *in situ* block size distribution is important for the migration of explosion gases and the attenuation of the shock wave. Finally, there is the density of the rock which affects the movement of the entire rock mass (Scott 1996). When investigating rock mass properties, scale must be taken into account. For example, the measurement of tensile strength with the Brazilian test does not represent the tensile strength of an entire rock mass which includes discontinuities that a small specimen does not have. A small specimen represents intact rock and the strength of it relates to its microstructure; in contrast, a rock mass is influenced by both its micro- and macrostructure. All of the above mentioned rock properties fall into the following five catagories (JKMRC 1996):

1) strength,
2) mechanical,
3) absorption,
4) structural, and
5) comminution properties.

Strength properties are measured by standard laboratory testing of smaller samples. Although a large number of tests are usually run, these methods are very often static and not representative for the loading condition caused by blasting. Rock, as with many other materials, is very strain rate sensitive and the strength increases with rising loading rate (Persson *et al.* 1970, Ross *et al.* 1996); hence, the dynamic strength is of greater importance than the static strength. Generally, the dynamic strength is higher, five to thirteen times (Hagan 1973), than the static, while the dynamic compressive strength is greater than the dynamic tensile strength (JKMRC 1996). The dynamic tensile strength is critical in two stages of the blasting process: first, in the initiation stage of cracks, and later when spalling might take place.

Mechanical properties are Young's modulus and Poisson's ratio, two parameters which describe how the rock behaves under loading. They are, just as the strength properties are, higher for dynamic situations than for static. They can both be calculated by measuring the velocities of shear and compressional waves through a cylindrical test sample. Measurements have shown that the velocities increase with stress, which would be explained by the closing of microcracks in the sample.

The capacity of the rock mass to absorb and transmit energy is the absorption property. Energy absorption can be caused by geometrical expansion of the stress wave, either stored in the material as internal friction or lost in the form of heat (JKMRC 1996).

Structural properties affect the blasting process in many ways. Open joints may reflect or absorb energy. Since the *in situ* structure influences the blast design, it is very important to map the bench before any blasting takes place. In full-scale blasts in two quarries, it was shown that the one with the higher joint frequency was affected more by the design of the blasting operation, while the other with fewer joints depended more on the blasting event (Gynnemo 1997).

Comminution is the reduction of the size of a particle through the application of energy. The term is often used for crushing and grinding processes but a familiarity with these characteristics of the material can also be useful in blasting.

Many researchers have tried to relate various rock properties to the blasting result and have succeded in the environment where the tests were made. However, it is hard to relate these results to the full-scale blasting operation used in quarries. Rakishev (1982) identified the rock mass properties with the greatest influence on the blastability to be: the density, the compressional wave velocity, Poisson's ratio, the modulus of elasticity, compressive strength, tensile strength, mean dimension of the *in situ* block size distribution, degree of opening and filling of fractures, and the properties of this filling material. Throughout many research projects, several factors and their influence on the fragmentation mechanism have been investigated and documented. The objective has been to both improve the blast design and try to extend general knowledge of the process.

Rock mass properties

The structure of the rock mass includes joints and faults, bedding planes, foliation and cleavage planes. Joints are discontinuities where no displacements have taken place. Faults are breaks in the rock mass where there is a displacement. Bedding planes are interruptions in the sequence of deposition: they mark the end of one deposit (sedimentary rock) and the beginning of another with different characteristics. Foliation is the parallel alignment of mineral grains found in metamorphic rocks, and cleavage planes are the result of breakage in weak bonding between or within minerals (Tarbuck *et al.* 1993).

Structures play an important part in the fragmentation process and are perhaps one of the most investigated factors that influence bench blasting. Structural zones interfere with the propagation of the shock wave by absorbing energy and by not transfering the entire wave from one side of the discontinuity to the other. Discontinuities have lower impedance, and complex wave interactions take place. If a discontinuity is wide enough, no energy can be transferred and the wave dies out or is partially returned as a tensile wave. The specific damping increases with the number of joints. The joints also vent the explosion gases so that there is less energy to do fragmentation work. A joint intercepting the charge column is opened up by the action of gas energy, which causes a sudden drop in the blasthole pressure (Singh *et al.* 1987, Persson *et al*. 1970).

Bhandari *et al*. (1990) have demonstrated, in a series of tests in jointed limestone slabs, the effect of differing orientations of structures in bench blasting. Not only was the structure changed, but also the S/B ratio. These tests (together with those by Badal 1995, Bhandari 1983, Hoek *et al.* 1981, Lizotte and Scoble 1994, Singh et al. 1983, Singh et al. 1987) show that horizontal weakness planes (Figure 2.5c) are generally favourable in bench blasting. The risk of toes being formed is low and loading conditions are often satisfactory. However, the floor (and the future bench below) is still damaged. As there are few joints "protecting" the remaining wall and the sides, there is likely to be some damage to them as well. Horizontal fissures are often responsible for unexpectedly large distances in throw. Horizontal jointing, as well as joints that angle outwards from the bench (Figure 2.5d), also seems to cause severe backbreak (Singh *et al.* 1983). This was observed in model-scale tests conducted in 25 mm sandstone slabs bound together by an adhesive. Another interesting observation from these tests was that no spalling at the free face took place in models having joint planes between the charge and the face. Internal spalling, crushing and cavities however, were observed near the joint plane in some of the models.

When there is vertical jointing parallel with the free face (Figure 2.5a), this direction is favourable because it directs the energy towards the unbroken rock mass. It is important to make sure that no rock mass between joints is left isolated, i.e. that the entire rock mass is affected by the explosive. Otherwise the fragmentation might become too coarse, even though the blast often leaves a clean wall. If there is a high frequency of joints close to the borehole, more intense fragmentation will take place. The cracks will not cut through a joint, and unexpectedly large breakout boulders can be the result (Persson et al. 1970). The sides very often suffer from overbreak, and the general fragmentation can vary considerably. Often, the floor is also uneven. Vertical joints perpendicular to the free face (Figure 2.5b) result in little overbreak from the sides, an uneven remaining wall, toes, and radial cracking that is very much controlled by the joint direction. This direction gave a finer fragmentation than blasts with vertical parallel joints in blasting conducted in a quarry with sedimentary rocks (Lande 1983). The capacity of explosive energy to propagate radial cracks is arrested by vertical open joints; the breakout shape is then no longer controlled by the propagation of radial cracks (Senyur 1998).

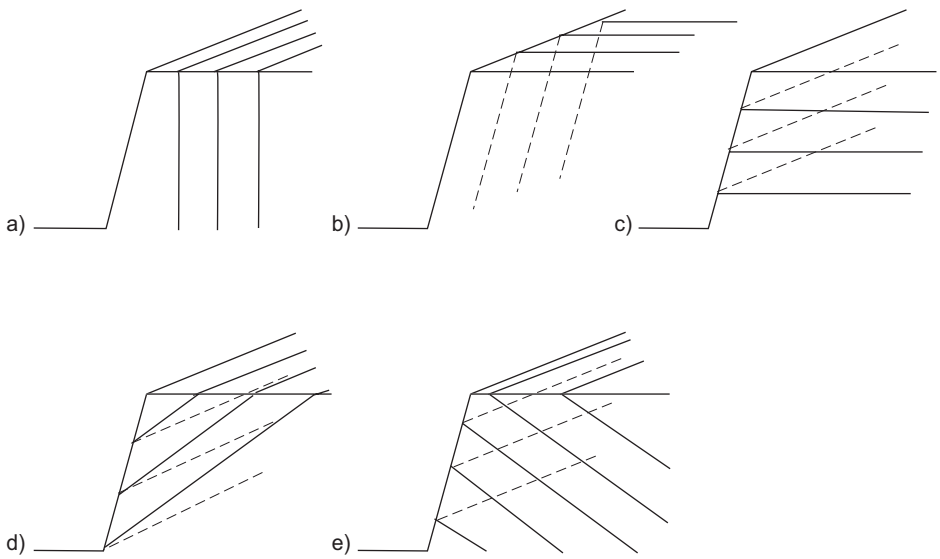

Figure 2.5 Rock mass stuctures with different joint directions: a) vertical parallel; b) vertical perpendicular; c) horizontal; d) joints that angle outwards from the bench; e) joints that angle inwards towards the bench.

Joints that angle inwards towards the bench (Figure 2.5e) can cause toe problems, and damage to the wall along with stability problems, such as overhanging. Joints that angle outwards from the bench (Figure 2.5d) often give severe backbreak and instability in the remaining wall, along with toe problems. Joints running oblique to the face produce a zigzag face with unequal, and sometimes severe, backbreak. It has also been suggested that bedding planes can affect the fragmentation result. Blasts in a Canadian iron ore mine consisting of different kinds of sedimentary rocks gave a better fragmentation, a finer one, if the blasting direction was against the dip of the bedding planes (Belland 1966). Ouchterlony *et al.* (1990) also showed that porous bands which appeared in the bench made the k_{50} value independent of the specific charge within the range of 0.30 - 0.56 kg/m^3. When there were no bands, the rock became much easier to blast and the k_{50} value decreased as the specific charge increased.

The shape of the fragments seems to be affected by characteristics of the pre-existing rock mass structure, such as joint orientation, cracks, bedding planes and other weakness planes (Persson 1990). Large fragments obtained from the vertical and horizontal models were plate shaped with a thickness equal to the slab thickness. When joints dipped away from the face, the fragments were more oblong, and if the joints dipped towards the face, more tabular (Singh *et al.* 1983). Yang *et al.* (1983) discovered that two perpendicular sets of weakness planes produces a greater volume of breakage than only one set parallel to the blasted surface. Moreover, the fragmentation seems to be more sensitive to the number of sets of weakness planes than to the number of planes within each set. The more weakness planes in the bench, the more difficult it will be to change the k_{50} value. This conclusion is also supported by full-scale blasts performed by Gynnemo (1997).

When it comes to the fragment sizes, it seems that finer fragmentation is achieved when the burden is small (20 mm in the model-scale tests in comparison to 30 and 40 mm) for all orientations except the vertical (Singh *et al.* 1983). When the joints were vertical, the fragmentation was finer for the larger burdens.

The degree of impedance of a discontinuity to stress wave depends on its aperture, filling material (Lizotte *et al.* 1994, Fordyce *et al.* 1993, Seinov *et al.* 1968) and the angle of incidence to the joint face (Lewandowski *et al.* 1996). Hard filling transfers the energy more effectively than fractures with soft filling or none at all. The shear strength of the filling material is also believed to influence blastability (Bohloli 1997). The finer fragmentation increased in laboratory-scale blasts, as the filling material became stronger (cement) compared to fillings of weaker material or to joints that were kept open (Bhandari 1996). Other experiments were conducted with models, fabricated from Hydrocal (a fast setting gypsum cement) which contained a layer of sand or clay, which were blasted and the travelling stress wave was studied by Fourney *et al.* (1997). The loss of stress wave velocity in the sand layer was found to be much greater than the loss for a clay layer. It has also been noted that the continuity of the fractures is more important for the fragmentation then the strength of them (Yang *et al*. 1983). Of course, the number of joints also plays a key role, since they absorb energy more effectively the more numerous they are. Rock mass with a lower joint frequency, i.e. a larger *in situ* block size distribution, has been observed to resist breakage succesfully (Da Gama 1983).

Most quarries are confronted with more than one kind of discontinuity as the blasting operation often takes place in different directions. Therefore, it is important for the operator to know what can be done for a variety of geological conditions. The drilling and its pattern can be changed, the timing altered, and the subdrilling and the powder factor regulated, among many other things. Most of the actions undertaken are the result of common practice, that is, years of trial-and-error have built up experience and knowledge

of what to do. The action taken is, thus, site specific and should not be regarded as common practice, since no quarry is like another. What works in one situation in a specific rock mass might not give the same desirable result in another.

Rock properties

Both the rock mass properties and the rock material are of great significance when studying the factors influencing blasting. The rock material, consisting of mineral grains of various sizes that are bonded together, is highly characterised by its inner stucture. A rock of magmatic origin behaves completely differently from a sedimentary rock; one magmatic rock can behave completely differently from another. The main difference is of course the mineralogy and the rock properties associated with it. It has, for example, been observed that rock of high density is more difficult to blast than that of lower density (Olofsson 1999). It is not hard to understand why the rock masses behave differently when considering properties such as strength, porosity, P-wave velocity etc, and seeing how they vary, both between different rock types and within the same type.

Microstructure is a primary factor to study, since it affects the behaviour of the rock material, for example by producing an anisotropic wave attenuation and strength characteristics, which may influence the crack growth and thereby the rock breakage (JKMRC 1996). **Mineralogy**, which is a part of the microstructure, highly influences the behaviour of the rock under dynamic loading. Some rock types have been identified as hard to blast, while others are easier. Small-scale blasting in rock cubes of dissimilar rock types show that a coarse-grained larvikite was more finely fragmented than a medium-grained granite. The granite was more finely fragmented than a fine-grained quartz-dioritic gneiss (Kristiansen 1995b). A gabbro was also blasted and presumably the grain size was similar to that of granite. In the resulting distribution curve it was also found that this rock type gave a finer fragmentation than the fine-grained quartz-dioritic gneiss. Hence, the conclusion can be drawn that the grain size does make a difference in the fragmentation process.

Kristiansen (1995b) also investigated the quality of the blasted rock in the form of impact value and flakiness. The results showed that the medium-grained granite gave the best quality, followed by the coarse-grained and, last, the fine-grained quartz-dioritic gneiss. No conclusions were drawn from these results. As for crack propagation, investigations made by Jern (2001) indicate that radial microfractures appear to pass through the grains, and those that are not radial to pass mainly around the grain boundaries. In crystalline materials, it is assumed that grain boundaries act as the predominant source of stress concentration. Laboratory uniaxial loading on rock types with different grain sizes was done by Eberhardt *et al.* (1999). The results showed that the grain size had a minor effect on the stress at which new cracks are initiated. These thresholds seemed to be related more closely to the strength of the constituent minerals, in this case feldspar and quartz. Primarily intergranular cracking (cracks which extend from a grain boundary into the grain) begins within the feldspar grains followed by secondary cracking at higher loads within the quartz grains. These intergranular cracks appear to be generated by point load contacts, with grain boundary cracks playing a secondary role. However, the size of the grains had a significant effect on the behaviour of the cracks, once they had been initiated. Longer grain boundaries and larger intergranular cracks provide longer paths of weakness along which growing cracks can propagate. Eberhardt *et al.* also refer to some other investigations where it was found that fracturing occurs primarily along grain boundaries, with secondary fracturing occurring within weaker grains, either between cleavage planes or at points where harder minerals induce a point load on softer, neighbouring minerals.

Many investigations, conducted in both artificial material and specific geologies, emphazise that flaws or **discontinuities** can either help or hinder fragmentation. Flaws can act as nuclei for initiation of cracks (Lizotte *et al.* 1994). In small-scale tests conducted in Homalite 100 (a stress optical material) and Plexiglas, there was a model in which flaws had been rooted into the material at various locations and with various orientations, while in another model, strips were bound together with cement (Fourney *et al.* 1983, 1985). The results show that both the flaws and the bond lines acted as initiators for the outgoing wave system; cracks began not only at the borehole and propagated outwards, but also began at the bondline, both above and below the charge. It seemed that they were initiated locally by the P and S waves.

Microstucture includes not only the mineral grains but also **porosity**. Sedimentary rocks have a greater porosity than rock of magmatic or metamorphic types. When a blasthole detonates, the shock wave generates a compressional wave moving outwards from the hole. The velocity of this wave is a measure of the propagating shock wave. The velocity is determined by the material through which it is travelling. A competent, high-density rock with few fractures (micro and macro) and low porosity will transfer the wave faster than the opposite kind of rock would. This competent rock will also resist compression breakage better (Hagan 1979).

To investigate whether or not the P wave is affected by the shock wave, Kim *et al.* (1998) made some tests using an explosively driven split Hopkinson pressure bar. The tests clearly indicate that the **P-wave velocity** is significantly lower after the blast, which suggests that considerable internal damage is accumulated in the rock during the passage of the shock wave. In practice this damage can play an important role in the crushing. The damage makes the material fall apart more easily, which would be preferable for grinding; this may not be so for aggregate production.

Water plays an important role in blasting operations, as most explosives are water-sensitive. Water resistant explosives have higher densities, which leads to higher energy and possibly a need to change the original design (JKMRC 1996). Another aspect is the behaviour of the rock material when wet. Tests performed by Bohloli *et al.* (2001) showed that the tensile strength, determined by the Brazilian test, of three rock samples was lowered by water saturation. This could be the result of water reacting with silicate to break the Si-O bond (Masuda 2001). However, it is not possible to say if these small-scale test results can be compared with a full-scale blasting situation.

2.2.5 Explosives and geometrical properties

When choosing the explosive to use, one should always do so by considering the environment in which the explosive is expected to work. For this, knowledge about the rock and the rock mass is vital. Thereafter, the geometrical parameters can be determined and the blast design settled. An important explosive property, the **velocity of detonation** (VOD), seems to influence heavily the outcome of the blast and it is perhaps not difficult to understand why. The VOD is the rate at which the detonation front travels through the explosive charge. It controls the release of energy and influences the partitioning of that energy into shock and heave. The velocity of detonation has a great impact on the fragmentation result. Explosives with a high VOD provide a greater proportion of shock energy and are better suited for blasting hard competent rock. An explosive with a low VOD releases its energy relatively slowly, and a larger proportion of its total energy takes the form of gas and heave.

A study by Kristiansen (1995b) used two explosives in three rock types, and the conclusion was that the higher the VOD, the finer the fragmentation. A complementary study of the

quality of the blasted fragments also indicated that better quality was obtained in the muckpile with a high VOD explosive. This was explained with the help of energy transfer. Explosives, that transfer less energy into the rock leave small cracks inside fragments without breaking them. More transfered energy not only causes cracks but also break the fragments apart. The use of less effective energy damages the rock more than necessary and the quality becomes poorer. Later, these investigations were compared with full-scale blasts in gneiss: it was once again observed that using an explosive with a higher VOD (as well as a higher specific charge) gave better quality in terms of impact value. The impact value can be seen as a measure of the inner strength of the material. As for the flakiness, it seemed to depend more on the foliation of the rock than on the VOD (Kristiansen 1994b). Another investigation conducted by Kristiansen *et al.* (1990) indicated that the fragmentation was affected more by VOD than by relative weight strength. These tests were a part of a full-scale tunnel experiment.

In a study of crack lengths when blasting with different explosives in granite blocks, a low VOD explosive seemed gentler on the rock than a high VOD explosive that subjected the rock to a higher impact pulse (Olsson *et al*. 2001). Emulsion for example, is a commercial high VOD explosive and has a fast rise time and a fast drop in pressure. An investigation concluded that the closer the product of density and VOD of the explosive (impedance) is to the product of P-wave velocity and the density of the rock, the better the energy transfer is (JKMRC 1996). Small-scale investigations have also shown that the impedance ratio is clearly correlated to the k_{50} value (Kristiansen *et al.* 1990). It has also been suggested that the higher the loading rate is, the lower the average fragment size becomes (JKMRC 1996). In full-scale blasts it is more difficult to detect the effect of different VODs. Gynnemo (1995) performed a number of blasts in two quarries and the change of VOD produced only a minor change in the fragmentation result. A series of blasts, conducted by Olsson (1995), in relatively homogenous granite, aimed to study the length of newly generated cracks. One of several conclusions was that there were more and longer finer cracks propagating from the blast hole if the VOD of the explosive was high.

The **amount of explosive** is of course also of importance to the fragmentation. A general rule of thumb would be the more explosive the finer fragmentation and vice versa. But naturally there are other influencing factors to consider as well. Ouchterlony *et al.* (1990) evaluated a number of bench blasts in andesite to find a correlation between fragmentation and the **specific charge**. Suprisingly, they found that when porous bands appeared in the bench, the k_{50} was independent of the specific charge within the range 0.30 - 0.56 kg/m^3. When the bands were absent, the rock was much easier to blast and the k_{50} value decreased as the specific charge increased. This meant that the presence of the porous band within the rock unit governed the fragmentation, and that increasing the amount of explosives had no effect on fragmentation. In smaller model-scale blasts in concrete, as well as rock material, performed by Rustan *et al.* (1983a), they also observed that the fragmentation, represented by the k_{50} value, decreased with an increase in specific charge. Another interesting find in the same investigation was that the mean penetration of radial cracks into remaining material was about the same for different charge concentrations (Rustan *et al.* 1983b)

A **primer** in the bottom of the blasthole is often used to initiate the detonation. The detonation begins and propagates at a constant velocity, at least theoretically, that is determined by the composition of the explosive, its density and the rock properties. The velocity of detonation contributes to a special ratio of stress energy to heave energy. If the velocity can be reduced, and thereby also the ratio, without the entire generation of energy being decreased, then the pulverisation around each borehole will be less. Hence, it is desirable to maximise the heave energy by controlling the VOD (Hagan 1979). There are two ways of accomplishing this: the first one is to replace the primer at the bottom of the

hole by several smaller ones placed a certain distance apart along the hole. Each primer reaches a constant velocity after a certain distance: by using several primers, the total initiation period will be longer and therefore decrease the VOD. The other way is to replace the primer at the bottom by a continuously detonating cord. In contrast to a bottom primer, the cord, placed along the side of the borehole, has a greater detonation distance, which means that the VOD is decreased (Hagan 1979). The fact that a side-initiated explosive gives a less pulverised rock, compared with ANFO, is well demonstrated by studing the perimeter holes after a tunnel blast; these have much less backbreak (Hagan 1979). When a blasthole is top-primed, the upper part of the burden will begin to move before the one below does. When a blasthole is bottom-primed, the burden near grade level (the bottom of the bench) almost always moves before the rock above does. This means that the rock exposed to the early detonation gases has a higher degree of confinement: it will not be able to move freely until the rock above it does. The explosion gases would thus be given more time to work on the rock mass, and overfragmentation is a likely result (Hagan 1973).

The **inclination of boreholes** is often 10 - 30° from the vertical, which gives better fragmentation and toe conditions. The backbreak problems are reduced and the subdrilling does not have to be as long as for vertical holes (Hagan 1973). With a shorter subdrilling the bottom of the bench is not overfragmented as much as if the confinement were greater. This could be of great importance when the bench blasting is done at more than one level. When using several levels, there is an extensive risk that the top of the second bench will be destroyed by the blasting in the first bench, even before the first round on the second level is fired.

By designing the blast as a V (Figure 2.6), the effective burden is less then the drilled burden. This means that the explosion gases do not crush the rock between the radial cracks as much as they would otherwise. It also becomes easier for the gases to move the rock. Another aspect of using the **V design** is that the fragmentation becomes finer, since rock collision is promoted by the initiation sequence (JKMRC 1996).

The **timing** of the initiation in bench blasting is of great importance. If timing is badly planned, the result can be overfragmentation of some parts of the bench and inadequate fragmentation of others. Simultaneous firing produces a very poor fragmentation result (JKMRC 1996). Anderson *et al.* (1985) carried out a series of large-scale blasts in granite in a production quarry. The results indicate that the most massive part of the face produces the finest fragmentation at 20 ms delay, and that fragmentation became increasingly coarse up through 60 ms delay. The most fractured portion of the face yielded the finest fragmentation at a delay of 40 ms. While it is hard to explain these results, there is a hypothesis that, the more massive the rock is, the faster the stress waves are transmitted, however, fewer fractures will be formed because there are fewer fracture sites. In more heavily fractured rock, stress-wave velocity will be lower and attenuation higher, but there are more fractures to serve as initiation sites.

The **stemming** material encloses the explosive gases to make them perform fragmentation work for a longer time than if they had been vented in open air. Sarma (1994) found that up to 35 % of the heave energy could be lost if no stemming material is used at all. In a series of small-scale blasts conducted in concrete, Armstrong *et al.* (1993) found that the mean fragmentation size decreased as the degree of confinement increased, due to a longer stemming. However, the stemming must not be too long, because the risk of too coarse fragmentation will be high. When stemming has to be long, placing a smaller pocket charge within the stemming material can be the solution, however care must be taken to prevent any flyrock and air blast (JKMRC 1996). Dry granular stemming is much more

efficient than material that behaves plastically. Crushed stones lock together better and the confinement of the gases is higher than with drill cuttings (Hagan 1973).

The larger the size of the borehole is, the more spread out the **drilling pattern** should be. This is also believed to give a coarser fragmentation. However, the rock structure makes it impossible to expand the pattern too much, as this would lead to poor distribution of the explosive within the burden rock; the muckpile will very likely consist of very fine material (from the vicinity of the borehole) and very coarse material (JKMRC 1996). The most effective way to reduce blasthole pressure and blast the rock mass a bit more carefully is to decouple the charge. The length of the cracks propagating from the blast hole is reduced, the more the charge is decoupled (Olsson 1995). Lateral **decoupling** is done either by using cartridged explosives or by pumping the bulk explosive into a hose inserted in the borehole. The latter method is probably the most effective one. Vertical decoupling means decking the hole so that parts of it are fully coupled but separated by "spacers". The blast hole pressure can be calculated by means of a method presented by JKMRC (1996).

$$P_b = N \cdot \rho_{ex} \cdot VOD^2 \tag{2.11}$$

where P_b = blast hole pressure [Pa]
N = conversion constant, 0.00123
ρ_{ex} = density of explosive [kg/m^3]
VOD = velocity of detonation [m/s]

The degree of coupling can then be expressed.

$$C.R. = \sqrt{C} \cdot (r_c / r_h) \tag{2.12}$$

where $C.R.$ = coupling ratio
C = proportion of the hole loaded vertically (50 % = 0.5)
r_c = radius of charge
r_h = radius of borehole

When combining the two, the new decoupled blasthole pressure can be calculated.

$$P_b = N \cdot \rho_{ex} \cdot VOD^2 \cdot (\sqrt{C} \cdot r_c / r_h)^{2.4} \tag{2.13}$$

The exponent 2.4 in equation 2.13 is the result of experimental work done by Bauer in 1967 (JKMRC 1996) and assumes adiabatic expansion of the explosion gases.

In dealing with the more geometrical factors when setting up a blast, the bench height and **burden** have to be decided. A larger burden and maintained specific charge yields a coarser fragmentation (Öqvist 1982). However, if the burden is larger than critical size, then there is a risk that the rock mass will not be liberated. Since the burden is fragmented, to a large extent, by bending cracks in the free face due to the movement of the rock mass (Rustan *et al.* 1988), it is important to design the blast in such a way that these cracks can be formed. The critical burden was found to depend on factors such as impedance of the rock and the static tensile strength (Rustan *et al.* 1983a). The **bench height** can vary considerably from quarry to quarry. Once the explosion gases penetrate the cracks and fractures, the free face begins to move and a bending mechanism or flexural failure takes place. This mechanism is controlled by the selection of proper blasthole spacing. As the

height of the bench decreases, the distance needs to be changed in order to overcome the problem of increased stiffness (Konya *et al.* 1990).

Uncautious blasting can do serious damage to the nearby rock. Such an operation not only destroys the material to be excavated by the blast, but also the material of future excavations or the stability of the rock left standing. If the fragmentation energy is transferred beyond the last row of blastholes, this will start to fragment the material in the next bench, which makes it more difficult to avoid overfragmenting the rock in the next blast. This damage zone can range from a couple of decimeters up to several metres in some quarries (Jern 2001). Overloading the bottom charge will also damage the rock underlying the bench. In many quarries this lower bench will at some point also be excavated and should be kept undamaged.

2.3 GENERATION OF FINES

Excessive fragmentation leads to the generation of fine material. In many quarries this becomes a problem since the material cannot be used; thus it is an economic loss for the producers, as the product is sold at a reduced price, if at all. This is often the most expensive fraction produced, since it is generated by every operation in the quarry, but it is sold at the lowest price. Another problem that arises from the generation of fine material is the environmental load the piles of material are becoming as they grow larger and larger. Other examples, more specifically connected with the mining industry, are disruption of the leaching operations in gold mines, difficulties in handling fine coal, and the need for pelletisation of iron ore fines (JKMRC 1996). Much research has been done on the overall fragmentation process but very little exclusively on fines generation.

2.3.1 Geological properties

Weakness planes, as discussed earlier, are very likely a source of fines, even if it is difficult to say to what extent. Generally, more weakness planes, and thereby more opportunities for the traveling shock wave to be reflected, can cause internal spalling to occur, which may give rise to more fines than would have been produced if the planes had not existed. In particular, more weakness planes around the borehole seem to counteract the generation of fines (Yang *et al*. 1983). Rock mass classified as good quality rock by the RMR rock mass rating scheme is more likely to disintegrate into small fragments, which indirectly means efficient use of the mechanical energy. The range of fragments will also be very narrow compared to a rock mass with a lower RMR rating. However, a rock mass of poor quality produces a larger volume of broken rock with larger fragments, whereas the blast in good or very good quality rock produces less material composed of smaller fragments (Senyur 1998). The amount of fines has been observed to decrease with greater distance from the blasthole, except for anomalous regions. Large discontinuities in oil shale disort the regular behaviour of the detonation wave and can produce as much as 15 % fines in weight fraction (Lizotte *et al*. 1994).

Fines present in the rock mass before blasting, often found in cracks and joints, has a significant influence on blasting results (Adhikari *et al.* 1990). At a marble site where the ***in situ* fines** were estimated to be 20 - 30 %, it was never possible to achieve a reduction below 35 %, while at another site, where most fines in joints were interlocked by cementing material, the fines could be reduced to 12 %.

The **dynamic compressive strength** is generally greater than the tensile. However, the compression stresses are of much greater magnitude than the tensile stresses so, in the end, it is the compression strength that is the most important when considering the crushing mechanism near the borehole. Crystalline rocks of very low porosity are expected to offer

the greatest resistance to compressive failure, whereas highly porous rocks (e.g. sandstone) crush relatively easily (Hagan 1973). Weak rocks, with low compressive strength and high porosity, are therefore likely to generate a lot of fine material. The crushed region absorbs a great part of the energy, which leaves less to perform fragmentation work on the rest of the rock mass. The result can be a muckpile consisting of very fine and very coarse material. An increase in macropores, on the other hand, reduces the spread of the detonation pressure, interrupts radial cracks and lead to coarser fragmentation. A laboratory experiment using the Brazilian test on gneiss cores indicates that the amount of fines is determined by the strength of the rock. The higher the **tensile strength**, the higher is the generation of fines (Bohloli *et al*. 1999). From a quarry perspective, this could mean that blasting in a more favourable direction, the one with the lowest tensile strength, could decrease the production of fines. Brazilian tests performed in a laboratory indicate that dry samples produce higher tensile strength values and approximately 20 – 30 % more fines than water saturated samples (Bohloli *et al.* 2001). Although this study was performed on drilled rock cores and is perhaps not a good representative for field blasting, the behaviour of the material is still interesting.

The properties of a material are due to its inner structure which for rock is composed of various combinations of minerals. The **minerals** do not have the same properties, and it is all of them together that comprise the material as a whole. Therefore, it is not surprising to find that different rock types behave differently under blasting conditions, and the fragmentation cannot be expected to be the same. One can perhaps even imagine that some weak minerals could act as initiators for crack propagation. Another interesting question is whether large lumps of weak minerals, such as mica, could act as reflecting surfaces and interupt the wave propagation. They could perhaps hinder travelling cracks, and the energy that is not transferred may cause local fragmentation of the mineral. Weak minerals are more susceptible to crushing (Hagan 1979). This would result in a high content of a specific mineral in the fines fraction; if the mineral were mica, it would be very undesireable in, for example, aggregates for road construction (Smith *et al.* 1993). However, very few research projects have studied this in detail, and none in full-scale production blasts has been found.

Those who have studied the behaviour of different rock types have done so in small scale. Core samples of gneiss with brittle minerals, such as alkali feldspar and quartz, generate more fines then the elongated minerals of greater tensile strength, such as amphiboles and pyroxene. This was shown in a series of Hopkinson Split Bar tests (Bohloli 1997). Also, coarse-grained cores seemed to generate more fines in Brazilian tests of three different rock samples (Bohloli *et al.* 2001). Glatolenkov *et al.* (1991) propose a basis for calculating the output of fines from the nature of the cracks, their spacing and the energy expended on breaking down the rock mass. If the rock mass has a granular structure, the formation of microcracks will develop along the grain boundaries, and their direction can differ from the direction of maximum tangential stress. This implies that the amount of fines would depend on grain size of the rock material.

Shock heating, which is what the rock closest to the borehole is exposed to, is a very efficient way to produce microcracks (Alm *et al.* 1985). The main factors governing the microcrack production are, first, the differences in thermal expansion coefficient, both of the different minerals in the rock and in the minerals themselves. The second and third factors are the maximum temperature the rock is exposed to and the rate of increase in temperature together with the thermal conductivity of the rock (Alm *et al.* 1985). In blasting, the maximum temperature and the rate of increase are very high, which favours microcrack formation. A scenario is that these microcracks could sooner or later generate more fines, if not during blasting, then at a later stage in the aggregate production process.

However, the conductivity of rock material is very low (Schön 1996), in comparison with metals for example, and the temperature might not spread beyond the crushed zone. Therefore, this aspect may not be worth taking into account, unless the temperature is spread with the explosion gases in cracks; it may then become important.

2.3.2 Explosives and geometrical properties

It is important to consider the rock mass when designing a blasting operation and choosing an explosive. If there is overcharging, there is a risk of too much energy being added, and the rock can be overfragmented. Having a high pressure in the early part of the expansion is not very effective, as a major part of the expansion work is expended on the small volume of rock in the region near the drillhole (Persson 1990). Optimum blasting would be to use fully coupled charges and achieve a peak blasthole pressure that just fails to cause crushing. Powerful, highly coupled explosives often cause excessive fragmentation at close range (Hagan 1973). Bench blasts in a salt mine, conducted by Bolger *et al.* (1996), showed that a lower level of energy, achieved through fewer blastholes per round, produced less fines. When a charge is not powerful enough, boulders are a common result and the cost of further fragmentation is very high. In South African gold mines, much effort is expended to decrease the density, and thereby the **VOD**, to avoid generating fines (Hagan 1979). By increasing the VOD from 3500 to 6000 m/s in small-scale blasts in larvikite (Kristiansen 1994a), the amount of fines (0 - 4 mm) was increased by 3 %. However, full-scale blasts in diabase and gneiss, reported by Gynnemo (1997), showed that a decrease in VOD did not affect the amount of fines (0 - 8 mm) generated to such a large extent.

The energy released during blasting depends on the type of rock and the **confinement** it provides. The percentage of shock energy is higher for a softer rock than in harder rocks. If unwanted crushing around the borehole is to be avoided, a low shock energy explosive should be chosen. A linear correlation was found between fines production (< 16 mm) and effective energy for small-scale blasting in granite (Sheahan *et al.* 1990). The fines also appeared to be generated around the boreholes since their mass remained constant as the pattern was expanded.

By decreasing the **borehole diameter**, from 150 mm to as little as 25 mm, the VOD is decreased dramatically (Hagan 1979) and, hence, the amount of fines. When the borehole diameter lies between the critical size and that for ideal detonation the VOD rises. As the charge diameter falls below a given value, the detonation is further from the ideal, and the detonation velocity decreases (Hagan 1973). When an increase in diameter no longer raises the VOD, the fines generation becomes a greater part of the muckpile (Hagan 1979). There is also a correlation between the borehole diameter, the length of the charge and the amount of fines (Stagg *et al.* 1990). Consequently, it was concluded that the fines are generated in a zone around the borehole. The size of the crushed zone around the borehole, and thereby the fines production, becomes greater with increased borehole diameter (Hagan 1979). Kristiansen (1995a) performed a series of full-scale blasts to study how the generation was affected by different borehole diameters. Four blasts were carried out in anorthosite with diameters of 76, 89, 102 and 114 mm. The specific charge was, for all blasts, 0.623 kg/m^3 and the number of holes varied accordingly. The result was an increase of the amount of fines (0 - 4 mm), in production scale, by 18 % for every half-inch increase in borehole diameter. The total increase was as high as 53 % when the 76 mm borehole was compared with the 114 mm one. Kristiansen also aimed to find a relation between fines and the amount of explosive per borehole area. Smaller test blasts were done in concrete specimens of various sizes, and these where complemented by larger full-scale blasts. The final formula can be seen below.

$$y = b_{rock} \cdot x + b_{explosive} \quad (2.14)$$

where y = precentage of fines (0 - 4 mm) generated in the blast
b_{rock} = rock constant depending on compression strength and bonding between mineral grains etc. (4.8 for concrete, 3.0 for anorthosite)
x = explosive per area borehole [g/cm^2]
$b_{explosive}$ = VOD, density and blast design (8.7 for Comp C-4[1] in concrete, 6.9 for Dynamite in concrete and 0.4 for Slurrit 50-10 in anorthosite with the blast design used)

Although the **borehole distance** can be varied, the specific charge is almost always kept the same. Hence, the burden needs to be changed as well. A decrease in distance between holes means increasing the burden and vice versa. If the optimal burden is exceeded, then the amount of fines will increase because of the greater confinement. If the distance between boreholes is increased, and the burden kept the same, the fines generation decreases, since each borehole needs to fragment a bigger rock mass (Hagan 1979).

As was mentioned earlier, it is generally believed that an increase in **specific charge** would yield an increase in fines. Stagg *et al.* (1990) found, in some reduced scale blasts, that an increase of the specific charge to over 0.84 kg/m^3 made 60 % of the total material originate from the crushed zone, with radial fracturing, around the borehole. Nevertheless, the average size of the fragmented material was not reduced very much. If the specific charge was below 0.65 kg/m^3, the average material size increased. Gynnemo (1997) also found, when studying a full-scale blast, that a decrease in specific charge lowered the amount of fines. Small-scale test blasts conducted by Yang *et al.* (1983) in magnetite concrete showed that a low charge concentration made the crushed zone around the borehole spread towards the burden. If the concentration was higher, then the zone was evenly distributed around the hole. By decreasing the charge factor to an optimum value, the amount of fines in a marble quarry could be reduced (Adhikari *et al*. 1990). At the optimum value of 0.3 kg/m^3, for the site concerned, the fines could be minimised to 36.5 %. A higher charge factor would result in a production of fines up to 64.4 %. Kristiansen (1987) performed model-scale tests in concrete which indicated that increasing amount of explosive per borehole area yielded more fines.

It is also generally believed (Hagan 1979, Stagg *et al.* 1990) that **decoupling** decreases the amount of fines generated, because the borehole pressure becomes lower. Decoupling can be achieved either by using cartridged explosives or by placing the bulk explosives in a hose inserted in the borehole. This gives the explosion gases more space, as a gap formed between the charge and the borehole wall lowers the pressure. When the unnecessary crushing is prevented, the fragmentation becomes more effective and there is little movement of the rock (Hagan 1979). Stagg *et al.* (1990) showed that there is a clear correlation between the degree of decoupling and the amount of fines generated. Gynnemo (1997) on the other hand, found that a high degree of decoupling and a lower specific charge reduces the fines (0 - 8 mm) in a diabase quarry. Decoupling alone did not affect the fines generation. These results agree with small-scale blasts in granite, where a strong decoupling only slightly reduced the mass of the finest material (Sheahan *et al.* 1990).

To achieve effective fragmentation, the blast must be fired towards a free face. The **length to width** ratio should be at least 3 if possible, because the blast has to be given the space to move forward without sealing the back rows. If a row is not allowed to move forward, the

[1]military plastic explosive consisting of 90 % hexogene (RDX)

explosion gases are trapped for a longer time and unnecessary fragmentation takes place. To prevent this from happening, the bench should be wide and shallow, not short and deep (Hagan 1979). Generally, it can be said that the amount of fines generated also depends on the **delay time** between every row. The rock in front of a row of boreholes must be loosened before the next section of rock behind it starts to move, if fines are to be minimized. The amount of fines rises with shorter delay times and a greater number of boreholes (Hagan 1979). With a V design (Figure 2.6), the blast is fired towards two vertical surfaces, which makes it easier for the rock to move; this also counteracts trapping of the gases and generating of fines (Hagan 1979). However, with this design the muckpile becomes concentrated, and secondary crushing of the fragments can take place as they fall on one another.

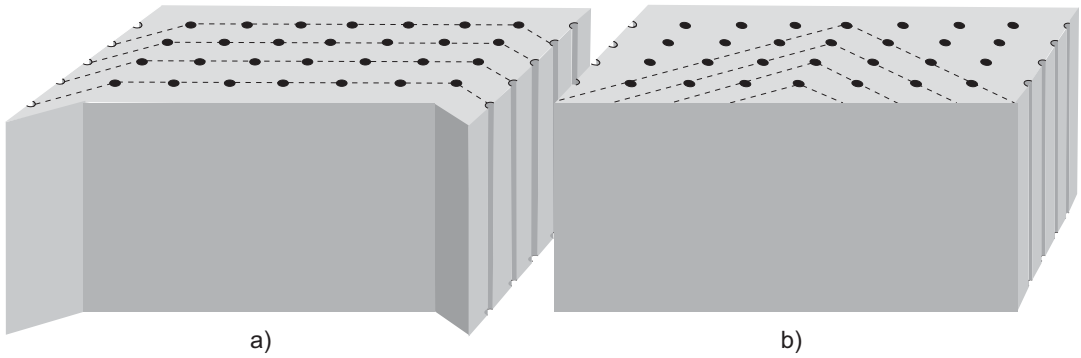

Figure 2.6 Ignition pattern for a blast with (a) one delay per row and (b) a V design.

When the **burden** is increased, the explosion gases are confined for a longer period and thereby do more fragmentation work. The risk of overfragmentation, and more fines, then also increases. An increase in burden and a decrease in the hole spacing lead to more fines (Adhikari *et al.* 1990).

Subdrilling is done to prevent toes being formed. This part of the borehole is confined to a much larger extent than the rest of the hole. The explosion gases are therefore given more time to fragment the rock, more fines are produced and overfragmentation is unavoidable. It is also important to remember the damage that is done to the underlying rock mass. This material is most likely to be of interest to excavate in the future; the material should not already be damaged even before any blasting takes place. The same amount of explosive used in this bench as well could perhaps mean overcharging and more fines could be the result.

The **stemming** influences the fines generation in two ways. First of all, it encloses the explosion gases for a longer time, which gives them a better chance to perform fragmentation work. Greater stemming length will also reduce the size of the explosive; as a result, less fines will be generated (Hagan 1979). However, the stemming length cannot be so great that the producers run the risk of boulders.

2.4 SMALL-SCALE MODELS AND FULL-SCALE FIELD TESTS

Much research done with small-scale models in the laboratory shows that the magnitude and ratio of the shock and gas energy are not consistent with explosive application in the field. Laboratory results are often misinterpreted because true field conditions cannot be accurately modelled, in particular shock and gas energy ratios and geometries of the charge

(Konya *et al*. 1990). One way of dealing with this problematic situation is to consider scaling and its effect on the differences between model material and the rock material.

2.4.1 Scaling

The importance of scaling must always be remembered when conducting model-scale tests. Even when the model material is taken from the same location that it should represent, there is a great difference. The rock properties measured in a laboratory are far from the rock mass properties that determine the production-scale process. Laboratory values have often exceeded *in situ* determinations by factors of five to eight (Hagan 1973). Another influential factor is the boundaries. Smaller models have boundaries that are likely to affect the fragmentation mostly because the reflection of compressional and tensile waves. The smaller the specimens are, the more they are affected by reflecting waves interacting with each other (Naarttijärvi 1978). In research, this problem can be solved by wave traps. A layer of aluminium, for example, is placed around the specimen and between them is a layer of oil. When the compressional wave reaches the surface of the specimen, it will try to reflect as a tensile wave; since the oil layer has no strength, the aluminium outside the specimen will fall off and the energy is consumed. No reflecting wave develops. Another approach is to place the specimen in liquid of density such that it is acoustically matched to the model material (Field *et al.* 1971). The propagating waves can then pass the free face, unreflected, into the liquid.

Few researchers have investigated the scaling problem. Most of them have settled for a material that "pretty much" acts like rock and where the results have been interpreted as equal for rock. This approach can of course be questioned, but one has to ask oneself whether it is possible to perform scaled model tests at all. If so, how should they be conducted? One approach has been extensively discussed by Naarttijärvi *et al.* (1980). The method is called dimensional analysis and, briefly summarized, it establishes a uniformity for energy and geometrical, kinematic and dynamic properties between model-scale and full-scale tests. The analysis requires knowledge about what really happens inside the rock during the blasting event, a decision as to what kind of rock is to be studied and what kind of blasting should be simulated. The technique is to generate dimensionless products which represent the relation between the model and full scale. One should identify the parameters that are necessary to take into account, place them in order of importance and choose one parameter that has a fixed relation to the others. The dimensions for all parameters are expressed in terms of mass, length and time. By a series of equations, the factors, in the end, become ratios between a parameter in model scale and full scale. For example, if the scaling factors are expressed as

$\frac{l_m}{l_f} = \frac{1}{\lambda}$ for the length, $\frac{\rho_m}{\rho_f} = 1$ for the density and the calculated factor λ is 36, then the characteristic length in the model is $\frac{1}{36}$ of the full scale, and the density of the model material should be the same as in a full scale test.

Dimensional analysis is far from trivial and several assumptions are made along the way, as the complex nature of the rock blasting mechanisms includes many parameters. Working with all of them is impossible, and the factors need to be reduced to a smaller number, which complicates the process. This is probably why the technique has not been extensively used. Naarttijärvi *et al.* (1980) tried the analysis with Plexiglas as the model material and as it turned out, this was not a suitable model material for studying cracks, even though it is the material that has been used in most research projects working with

crack propagation. Naarttijärvi (1978) has also found that Plexiglas gives a much coarser fragmentation than rock and cannot therefore be considered scaleable.

The most difficult task is to understand how smaller specimens behave in comparison with full-scale benches. Panchenko stated that the most critical tasks, when designing smaller scale blasts, are keeping the geometries and distribution of the charge scaled (Naarttijärvi 1978). If this can be achieved, the volume of the fragmented zone should be proportional to the scale factor of the model. Panchenko concluded this from investigations conducted in concrete.

Another approach is the "scale distance" stated by Hopkinson (Naarttijärvi 1978).

$$z = \frac{R}{Q^{\frac{1}{3}}} \tag{2.15}$$

where z = scale distance
R = distance
Q = amount of explosive

The shock waves, generated at the same scaled distance, produced by two charges of the same shape and explosive, but of different sizes, are equally great. All parameters with pressure or speed dimensions are given a scale factor of one, i.e. they are the same in model and full scale.

Kristiansen (1987) suggested another method for scaling model tests. Some explosives do not detonate completely at diameters as others do. Consequently, it became important to find a way to scale different test results so that they were comparable. Kristiansen describes a method for this by calculating the new surface area formed by the explosive. It was assumed that all of the fragments are cubical and that the length of a cube is the average side of a sieve opening. For example, the fraction passing the 64 mm sieving deck and landing on the 32 mm deck is assumed to have a length of (64 + 32)/2 = 48 mm. The new surface area is calculated as:

$$A = \frac{V}{L^3 \cdot \rho} \cdot L^2 \cdot 6 = \frac{6 \cdot V}{L \cdot \rho} \tag{2.16}$$

where A = surface area of the fraction formed by the explosive [cm^2]
V = weight of the fraction [g]
L = the average side length of the fragments in the fraction [cm]
ρ = density [g/cm^3]

A ratio is given for dividing the surface area of all fractions formed by the explosive and the volume of the cubical model. This ratio was then plotted against the side length of the model cube for two types of explosive, Comp C-4 and dynamite. The resulting diagram was two straight parallel lines that could be described by the following equation.

$$Y = B + k \cdot x \tag{2.17}$$

where Y = surface area/volume of the cubical model [cm^{-1}]
B = variable depending on type of explosive
k = constant
x = side length of the cubical model [cm]

The positive inclination of the lines indicates that the amount of fines increases with increasing borehole diameter; the boreholes become larger with increasing cubical models. Between 60 - 70 % of the generated surface area originates from the fractions less than 2 mm in size. Since the crushing of the zone surrounding the borehole becomes greater when the cube size increases, the ratio surface area/volume also increases which gives the line a positive inclination. This proposed scaling method has been validated only by Kristansen's own tests; more tests need to be done to further verify the method.

The choice of scaling method is difficult, as they all contribute interesting approaches, but at the same time there are weaknesses worth noting to study further. Probably the most obvious and important problem when scaling rock blasting is the effect of rock mass properties, such as inhomogeneities and discontinuities in the rock material. These rock mass properties are almost impossible to simulate in small-scale blasts. It is also interesting that when the characteristics of today's explosives are given, they have very often been transposed from experiments in materials other than rock. There has been some work done on this. Vestre (1992) has investigated whether concrete would be a more suitable material, if rock cannot be used; however, more research on this is needed. Therefore, one can ask: Are the values really representative for all blasting applications?

The model-scale test conducted in this project was not developed with any reference to scaling. The material was simply chosen because of its capacity to be formed and coloured so that the method could be tested. It was decided to use the strongest concrete that could be produced. The amount of explosive was given by the specific charge, which was to be kept approximately the same as in a production full-scale blast. Safety precautions were the reason for using the detonating cord. It could easily be handled and the charging was as constant as possible, since it was easier to measure and cut off a certain length than to compact an explosive paste by hand.

2.4.2 Confinement

For model-scale blasts, the confinement, unfortunately, is usually almost nonexistent. Nonetheless, it is easy to understand that this ought to be an important factor. A confined rock mass offers a much greater resistance to breakage: first, because of the increase in strength, both compression and tensile, and second, because the energy from the explosive has a longer time to fragment the material. Also, more energy is needed in the liberation and movement of a rock mass. Tien *et al.* (2000), for example, found that the higher the confining pressures a test sample (of mortar or concrete) was exposed to, the higher failure strengths the material offered. This demonstrates very well why the confinement is critical for blasting situations. Confinement also affects the strain rate dependence of the failure strength of granitic rocks (Masuda 2001). The failure strength becomes more dependent on the strain rate at higher confining pressures.

If the confinement is to be modelled, then it also needs to be measured at the site the study aims to investigate. This is, as with many other considerations, desirable but highly unlikely to be done for economic reasons. The reasonable thing to do is to leave this

parameter at model-scale level and try to confirm results from the laboratory in a field study where the confinement is a reality.

3 MODEL-SCALE BLASTS

To investigate the hypothesis that fines originate to a large extent from the crushed zone around a borehole, it was decided to make small-scale experiments, as this would be impossible to study for full-scale production blasts. It would also be extremely difficult to fully replicate any experiment, because of the inhomogeneous nature of the rock and the non-ideal behaviour of the explosive. Moreover, it is seldom possible to repeat an experiment enough times to make a statistically significant analysis of the results (Winzer *et al.* 1983). However, by repeating the blasts even as few as three times, the result would still be more reliable than only being able to do it once. Since the 1970s most work reported in literature of rock fragmentation has been conducted in materials such as Plexiglas, Homalite and concrete, which is fully understandable when considering the complex nature of rock material.

3.1 DESIGN OF THE METHOD

As the objective was to study where, from the inside of a test specimen, fines orginate, a method had to be designed so that each fraction could be traced after the blasting was done. Finally, the design arrived at was a cylinder divided into three segments. These segments needed to differ from one another in some way so that the material in each segment could be separated after the blast. To conclude, the cylinder needed to be homogeneous in each segment, but have a property that differed for each, and also consist of a material which allowed the tests to be repeated. The only material that could be thought of was concrete, for which the properties could be controlled and the different segments separated by colour. Colour pigments can be added when mixing the concrete, and they do not affect the properties of the final hardened product. After the blast and sieving process, each colour would represent a segment and the origin of a fraction would be obvious. The cylinder was 600 mm high and 300 mm in diameter. The two inner segments would consist of smaller cylinders inside an outer final one (Figure 3.1). The innermost cylinder was given a diameter of 120 mm, the middle one a diameter of 200 mm and the outermost 310 mm.

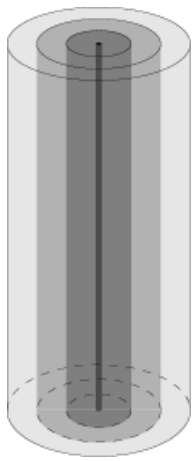

Figure 3.1 The test specimen was designed as a concrete cylinder consisting of three segments with different colours.

3.2 MODEL MATERIAL

Concrete is a multiphase complex material consisting of aggregate particles, of various sizes and irregular shape, which are dispersed and embedded in hardened cement paste, i.e. the matrix of concrete differs from that of rock material. To give the concrete a more rock-like matrix, the aggregate particles were limited to a size of 0.5 mm or smaller and consisted of 94.7 % quartz. This mix is considered to be closer to mortar than concrete. The mixture was designed to produce a high-strength mortar with low porosity. To achieve this, the water-cement-ratio was set to 0.35 and a superplasticizer was added. The superplasticizer not only decreased the air voids, but also gave the mortar a lower viscosity (an essential property in the casting procedure). The complete mixture can be seen in Table 3.1.

Table 3.1 The mortar mixture

Sand	Industrisand (Askania)
Cement	White Std. Cement (Aalborg, Cementa)
Superplasticizer	1.7 % (Cementa SSP20)
Pigment	4 % (BKN Byggekemi AB)
Water-cement ratio	0.35
Sand-cement ratio	1.5:1

To colour the mortar, two oxides of iron and one of chromium were chosen. The colours were selected after studying their intensity when mixed with white cement and hardened to mortar. Black, yellow and green were chosen because they are easy to distinguish visually. Each pigment was tested, for any colour changes due to high temperature or pressure, by blasting small specimens (Figure 3.2). Although no changes could be detected, the remains of the explosive blackened the material surrounding the charge (Figure 3.3). Therefore, it was decided to place the black mortar closest to the charged hole.

Figure 3.2 Small mortar specimens were blasted and colour changes due to high temperature or pressure were studied.

Figure 3.3 The remains of the explosive blackened the material surrounding the charge.

3.3 CASTING PROCEDURE

The casting procedure suitable for the cylinder shaped specimens turned out to be a bit more complicated than expected. First of all, the outer mould was manufactured by cutting open a steel cylinder (Figure 3.4). With screws, it would then be possible to close the cylinder when the mortar was poured into the mould and, after it had hardened, the screws could be loosened and the steel cylinder easily removed. The cylinder was covered with a plastic paint which would make the hardened mortar release the mould. Then two smaller steel cylinders were welded together and centred inside the big cylinder (Figure 3.4). These were to act as a sliding form. The bottom was tightened with a wooden plate which also kept the inner cylinders in place. In the middle of the inner cylinder, a steel rod with a diameter of 9 mm was placed.

Figure 3.4 The first casting procedure consisted of one outer cylinder and two inner ones that had been welded together. These were to act as a sliding form.

The casting procedure was tested with a non-coloured mortar mixture. The mixture was poured into the three sections; as the inner cylinder was so narrow, it was important to keep the mortar as low in viscosity as possible. No vibration was performed, since the mixture was considered self-compacting. The mortar was kept moist: after one day the steel rod was removed and, one day later, the mould. The mortar body was wrapped in plastic film with moisture inside and left for 26 more days to harden. The test body was blasted in a container designed for the purpose (Figure 3.10) and the explosive used was explosive paste compacted with a wooden stick. The detonation was incomplete, and it left

half of the cylinder intact. However, it could be seen that the casting procedure was not successful, as the cylinder had separated where the form had been pulled up (Figure 3.5).

Figure 3.5 Weakness planes formed during casting.

The weakness planes were probably formed when the form was pulled up: a layer of water was left enclosed under it. Consequently, this casting procedure was abandoned. The new method consisted of three stages. The outer painted mould was kept, but two new moulds were produced (Figure 3.6): one for the inner black cylinder and another for the middle yellow one. First, the inner black part was cast, left to harden for one day before the mould was removed, and then left to harden for another day in plastic film. To remove the weakness layer that might arise on the envelope surface, from the contact with the mould, the mortar body was sand blasted. Then, the black mortar body was placed, centered, inside the middle mould and the yellow mortar was poured into the remaining space. As the contact between the two mortar mixtures had to be tested, no outer layer was cast. The mortar body, which then consisted of two layers, was left to harden for 28 days.

Figure 3.6 The new method consisted of a three-stage process by which the mortar body was cast with different moulds.

To test the strength of the area of contact between the black and the yellow mortar, four cores were drilled through the body and their tensile strength was tested (Figure 3.7).

Figure 3.7 Cores were drilled into the mortar body, and the tensile strength of the area of contact between the yellow and black mortar was tested.

The result of the test showed that there were no weaknesses between the two mortars: the cores broke in the black layer in every test made. The test also revealed that the black layer was weaker than the yellow one, even though the mixtures had been identical. The black mortar was observed to have more voids, which could explain the behaviour. This demonstrates how difficult it is to produce two identical batches of mortar even when the ingredients and mixing routine are identical.

When the casting procedure had been considered successful, the process of producing three mortar bodies in three colours was started. The blasting was to be carried out three times to obtain a more reliable result. The test bodies were produced in three stages. The first stage was the innermost layer, which was cast in three cylinder moulds with a diameter of 120 mm (height 600 mm). Before the mortar was poured into the moulds, a stick, 9 mm in diameter, was placed in the middle of each cylinder to form a hole for the charge. After two days of hardening, the mortar was strong enough to remove the moulds. The envelope surface of the black cylinders was sand blasted to roughen it and to remove any weaker material. Thereafter, the cylinders of 120 mm diameter were placed inside three 200 mm diameter moulds and the second mixture, yellow mortar, was poured into the remaining space. The same sand blasting procedure followed after another two days and, finally, the green mortar was placed, in a 310 mm diameter mould, outside the yellow one. The final three-layered cylinders were left to harden for 28 days at 20°C. This approach produced cylinders consisting of 15 % black mortar, 28 % yellow and 57 % green (Figure 3.8). During casting, standardised test specimens were also made for each mortrar mixture to facilitate determining the properties of the mortar. The measurements were most important for the green mortar mixtures, since these were separately mixed for each cylinder. The properties were determined 28 days after casting and also on the day of blasting.

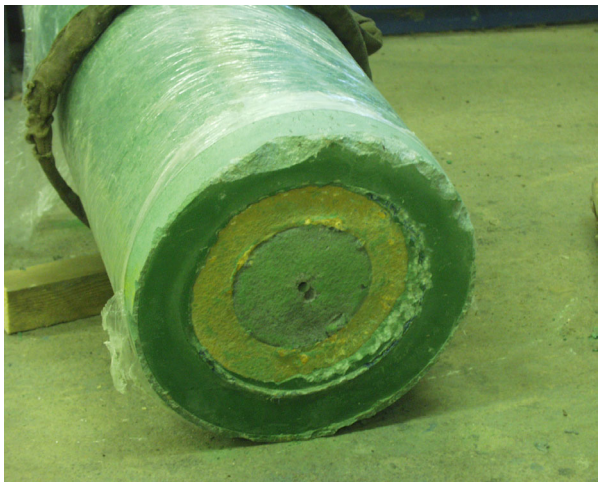

Figure 3.8 One of the final mortar bodies to be blasted.

3.4 MATERIAL PROPERTIES

Both fresh and hardened properties were tested at the time of casting, after 28 days, and on the day of blasting. Measured properties on the day of blasting can be seen in Table 3.2. The first two layers, black and yellow, for all three cylinders, were mixed in the same batches; unfortunately, this was not possible for the last layer, since the volume of mortar was too large for the existing equipment. The only way to proceed was to accept having three batches of green mortar and to carefully repeat the mixing procedure.

Table 3.2 Mortar properties on the day of blasting

Layer	Fresh density [kg/m^3]	Density [kg/m^3]	Compressive strength [MPa]	Flexural tension strength [MPa]	P-wave velocity [m/s]
Black	2214	2253	76.6	7.8	3922
Yellow	-	2266	98.4	7.8	4143
Green 1	2055	2039	62.2	7.2	3803
Green 2	2325	2338	85.3	7.6	4078
Green 3	2316	2340	86.3	8.7	4178

As can be seen in Table 3.2, the first green batch showed lower values for all properties. The fresh density indicates that something differed for this mixture from the beginning, despite the use of the same mixture, mixing procedure and equipment. To get an indication of the porosity, the P-wave velocity was measured: it was relatively similar for all five batches of mortar. It can also be seen that the objective to mix a high-strength mortar was successful.

Since it was not possible to obtain a stress-strain curve in the traditional way from the type of tests used, neither Young's modulus nor Poisson's ratio could be calculated. Instead, as an approximation, the following equation was used:

$$E_d \cong \rho_{rock} \cdot V_p^{\ 2} \tag{3.1}$$

where E_d = Young's dynamic modulus [MPa]
ρ_{rock} = density of the rock [kg/m^3]
V_p = P-wave velocity [m/s]

Equation 3.1 is based on an equation for an explosively driven split Hopkinson pressure bar, where the velocity of the bar is the square root of the modulus divided by the density. However, a simplification suggested by the ASTM Standard (C769-80) (Kim *et al.* 1998) is that the velocity of the bar be assumed equal to the compressional wave velocity. This Young's modulus is a dynamic one (Table 3.3): it is not comparable to the Young's modulus used in traditional concrete testing. This is the equation that is also used for the Bårarp gneiss (see Chapter 4). It is also possible to calculate the Poisson ratio with another equation based on ultrasonic testing, but then it is necessary to determine the shear wave velocity, which was not possible here.

Table 3.3 Young's dynamic modulus for the three mortar layers.

Layer	P-wave velocity [m/s]	Density [kg/m^3]	Young's dynamic modulus [GPa]
Black	3922	2253	34.6
Yellow	4143	2266	38.9
Green 1	3803	2039	29.5
Green 2	4078	2338	38.9
Green 3	4178	2340	40.8

The calculated Young's modulus seems reasonable, since concrete in general has a static modulus between 10 and 40 GPa (Tepfers 1995). The dynamic modulus is somewhat higher, as the specimen is exposed to a sudden pressure loading: there is no time to respond to the loading. The pressure does not have time to find the weakest places to pass through, as it would otherwise.

3.5 CHOICE OF EXPLOSIVE

The first choice of explosive was explosive paste, however, since a detonation stop occured during a test blast, it was assumed that the explosive could not be compacted enough by hand. Hence, the final choice was to use a detonating cord, which was both safer and more convenient to handle. In the matter of amount of explosive, two detonationg cords were tested: one 20 g/m which would give a specific charge of 0.27 kg/m^3 and one 40 g/m (0.53 kg/m^3). Two cylinders had been cast for this purpose and those were blasted. The material was collected and sieved. The sieving curves (Figure 3.9) showed that the 40 g/m cord gave more fines to work with; it was therefore decided to use that one. Also, the specific charge was quantitatively more like one used in a real quarry.

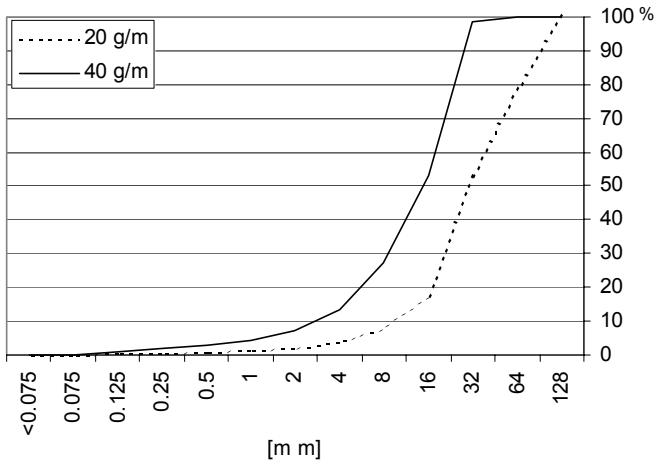

Figure 3.9 The sieving curves for the blasting of two mortar cylinders when investigating which detonating cord to use.

3.6 BLASTING

The blasting of the three coloured mortar cylinders took place in a container designed and constructed for the purpose (Figure 3.10). The container, reinforced with 10 mm walls of steel, was lined with a layer of rubber. The rubber was to reduce the risk of further fragmentation of the pieces when they hit the wall after the blast. The 40 g/m detonating cord was placed inside the 9 mm diameter hole in each mortar cylinder. This gave a specific charge of 0.53 kg/m^3. An initializer initiated the blast and afterwards all fragments were collected.

3.7 SIEVING

Concrete material has a tendency to break apart easily when it is sieved, since it is brittle. This was thouroughly investigated by test sieving the mortar material collected from the test blasts with different detonating cords. To make sure that no more fines were produced, apart from those generated by the blast, the sieving process was changed from the ordinary laboratory method to a gentler one. The first stage of this process consisted of six screen decks, which were shaken by hand; the smallest mesh was 4 mm in size (Figure 3.11). Although the material smaller than 4 mm was placed in ordinary laboratory sieving equipment, it was sieved by hand for 2 to 3 minutes instead of sieving it for 10 minutes automatically.

3.8 TEST SAMPLING

When all three cylinders had been sieved, the process of separating the different colours in all the fractions began. When the separation had been done this information was used to construct size distribution curves.

Each of the larger fractions (> 8 mm) was separated, by colour, by hand. The total number of mortar fragments within each colour group was then counted. As there were too many fragments of the material less than 8 mm in size, test samples were taken instead of counting them all (Figure 3.12). For the fractions of 4 - 8 and 2 - 4 mm, the randomly taken test samples together made up 15 % of the entire fraction. For the fractions smaller than 2 mm, even 15 % was too much to count: instead, enough samples were taken to obtain confidence limits of 2 % or less with a significance level of 0.05. This meant counting a total of approximately 6000 – 11000 fragments per fraction in no fewer than 5 test samples. As the fragments were too small to handle with fingers, they were spread on a piece of paper and put in a scanner. When the picture was scanned, it was easier to count the fragments by looking at the printed picture (Figure 3.12). After considering whether some image analysis software would be useful when counting the fragments, it was decided to use the scaning method instead.

Figure 3.10 The blasting took place in a steel-reinforced container in which all the fragments were collected afterwards.

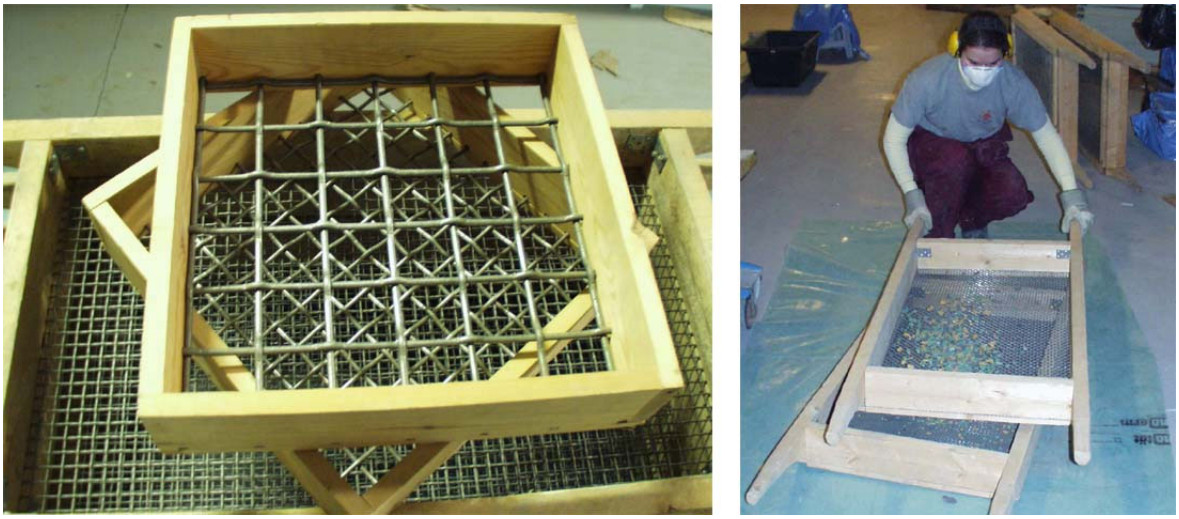

Figure 3.11 As the mortar easily broke apart the sieving was done by hand instead of automatically.

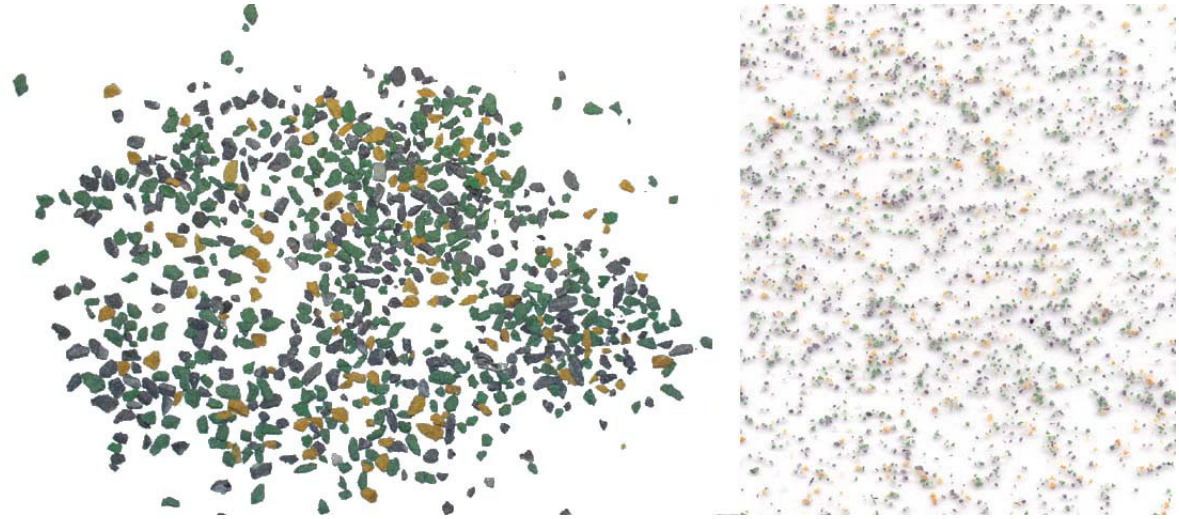

Figure 3.12 Scanned and printed pictures made it easier to count the fragments in the smaller fractions: on the left cylinder 1 fraction 2 - 4 mm, and on the right cylinder 1 fraction 0.25 - 0.5 mm.

3.9 THIN SECTIONS

To further study the crack propagation in a mortar cylinder, seven thin sections were made. These were taken from two fragments which both consisted of all three layers, however, one had the envelope surface intact and the other did not. Figure 3.13 illustrates the location of each thin section.

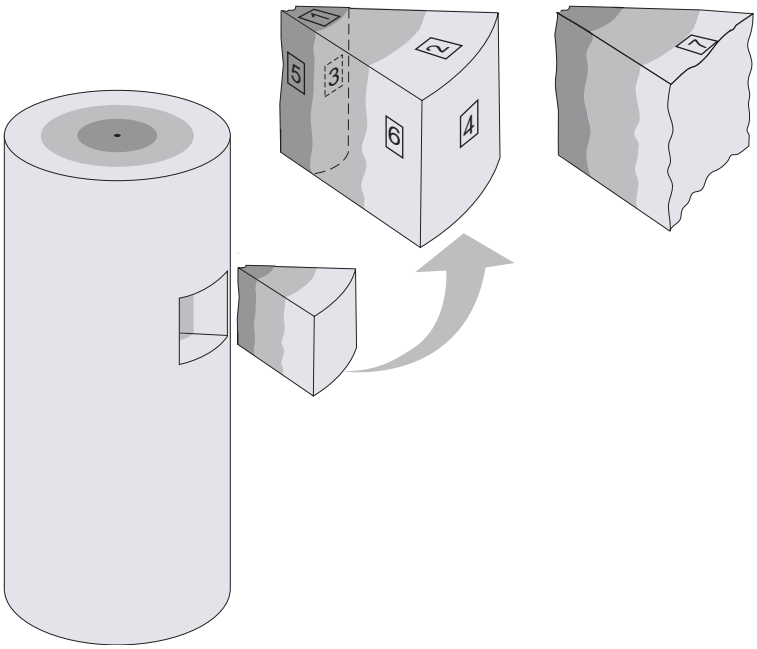

Figure 3.13 Thin sections were made from two fragments which both consisted of all three layers. Thin sections 1 - 6 represent the inner or the outer layer of the intact fragment; thin section 7 the outer layer in the fragmented piece.

The thin sections were prepared in a standard way with one addition. Before starting the preparation, the mortar pieces were soaked in a red epoxy paste. This paste penetrated all cracks in the piece and made them easy to observe in a microscope.

4 HALF-SCALE BLASTS

The objective of the half-scale blasts is to study the effect on fragmentation, specifically the fines generation, of different borehole diameters when keeping the specific charge constant. This has been investigated before, for example by Kristiansen (1995a) who found that a decrease in borehole diameter generated less fines (0 - 4 mm). It was decided to do this in smaller blasts in a quarry, as this would make it possible to sieve the entire muckpile. The results would also be more reliable with rock material than in another model material. Mats Olsson (SveBeFo) designed and performed the blasts.

The quarry site, Bårarp, is located south of Falkenberg and north of Halmstad, in Getinge, just off highway E6 (exit 47). It was chosen because the geology is quite homogeneous and the *in situ* block distribution very large. The homogeneity was important so that the blasts could be considered repeatable. The quarry is owned by Emmaboda Granit AB and used for producing armour stones, which means that the blasting technique used is very cautious and the bench remaining after a blast is relatively undamaged.

4.1 GEOLOGY

4.1.1 Regional geology

The county of Halland, in which the Bårarp quarry is located, consists to a large extent of crystalline bedrock which is part of the western section of the Southwest Gneiss region. The region stretches from the Tornquist zone in the south of Sweden to the southern part of Norway. This region can be divided into two zones separated by the Mylonite zone (Lundqvist *et al.* 1998).

The quarry activities in the region are dominated by the production of armour stones and aggregates. This is because the polished gneiss has a very attractive colour, as well as good technical properties and resistance to weathering, all of which make it a desirable export product. When producing armour stones, there is much waste rock material. This waste product is a suitable aggregate source for local use (Lundqvist *et al.* 1998).

4.1.2 Local geology and the test site

The quarry at Bårarp, in which the test site is located, consists mainly of grey-red, alkali rich gneiss with a grain size ranging from 0.5 to 5 mm, however the average grain size is close to 2 mm. The rock has been metamorphosed, a process that resulted in partial melting and a more or less phaneritic texture (Ronge 2000, SP 1997). Pegmatite can be found at various places, which is also a result of the melting. The dominant minerals are quartz, alkali feldspar (microcline), plagioclase, biotite and muscovite. Quartz and potassium feldspar are the first minerals to melt, thus they gather in large volumes. The rock can also include xenoliths. Mineral grains grow in the direction of least pressure and become parallel. Variations in temperature and pressure cause different degrees of transformation, which give the rock a somewhat foliated look. The strike of the foliation is to the north-northeast and dipping to the southeast.

The rock at the test site at Bårarp consists of the same gneiss as that described above. The measured strike of the foliation is N40°E and the dip 35 - 45°SE. The rock is brittle and the joint frequency low. However, the few existing joints are quite dominant and wide open. Some are closed and almost sealed. Joints wider than 50 mm have filling consisting of crushed sand material.

4.2 MAPPING

Before any blasting operations took place, the geology and all joints in the bench were mapped. The surface of the bench was divided into squares so that all joints could be more easily identified. They were all marked with paint and photographed digitally. Later a sketch of the area was made (Figure 4.1).

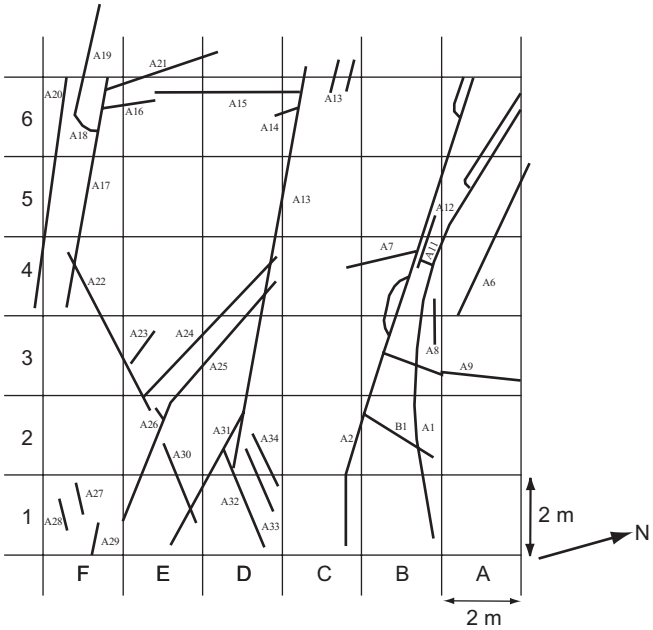

Figure 4.1 During the mapping process the bench was divided into squares so that all joints could be identified more easily.

When the strike and dip of all joints were measured, a rose diagram and a stereoplot could be made (Figure 4.2). Since the joints were relatively few, the statistics for the plots are not very reliable for the whole Bårarp area, however they are more accurate for the specific test site.

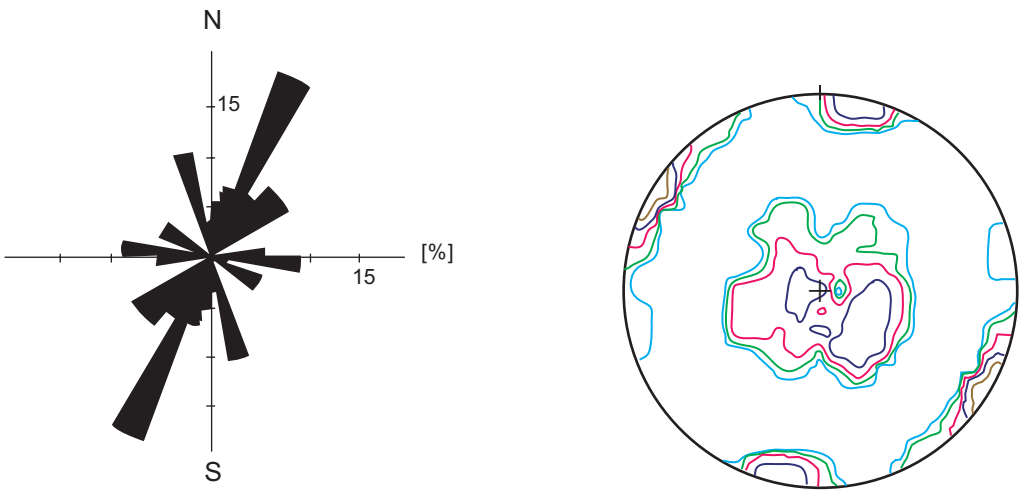

Figure 4.2 Rose diagram and stereoplot for the Bårarp test site. (Stereoplot: light blue line 1 %, green 2 %, red 4 %, dark blue 8 % and brown 16 %)

4.3 TECHNICAL PARAMETERS

The technical parameters of the rock at the Bårarp test site were determined by investigating five cores that were drilled into the bench. These were located according to Figure 4.3.

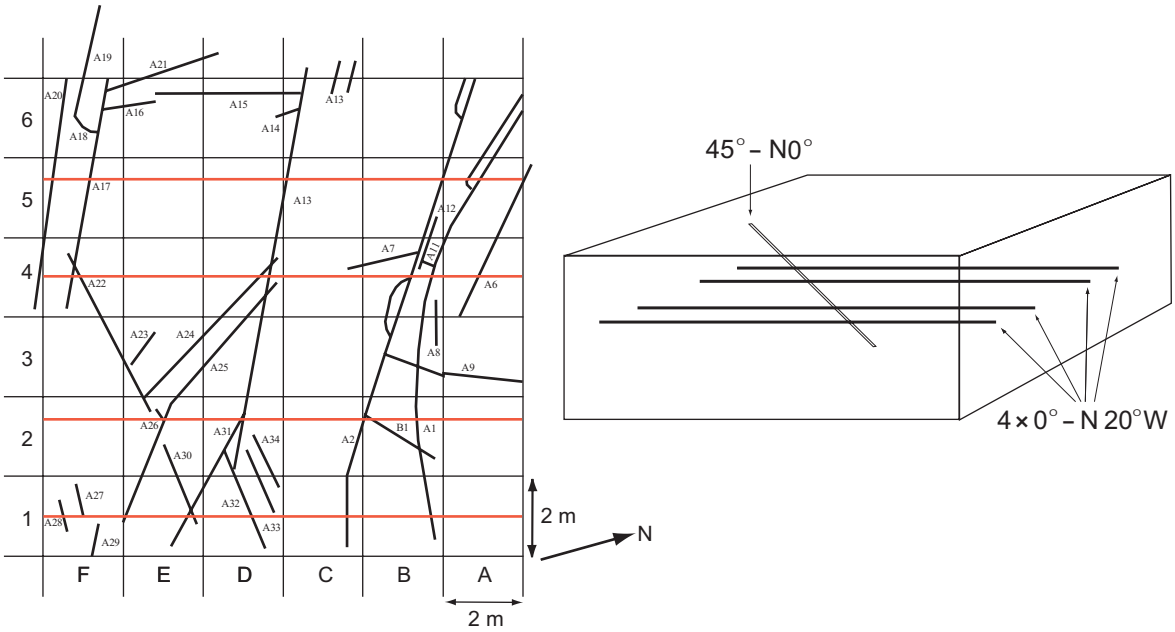

Figure 4.3 Five cores were drilled into the bench so that technical parameters could be determined for the rock. The red lines represent the horizontal core drilling.

The cores were also used for studying the joint frequency. It was found that the joints which were visible on the surface of the bench represented the number of joints inside the rock mass very well.

The compression and tensile strengths were determined, as well as the P-wave velocity, by standard methods. Tests of rock parameters have also been made by Lundqvist *et al.* (1998), Swedish National Testing and Research Institute (SP 1996, 1997) and the Geological Survey of Sweden (SGU 1997). All parameters can be seen in the tables below (Tables 4.1 – 4.3). For further information about the standard test methods for the parameters below see FAS (1995), Pells (1993), Schön (1996) and Brook (1993).

Table 4.1 Compression, tensile strength and P-wave velocity for the Bårarp gneiss.

$\sigma_{c,\ Point\ load}$ [MPa]	$\sigma_{t,\ Brazilian}$ [MPa]	V_p [m/s]
244 ± 37	13.2 ± 1.4	5526 ± 185

Table 4.2 Some technical parameters for the Bårarp gneiss (Lundqvist et al. 1998).

Impact value [weight%]	Average flakiness [weight%]	Density [kg/m^3]	Abrasion value [cm^3]	Mica content [vol%]
55	1.35	2.7	3.09	6

Table 4.3 Some technical parameters for the Bårarp gneiss (SGU 1997, SP 1996, 1997).

Length-thickness index [weight%]	Point load index (dry) [MPa]	Point load index (wet) [MPa]
14.0	9.3	8.4

It is possible to calculate a Young's dynamic modulus from the compressional wave velocity and the density of the rock (see Section 3.4). This was done for cores of Bårarp gneiss from the test site: an approximation of the Young's dynamic modulus is 82.5 GPa.

4.4 *IN SITU* SIZE DISTRIBUTION

By mapping the test site it was possible to make an *in situ* size distribution curve for the rock blocks. This was done statistically by assuming that the joints were randomly distributed in space and that dominant joint sets based on orientation could be determined. This was decided by studying the stereoplot of poles to joints. Since no discernible joint orientation clusters could be observed in the stereoplot, and furthermore, the number of joints mapped was rather small, all statistical clustering attempts proved to be of low significance and, as such, gave no evidence for any clear pattern in joint orientations. Monte Carlo simulations gave 100 in situ distributions (Dershowitz et al. 1998); of these, 10 were randomly chosen to represent the rock block distribution at the site. This distribution was a log normal-distribution with a mean value of 5.7 m^3 and standard deviation of 0.84 m^3. The final cumulative *in situ* distribution curve can be seen in Figure 4.4.

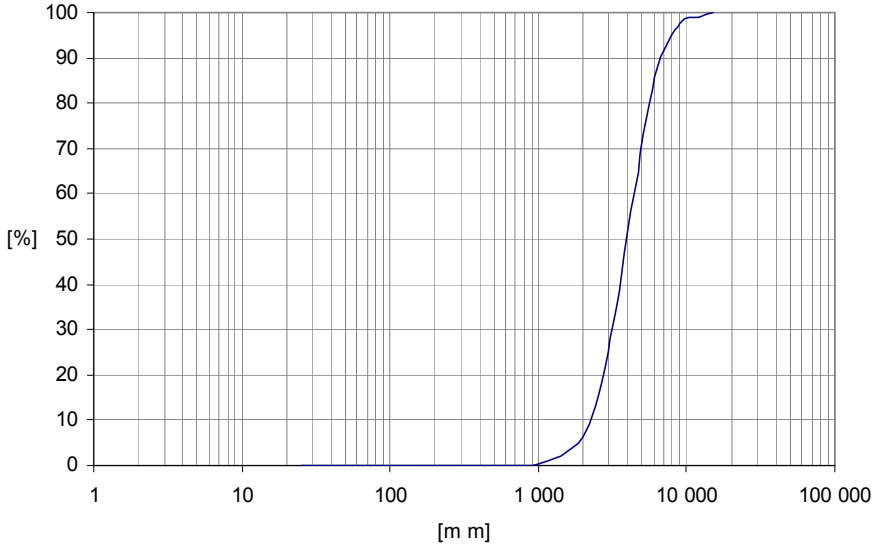

Figure 4.4 In situ *distribution curve for the Bårarp test site.*

4.5 BLAST DESIGN

The test site was chosen for its quite homogeneous character and very low joint frequency. The bench was approximately 5 m high and 13 m wide. This bench was used for the first three test blasts, and the mapping of it is described above. The objective was to keep the specific charge constant, vary the borehole diameter and study any changes in fragmentation (Olsson 1999). This meant changing the geometry of the blast design so that the amount of explosive was the same for each unit of rock mass (Table 4.4). All test holes, except for the holes in round two, were fully charged. Round two had decoupled 51 mm charges in 76 mm boreholes. The decoupling was done by placing a 51 mm tube, which was later filled with explosive, centered inside the borehole. To achieve fully coupled boreholes, cartridges were slit open and dropped down into the hole. This technique gives the desired degree of packing. These first three blasting tests were made during June to October 2000 (Olsson 2002). After the evaluation of the results, it was decided to continue with three more blasts, however these could not be made in the same bench, as there was not enough rock mass remaining. Instead, another bench was chosen, just in front of the

old one but one level down. The geology of this rock mass was considered to be the same as the other, hence no mapping was done. The fourth test blast was a repetition of the first blast (Olsson 2002). The fifth and sixth rounds were designed with borehole diameters of 38 and 64 mm, respectively. These three rounds were fired between August and December 2001. Together, the six test blasts were thought to give enough information about how the fragmentation result is affected by different borehole diameters with a constant specific charge, and how a decoupled charge fragments the bench in comparison with the other fully coupled blasts.

Table 4.4 The blast design for six test blasts (Olsson 2002)

Blast no.	Borehole diameter [mm]	Burden [m]	Hole spacing [m]	Number of holes [-]	Volume of rock [m^3]	Stemming [m]	Specific charge [kg/m^3]
1 (00-06)[1]	51	1.80	2.10	6	95	1.4	0.55
2 (00-09)	76/51[2]	1.80	2.10	6	95	1.4	0.57
3 (00-10)	76	2.70	3.40	4	138	1.8	0.55
4 (01-08)	51	1.80	2.20	6	103	1.2	0.55
5 (01-10)	38	1.35	1.65	8	81	1.1	0.52
6 (01-12)	64	2.30	2.85	5	139	1.2	0.55

[1] Date of test blast, 00-06 = June 2000. [2]A 51 mm charge was decoupled in a 76 mm borehole.

Blast no.	Bench height [m]	Hole depth [m]	Initiation sequence	Explosive	Coupling ratio [-]	Charge weight per hole [kg]
1 (00-06)	5.0	5.60	321123	Emulite	1.00	9.0
2 (00-09)	5.0	5.50	321123	Emulite	0.66	9.0
3 (00-10)	5.0	5.50	2112	Emulite	1.00	19.0
4 (01-08)	5.2	5.50	321234	Kemix	1.00	9.4
5 (01-10)	5.2	5.35	32101234	Kemix	1.00	5.3
6 (01-12)	5.3	5.60	32123	Kemix	1.00	15.3

The change in the emulsion explosive after the first three test blasts was made because another supplier had to be used. The explosive is however fully comparable. Electronic detonators initiated each blast and in two blasts (the second and fifth) the VOD was measured to check the performance of the explosive. Electronic detonaters were used to secure the initiation sequence.

4.6 SIEVING AND ROCK QUALITY TESTING

The sieving process was carried out in three steps. First, all rock material in the muckpile was transported to a Hercules drum sizer (Figure 4.5) and sieved to five fractions; < 200, 200 - 350, 350 - 400, 400 - 450 and > 450 mm. All fractions, boulders included, were weighed. The material < 200 mm was transported to a second siever, an Extec, and sieved into four fractions (0 - 25, 25 - 90, 90 - 120 and > 120 mm). Test samples were taken from the 0 - 25 and 25 - 90 mm fractions and transported to a nearby laboratory where the last sieving took place. The complete sieving process gave fractions ranging from > 450 mm to < 0.075 mm (Olsson 2002).

Figure 4.5 The first sieve to be used at Bårarp, a drum sizer.

When aggregates are evaluated for road construction, some rock quality parameters are of importance. Therefore, parameters such as density, average flakiness, impact value and abrasion value were determined from the material that was sieved in the laboratory.

5 RESULTS

As for many other research projects within the field of rock blasting, where the material is used for aggregates, the result from the blasts is presented in the form of different types of size distribution curves. The objective is to find a trend in the fragmentation, rather than to study absolute numbers. For many reasons, it is not a meaningful task to try to compare the amount of fines generated in model-scale blasts, conducted in rather small mortar specimens, with full-scale production blasts in rock. This is further discussed in Chapter 6. Apart from studying the outcome of the sieving process, from both the small-scale blasts and the Bårarp quarry, seven thin sections were made to facilitate investigating crack propagation. These are presented in the same section as the model-scale blasts.

5.1 MODEL-SCALE BLASTS

After all of the fractions for all three cylinders had been weighed (Appendix V), cumulative size distributions were plotted to see if the fragmentation was similar for all specimens (Figure 5.1).

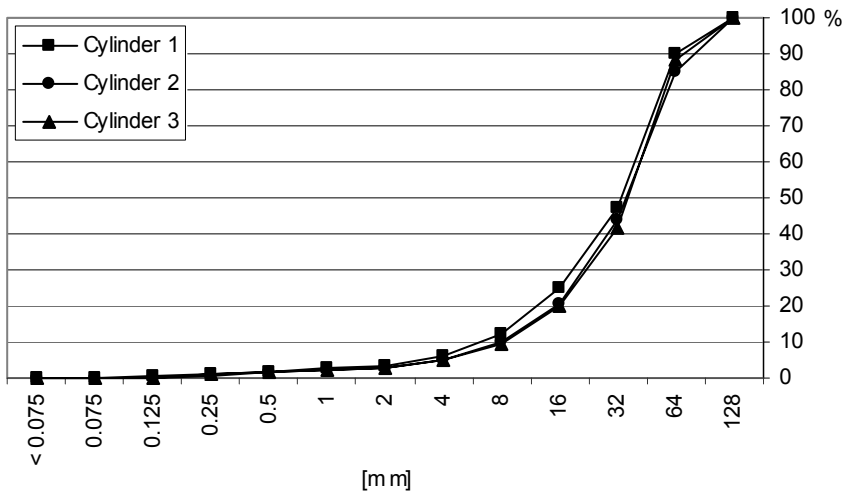

Figure 5.1 Cumulative size distribution curves for all three cylinders.

All three cylinders show very similar fragmentation and the next step was to separate the fragmentation of the different layers.

5.1.1 Size distribution curves

To find possible trends in the sieved blasted material, the percentage of each colour in every fraction (Appendix V) was plotted for the three cylinders (Figures 5.2 – 5.4).

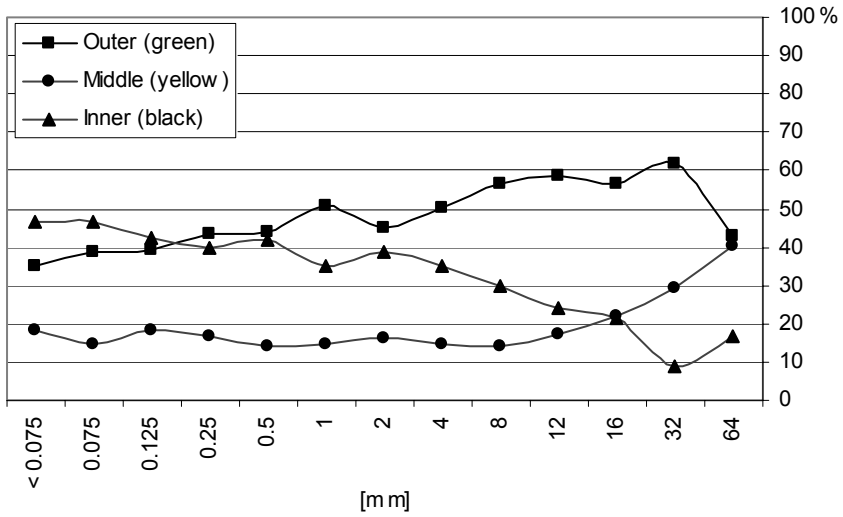

Figure 5.2 Cylinder 1: Percentage of each colour for the fractions.

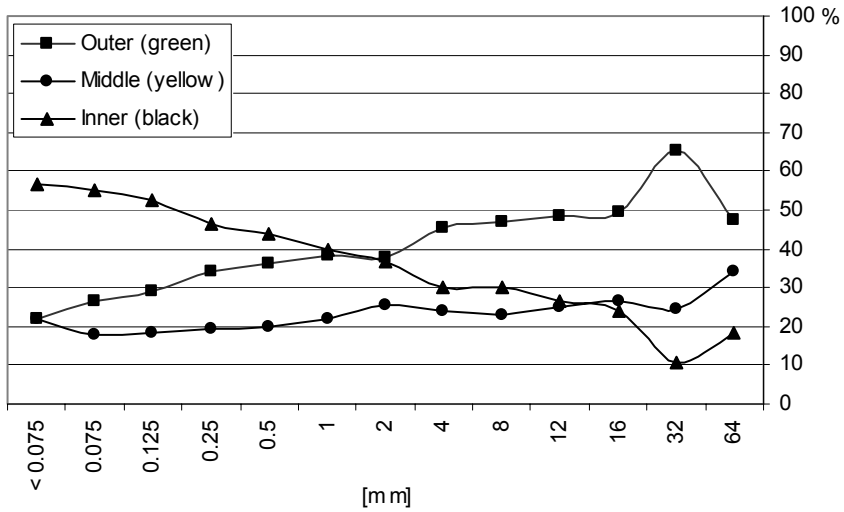

Figure 5.3 Cylinder 2: Percentage of each colour for the fractions.

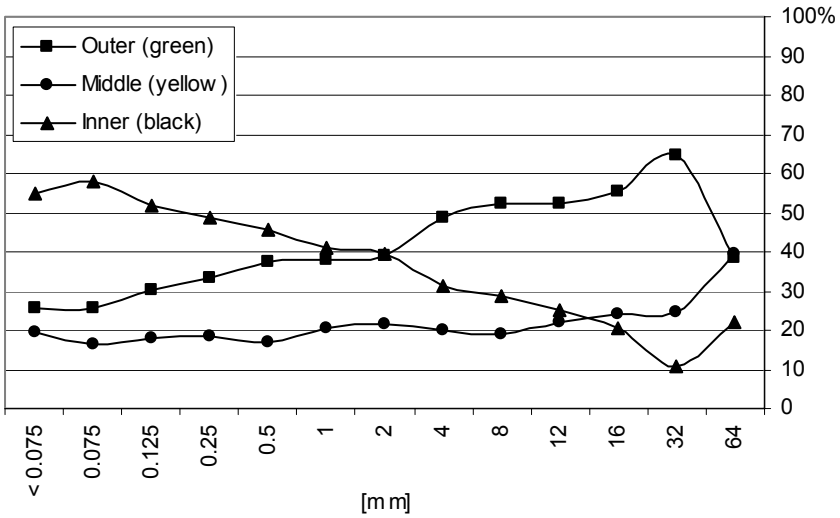

Figure 5.4 Cylinder 3: Percentage of each colour for the fractions.

Comparing the three cylinders shows that the first one has a slightly different fragmentation. The green layer of cylinder 1 is more finely fragmented than that of the other two cylinders, which could be the result of its weaker mortar properties. The cylinders blasted second and third have very similar curves, which is why these two are discussed further.

It was observed that the yellow layers in all three cylinders are not represented in the smaller fractions to the extent that was expected. The amount of yellow is always less than the amount of green, which is natural since the cylinders consist of more green mortar than yellow. However, the amount of yellow is outrun, in the fraction 16 – 32 mm, by the black layer, even though the amount of yellow mortar is almost twice the amount of black. A likely explanation is the few, but very large, pieces in the > 64 mm fraction. Although these pieces had all layers in them, only the yellow one extended intact from the black to the green. These pieces thereby "stole" a great part of the yellow mortar; hence, relatively little was left to be further fragmented and end up in the other fractions.

During the sieving process, it was noticed that for most of the pieces from the > 64 mm fraction, where all three layers were present, both the inner black layer and the outer green layer had been fragmented. The fragmentation of the inner layer was because of the crushing near the explosive, but what caused the fragmentation of the outer layer can be discussed. The most likely explanations are the spalling that might take place when the compressional wave meets the free face, the reflecting wave causing crack initiations in the material, and the radial cracks forming the piece that is finally liberated and thrown against the wall of the container. The spalling of a free face when bench blasting in rock material is a recognised phenomenon (Langefors *et al.* 1963, Jimeno *et al*. 1987, Persson *et al.* 1994). The compressional wave is travelling at an approximate speed of 4000 m/s, which is the average measured V_p for the mortar. The speed of the crack propagation is always less than the speed of the compressional wave, around one fifth to a quarter of it (Persson 1990). It is slower than the Rayleigh wave in the material, which is slightly slower than the shear wave velocity (Ouchterlony 1974). The shear wave velocity is always slower than the compressional wave. It can be concluded that the fragmentation of the green outer layer is a combination of all of these fragmentation mechanisms; it is not just a result of the radial cracks liberating a piece that is thrown into the wall.

The fragmentation described above produces more green pieces in the finer fractions. However, even with these mechanisms acting on the specimen, it can generally be observed that the finer the fractions are, the more the proportion of fragments from the black layer increases. For the green layer, this is reversed. All of this shows that the finer fractions originate from the vicinity of the charged borehole.

It is also of interest to look at the distribution curves for cylinders 2 and 3. These curves (Figures 5.5 and 5.6) give an idea of how much of each colour was present in each fraction. It is important to take this into account because the original amount of each colour was not the same in the cylinders.

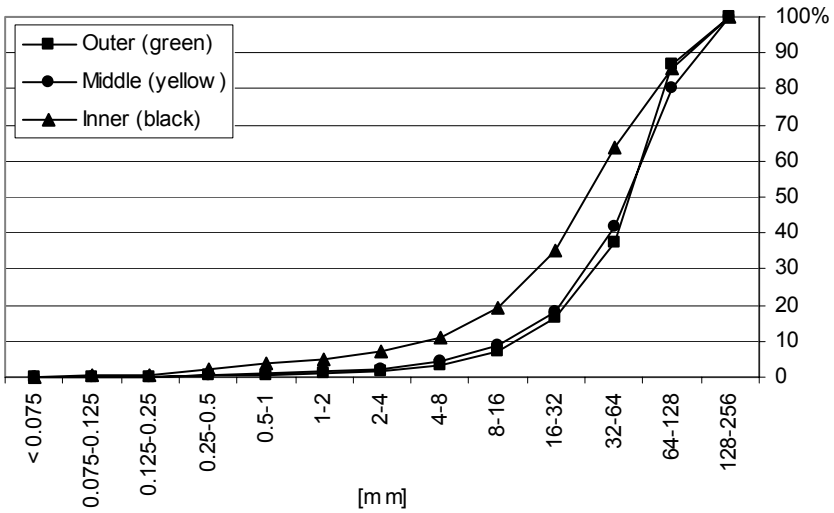

Figure 5.5 Distribution curves för each colour of cylinder 2.

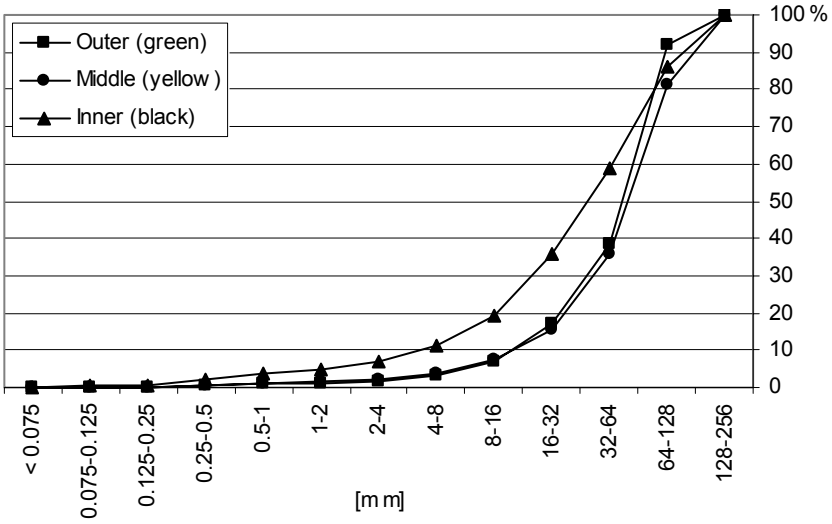

Figure 5.6 Distribution curves för each colour of cylinder 3.

For the fraction < 8 mm, approximately 12 % of the black mortar is found but only about 4 % of the green. When studying finer fractions, such as < 4 mm or < 2 mm, black is still the dominating colour, although the percentages are very small. It should be kept in mind that the test samples all have confidence limits of 2 % or less (Appendix I), for example 12 % ± 2 %, which means that it is hard to draw any solid conclusions if the percentages are too close to one another. However, a clear indication that the black layer is more finely fragmented can be seen in the entire distribution curve.

The results confirm that a great part of the fines do originate from the area surrounding the borehole. This can also be illustrated by plotting the amount of fines for the volume of each layer (Figures 5.7 – 5.9). The values on the x-axis represent the radius of the cylinder, where 0 is the location of the charged borehole and 0.15 is the envelope surface of the cylinder. The values for the layers are given at the radius of the middle point in each layer.

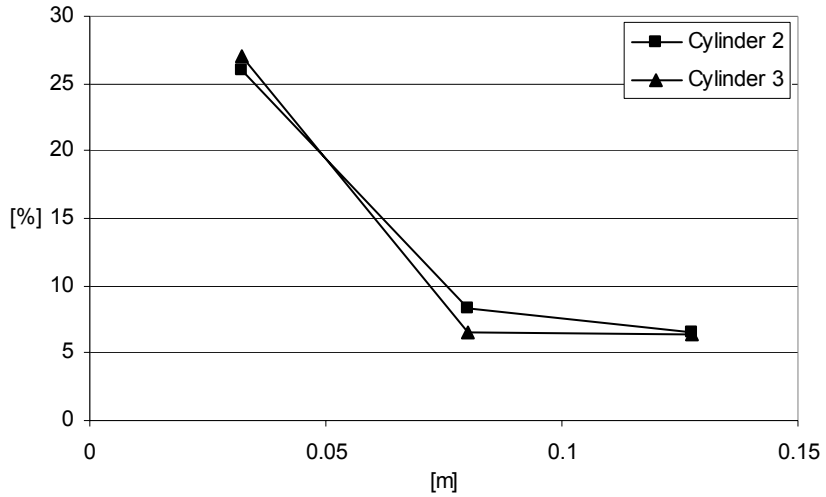

Figure 5.7 The percentage of fines, < 8 mm, for each colour as a function of the distance from the charged borehole for cylinders 2 and 3.

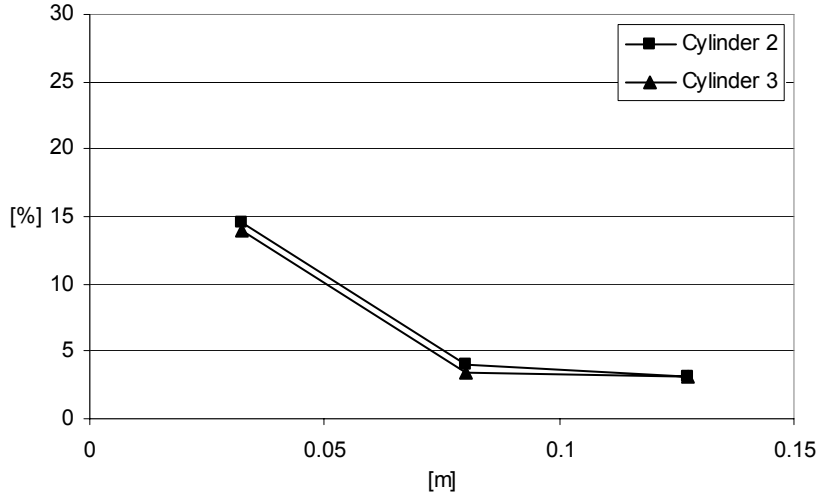

Figure 5.8 The percentage of fines, < 4 mm, for each colour as a function of the distance from the charged borehole for cylinders 2 and 3.

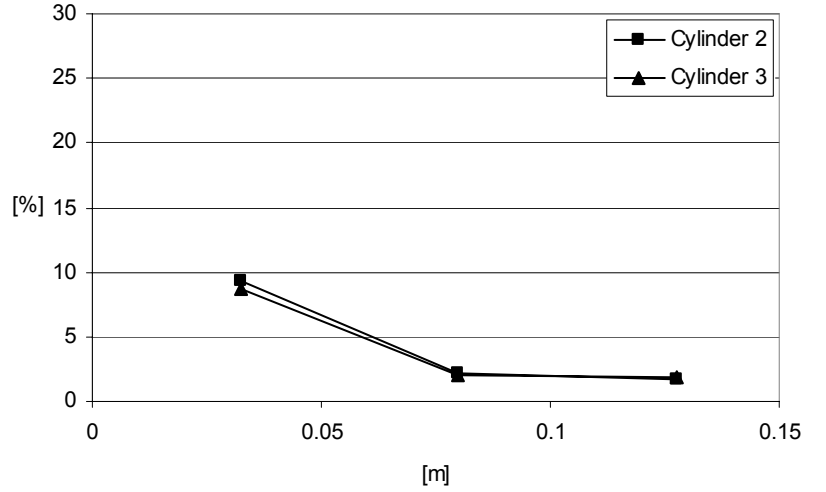

Figure 5.9 The percentage of fines, < 2 mm, for each colour as a function of the distance from the charged borehole for cylinders 2 and 3.

Once again it can be seen that the middle yellow layer and the outer green layer do not differ much in the amount of fines produced. The inner black layer, however, shows a much higher amount of fines, which supports the previous statement.

5.1.2 Crack propagation in thin sections

As it could also be of interest to study the crack formation in remaining mortar pieces, seven thin sections were made to investigate this further. The fragments, from which the thin sections were made, were chosen from the third cylinder; each thin section represents a layer in a specific direction (Figure 3.13).

The first thin section shows the radial crack formation in the inner layer close to the detonating charge. It was studied under a microscope and all cracks were identified. In Figure 5.10 the original thin section can be seen together with one where all cracks are highlighted. The micrograph to the right clearly shows that the crack propagates only in the cement phase and not through any aggregates. By thoroughly investigating every crack, it can be concluded that this is true for all cracks present in this thin section.

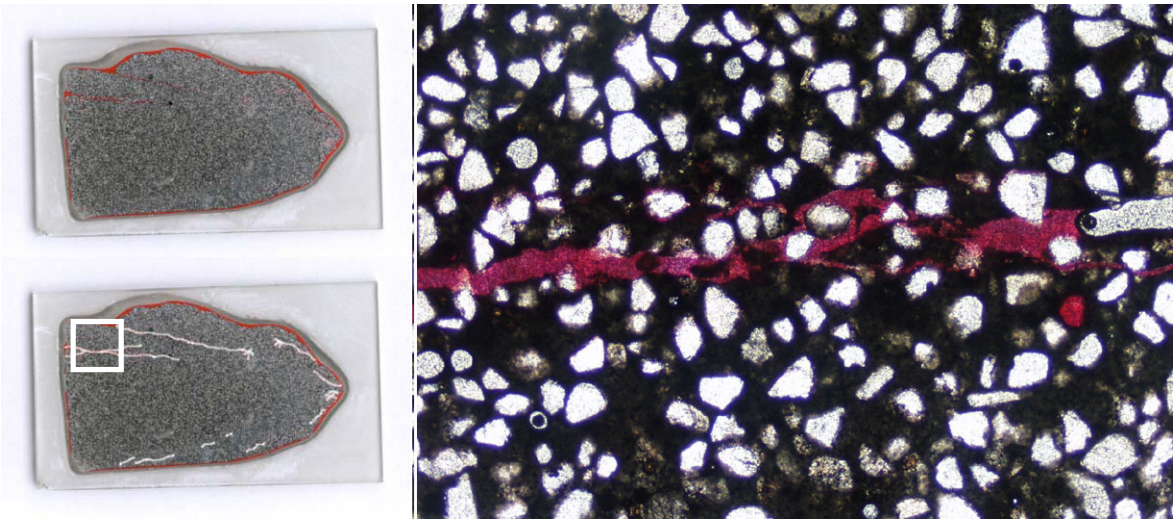

Figure 5.10 Horizontal thin section (no. 1) of the inner, black, layer closest to the detonating charge.

In thin section number two, which is taken from the green outer layer of the same fragment as the first thin section, it is evident that no severe damage has been caused (Figure 5.11). However, the few cracks that could be found propagate in the same way as in the previous thin section: through the cement phase. The fragment from which these two thin sections were made was intact at the envelope surface; this should be kept in mind.

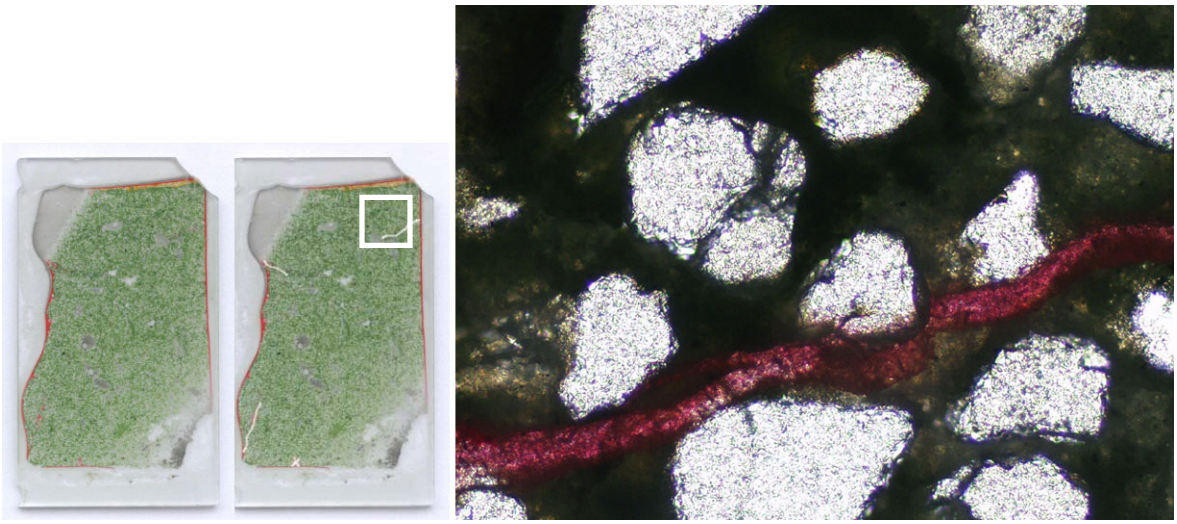

Figure 5.11 Horizontal thin section (no. 2) of the outer, green, mortar layer at the envelope surface of the cylinder.

The third (Figure 5.12) and fourth (Figure 5.13) thin sections, which represent the same fragment as thin sections one and two, are vertical and parallel to the outer surface. The inner layer seems to have been damaged more than the outer one, which is in agreement with the horizontal thin sections. The cracks in the fourth thin section are located at the perimeter, and it is possible that those cracks could have been caused during the production of the thin section. Once again it can be demonstrated that the cracks have propagated exclusively in the cement paste.

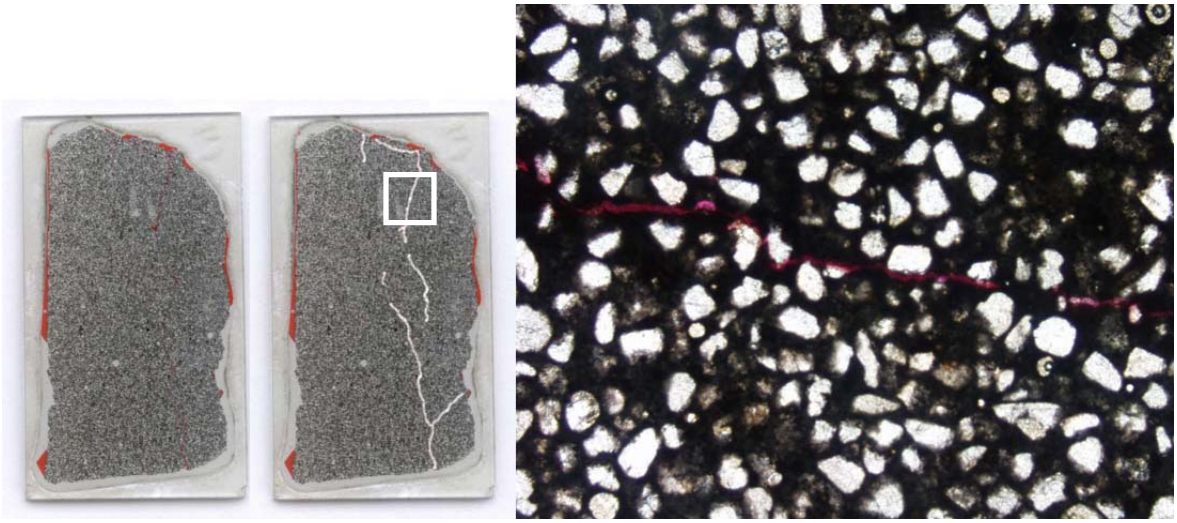

Figure 5.12 Vertical thin section (no. 3) taken from the inner black mortar layer parallel to the envelope surface.

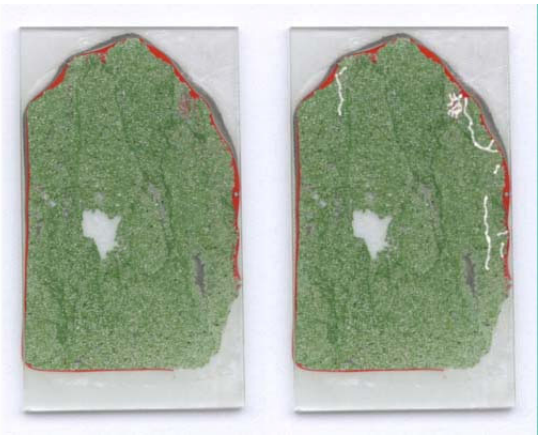

Figure 5.13 Vertical thin section (no. 4) taken from the outer green mortar layer parallel to the envelope surface.

The fifth (Figure 5.14) and sixth (Figure 5.15) thin sections represent a cut vertical and perpendicular to the outer surface in the inner black and outer green layers. These thin sections show, as expected, no damage at all. This is probably due to their location. Up to this point, the damage that has been discovered is most likely the result of radial cracks, and these would be very hard to come across in a cut in the same direction as they are propagating.

Figure 5.14 Vertical thin section (no. 5) taken from the inner black mortar layer perpendicular to the envelope surface.

Figure 5.15 Vertical thin section (no. 6) taken from the outer green mortar layer perpendicular to the outer surface.

The thin section above (Figure 5.15) might look a bit peculiar as there are parts missing. This is due to unsatisfactory mixing of the mortar, which has left aggregates unmixed with the cement. These lumps of quartz grains do not have the strength to hold together, which is why they are easily lost during the preparation of the thin section.

The seventh thin section is, once again, from a horizontal cut in the outer green mortar layer. However, this one is taken from a piece of mortar that has been fragmented at the envelope surface. Figure 5.16 reveals some damage. It is hard to say what source gave rise to these cracks. One possible explanation is the spalling effect that a tensile wave would give; another is the throw that the fragments were subjected to after detonation. This would very likely cause cracks as the fragment struck the wall of the container. No matter what caused the cracks, they seem to have propagated in the same way as the other cracks studied in the thin sections described above.

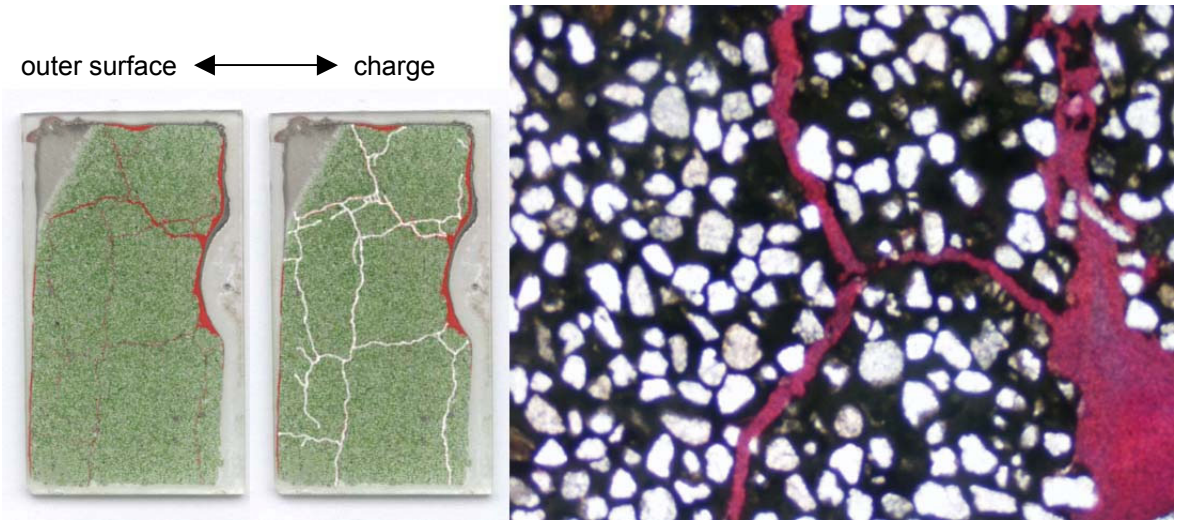

Figure 5.16 Horizontal thin section (no. 7) of the outer, green, mortar layer from a fragment that had been fragmented at the envelope surface.

The thin sections above were made to briefly study the crack propagation. Since it is not possible to identify the source of the cracks, any comments are highly speculative. It is also important to remember that each thin section represents a very small part of the entire cylinder; to be sure of any of the indications that these sections might give, a more thorough investigation needs to be done.

5.2 HALF-SCALE BLASTS

5.2.1 Bårarp test blasts

After blasting and sieving, all data were collected and summarized in six cumulative size distribution curves (rounds 1 - 4 Olsson 2002; all blasts are to be published in SveBeFo Report 60 by Mats Olsson in 2003), one for each test blast (Figure 5.17).

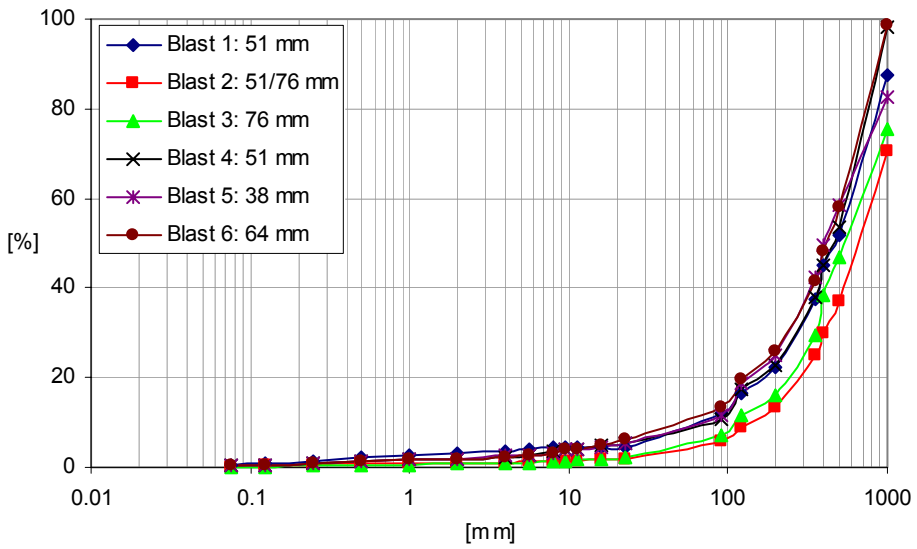

Figure 5.17 Cumulative size distribution curves for all six test blasts in Bårarp (blasts 1-4 Olsson 2002; all blasts are to be published in SveBeFo Report 60 by Mats Olsson in 2003).

The least fragmented of all six test blasts is, not very surprisingly, the decoupled round. That is also according to the project hypothesis. Tests made by Olsson *et al.* (2001) have clearly pointed out that the length of blast-induced cracks around boreholes is reduced when decoupled charges are used. It has long been believed that decoupling leads to less fragmentation and, thereby, also less fines. The 0 - 8 mm fraction is only 1.3 %. However, the size distributions also reveal another, not expected, finding: among the fully coupled rounds, it is the one with the largest boreholes that gives the coarsest fragmentation. The general opinion so far has been that the smaller the boreholes, the coarser the fragmentation. As previously mentioned in Chapter 2, there are research projects that have established this in full-scale blasts; however this one indicates the opposite. Since the distribution curves for the rest of the test blasts are hard to distinguish from one another, they were plotted in a log-log diagram (Figure 5.18).

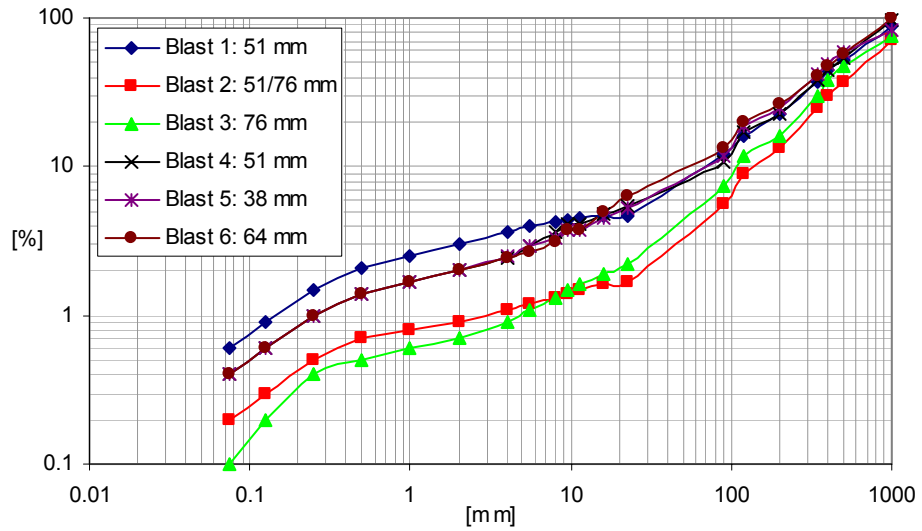

Figure 5.18 Cumulative distribution curves in a log-log diagram (blast 1-4 Olsson 2002; all blasts are to be published in SveBeFo Report 60 by Mats Olsson in 2003).

This diagram separates the different fragmentation results more clearly, especially in the finer fractions. Once again, it can be seen that the decoupled and 76 mm rounds produce less fines. Among the others it is hard to see any difference between them down to 10 mm. At approximately 15 mm, the curves from blasts 4 - 6 and blast 1 seem to cross and become reversed. This is also evident for the decoupled blast and the 76 mm test blast. The only resonable explanation for this is the change of sieving procedure for fractions below 22.4 mm. These fractions are the ones that have been test sampled and sieved under laboratory conditions.

As the blasting site was changed after three blasts it could also be of interest to separate the first three rounds (Figure 5.19) from the last three (Figure 5.20). In this way it would be possible to detect any changes in fragmentation due to the geology. The assumption was that the geological conditions were the same for the two sites; however this was confirmed with neither mapping nor testing of rock parameters.

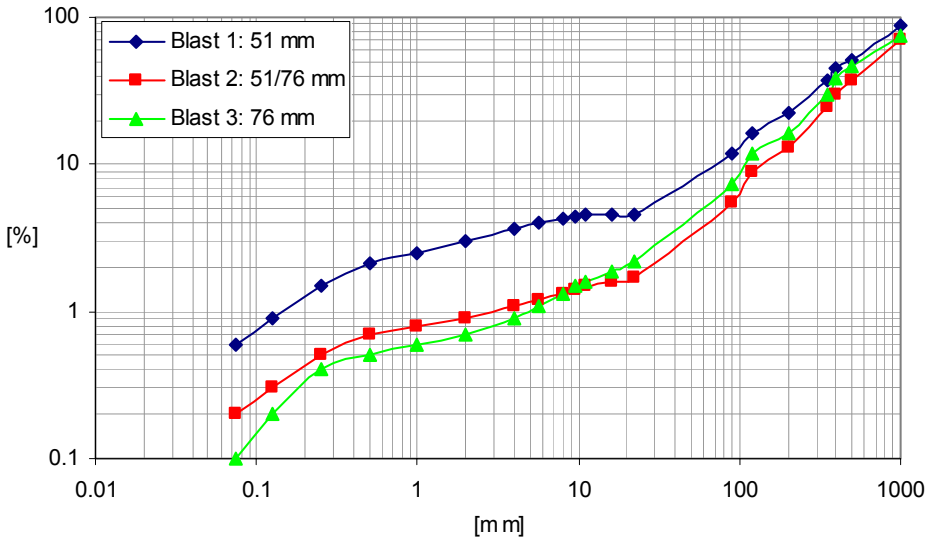

Figure 5.19 Cumulative size distribution curves for the first three test blasts in a log-log diagram (Olsson 2002).

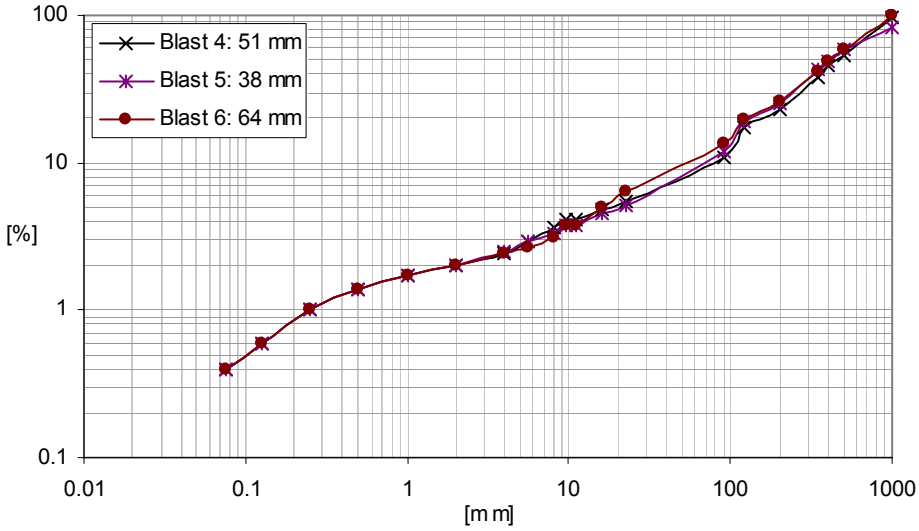

Figure 5.20 Cumulative size distribution curves for the last three test blasts in a log-log diagram (blast 4 Olsson 2002; all blasts are to be published in SveBeFo Report 60 by Mats Olsson in 2003).

It is worth mentioning that the last three rounds show very little difference, although they have a wide variation in borehole diameter. Looking at the two 51 mm rounds, which were expected to be identical, reveals that this is nearly so (Figure 5.21).

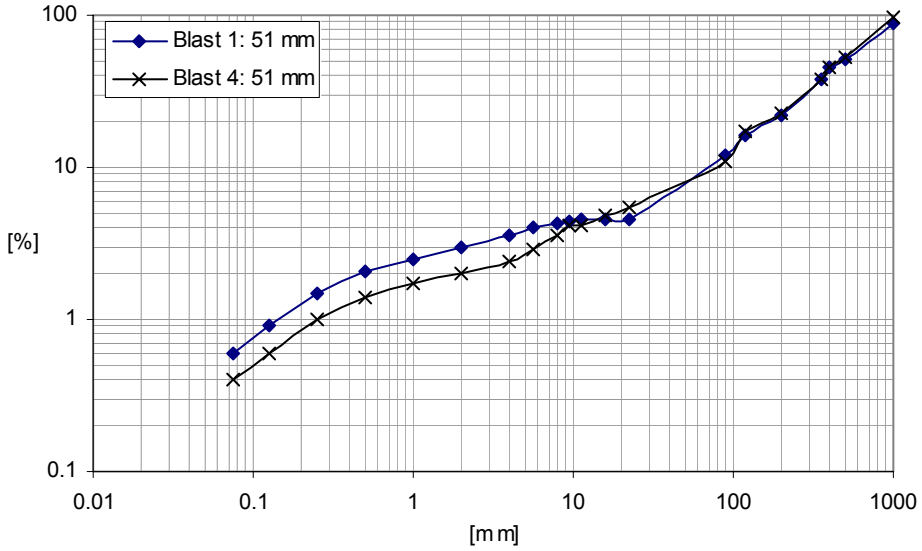

Figure 5.21 Cumulative size distribution curves for the blasts with 51 mm boreholes in a log-log diagram (Olsson 2002).

The two blasts with 51 mm boreholes that are almost identical show a very similar curve in the coarser fractions; however below 15 mm they also cross. Studying the smaller fractions shows that the fragmentation at the first test site is a bit coarser than that at the second. The crossing curves (Figure 5.18) indicate that, if the sieving process is not the explanation for it, perhaps the site, and the geological conditions, could be.

5.2.2 Rock quality

The rock quality parameters that were tested were density, average flakiness, impact value and abrasion value (to be published in SveBeFo Report 60 by Mats Olsson in 2003)(Table 5.1).

Table 5.1 Rock quality parameters for the fragmented Bårarp gneiss

Blast	Density [kg/m^3]	Average flakiness [weight%]	Impact value [weight%]	Abrasion value [cm^3]
1	2.67	1.46	-*	-*
2	2.67	1.41	-*	-*
3	2.67	1.42	-*	-*
4	2.67	1.42	59	17.2
5	2.67	1.37	56	16.7
6	2.66	1.36	56	15.4

*The missing parameters are due to an insufficient amount of test material.

All parameters resemble those previously presented in Chapter 4, except for the abrasion value. This value is 5 - 6 times as large as in the investigation conducted by Lundqvist *et al*. (1998). An explanation could be that Lundqvist *et al.* (1998) made their tests on blasted and crushed aggregates, whereas here the testing followed blasting alone. A likely

difference would be that the quality of the material will improve during the crushing procedure, and the abrasion value improves.

6 DISCUSSION

The results presented in Chapter 5 clearly show that most fines are produced in the near vicinity of a borehole for the model-scale tests that were performed in mortar. However, the results cannot, without careful consideration, be applied to rock. This chapter begins with a discussion of how the results may be transposed to a rock-blasting situation. Thereafter, the model-scale test and half-scale blasts are analysed and an attempt is made to bring the results together.

6.1 CAN THE RESULTS BE APPLIED TO ROCK?

6.1.1 The model material and its properties

The material must be of importance when working with blasting experiments, but it is not yet fully understood what properties should be considered when choosing the model material. Very often the most convenient and easily handeled model material is used. Most of the time it is the objective of the research that guides the choice; for example, when studying crack propagation the best material to use is one for which the cracks can easily be studied after the blast. Thus, one can find that this kind of research is often done with glass or plastic materials; these visualise the crack propagation very effectively.

It would be a mistake to say that the results from model-scale blasts can easily be compared to any rock type. It is closer to the truth to state that the results could resemble some types of rock and the way they would behave. When conducting model-scale blasts the aim should be to choose the material and geometry so that the tests resemble, as much as possible, the real production blast. The question is: How can this be done? Scaling methods are one solution, but in the end, the most important criterion for the selection of material is that the mechanical behaviour of the artificial rock should be similar to that of natural rock (Tien *et al.* 2000). The five most important properties of the material were stated by Tien *et al.* (2000) to be: the uniaxial compression strength (UCS), Young's modulus, the Poisson ratio, the cohesion, and the friction angle. This is quite a few parameters in comparison with what can be included in a dimensional analysis. If possible, the most desirable approach would be to perform the tests in both a model material and in rock for comparison, so that more can be learned about the comparability of different materials. Surprisingly, Langefors (Naarttijärvi 1978) found that model-scale blasts in rock did not at all represent the crack propagation or fragmentation that would occur in production-scale blasts; he concluded that rock is an unsuitable model material to use for studying fragmentation mechanisms in production-scale rock blasts. This finding was based on an empirical equation by which the amount of explosive could be calculated by knowing the burden. The equation was developed for Swedish bedrock. It was found that the specific charge increased considerably when the geometrical scale decreased. Also, the crack pattern from some model tests in limestone did not look anything like crack propagation in larger scale.

Aspects that are seldom considered when working in smaller scale are the inhomogenous nature of rock, reflections from boundaries, and the static stress field (Naarttijärvi 1978). In the past, the choice of material has often been based on a "feeling" that the model material behaves quite like rock material would. Naarttijärvi (1978) summarized several model-scale tests performed between 1959 and 1976 and found that the material with which the test blasts had been conducted, varied considerably, from glass and plastic materials, such as Homalite and Plexiglas, to cement. Not only does the material vary, but also the shape of the specimens, which can often be explained by the objective of the blasts. The most

common shape to be used is the block, either homogenous or consisting of slabs jointed together.

Kristiansen *et al.* (1990) blasted several cubical samples of concrete, larvikite and gneiss, all with the specific charge of 0.625 kg/m^3. Concrete was thought to be a good model material, as it has a density and P-wave velocity similar to rock. The resulting particle size distribution showed that the concrete gave a finer fragmentation than either the larvikite or gneiss samples, however the shape of the distribution curves was similar. Hence, it was concluded that concrete could be used as a rock-like material for further blasting experiments, even though the absolute value of the amount of each fraction was not representative for rock material.

The first parameter to be considered when choosing the model material is often the strength. Crater tests in mortar showed that a test specimen with a higher strength was more easily fragmented and thereby gave more pieces than one with 50 % lower strength. The fragments were also thrown much further (Honma 1990). Small-scale blasts in concrete conducted by Armstrong *et al.* (1993) aimed at investigating the mean fragmentation size and face velocity with increasing confinement. The results indicated that the trend of the fragmentation was independent of the strength of the concrete. This demonstrates what is sometimes also believed for the dimensional analysis (Section 2.4.1): the strength parameter should be kept the same in model-scale blasts as in full scale. Unfortunately, it is hard to find a material with a rock-like matrix and a compressive strength in the magnitude of 200 MPa.

Another approach, classifying blasting resistance by using a "blastability coefficient" has been suggested by Hino (1959), (see Mäki 1983). The coefficient is defined as the ratio of the compressive to the tensile strength. The compressive and tensile strength ratio for some rock types, as well as Plexiglas, was put together by Ash (1969), (reported by Rustan 1981). It can be observed in Table 6.1 that although Plexiglas shows a completely different behaviour, it has nevertheless been a valuable model material for studying fragmentation mechanisms. In comparison, concrete could be considered a more rock-like material when studying this ratio.

Table 6.1 Compressive/tensile strength ratio and shear/tensile strength ratio for rock and other model materials (Rustan 1981)

Model material	σ_c/σ_t	σ_s/σ_t
Dolomite	41	34
Granite	10	5
Hydrostone	3.6	3
Concrete	20	4.4
Plexiglas	1.5	0.72
Sandstone*	3.8	-

*Calculated from Johnson *et al.* (1988)

In the model tests conducted in this project the parameter taken into account was the compressive strength of the concrete, and the aim was to use a rock-like matrix. This was obtained with mortar and by choosing aggregate particles with a maximum size of 0.5 mm. Also, the ratio of the compressive strength and the tensile strength was chosen to be similar to rock. The ratio for the model-scale specimens is in the range of 9 – 12, while for the Bårarp granite it is approximatelly 18. A low porosity was also wanted; this was a natural aspect of designing the high strength mortar.

6.1.2 The shape of the specimen

The significance of specimen shapes was tested when the search for a new material to test explosives began in the beginning of the 1980s (Vestre 1992). A cube, a sphere and a cylinder in concrete were blasted and the distribution curves were compared. The cube and the sphere behaved quite similarly even though the cube gave a finer fragmentation. The cylinder, however, differed slightly in behaviour from the other two. The differences in fragmentation are most likely due to the boundary conditions. In the research that followed, the cube was chosen, as this was the only shape that was possible to extract from rock. Three cube sizes were blasted, with the same specific charge, and the evaluation showed that the largest cube gave more fines, and larger pieces, than the smaller ones. This supports the theory that it is the amount of explosives per area of borehole that strongly affects the fines generation (Kristiansen 1995a). As the area around the borehole is crushed, a large amount of the energy is consumed, and little is left to fragment the rest of the material; this means fewer intermediate particles.

Since the different shapes seem to be fragmentated in a similar way, the most critical choice does not seem to be which shape to use. Boundaries will always make the fragmentation a bit more complicated, but the results may still be valid. Without a proper confinement it would hardly be possible to model the situation anyway.

In the model-scale tests conducted, the cylinder shape was a natural choice because it was desirable to have the same amount of free surface all around the specimen. This also reduced the risk of generating complicated reflection patterns. With a cube, some parts of the wave would have been reflected towards a flat surface and some towards a corner. With a cylinder, all travelling waves would hit a surface normal to their direction and be reflected back in the same direction from which they came.

6.1.3 Loading rate

Mohanty (1987) found that a variety of rocks could withstand repeated shock loading up to five times their static strength. The strength for granite at different strain rates indicates an increase in strength by a factor two from normal laboratory strength measurement conditions to those prevailing in a shock wave (Persson *et al.* 1970). This may mean that the dynamic strength can be considered more relevant when characterising the behaviour of rock during blasting. It was also noted by Grady *et al.* (1980) that the strength properties seemed to be proportional to the strain rate in a variety of rocks (see Mohanty 1987).

With fast loading rates, as in blasting, the material resists breakage (in crushing and grinding) more easily because there is not time for the stress to find the weakest and fastest zones to escape through (Bond 1952). In 1971 Mellor and Hawkes investigated the influence of the loading rate on the Brazilian tensile strength (Mäki 1983). The results indicate that the tensile strength is little affected by loading rates less than 0.1 cm/minute. However, in blasting the loading period is less than 0.01 ms (for fully coupled charges) and the relationship between compressive strength and loading rate cannot be accurately defined (Hagan 1973). This relationship can differ from one rock type to another. Rock types with low porosity, such as andesite, granite and marble, are less likely to contract as the compressive load becomes higher. Rock with high porosity, such as sandstone and limestone, contract much more easily, and stress waves are quickly and extensively decayed in their transmission. The strain rate dependence of rock strength for two types of granitic rocks (granite and andesite) is also different (Masuda 2001), but typically the increase in strength was 5 to 10 % per tenfold increase in strain rate. Thus, the rock becomes more resistant to dynamic crack propagation as the loading rate increases (Zhang

et al. 1999). The failure strength of granitic rocks decreased linearly as the logarithm of the strain rate decreased (Masuda 2001).

In dry concrete the strength also increases significantly when the strain rate rises (Ross *et al.* 1996). Wet concrete give a slightly better strength (both compressive and tensile) under high strain rate loading. The strain rate effect is more apparent on the failure strength of wet rock samples in the lower confing pressure range (≈ 0.1 MPa).

Both rock material and mortar show a significant rise in strength when the loading rate is as fast as in blasting. The increase for both materials is approximately a factor two. The behaviour of the two materials is thus strongly related.

6.1.4 Variation in fines generation

To conclude the comparison between mortar as a model material and rock, the material to be studied, it can be stated that they have several properties in common, therefore they show similar fragmentation behaviour. The strength, which is often thought of first, is, however, not comparable. If the results are not looked upon as absolute values, then this is not critical. The objective with models, in general, is to study a mechanism and for that, this cement matrix material seems to work. The scaling effect cannot be overlooked, however. Previously mentioned research indicated, suprisingly, that small-scale models in rock did not give an accurate picture of crack propagation in full scale rock blasting (Naarttijärvi 1978). It would be desirable to study the scaling effects further.

When it comes to the generation of fines, there is a possibility that the mortar might give a false picture. When the sieving took place, it was first noticed that the material was so brittle that it started to fall apart very easily during the handling of the fragmented product: consequently, the traditional laboratory sieving equipment was abandoned. It is likely that the blasting, transport and sieving of the mortar increased the amount of fines. However, since all specimens were treated the same, they should be comparable, and then the trends are still correct.

Another aspect of using mortar as a model material is the lack of geological features. There are no cracks, joints or discontinuities apart from voids that might resamble a sedimentary rock texture. However, the model-scale tests aim at studying the small area closest to the borehole, where the effect of discontinuities is probably of minor importance.

In a characteristic magmatic rock, the mineralogy is a critical factor. Some minerals, e.g. amphibole, can act as reinforcement and make the rock more difficult to blast, while others, e.g. micas, may act as initiators of cracks or energy absorbers. Micas, for example, could even be a major source of fines as they are brittle and an easily fractured material. Today, little is known about how different minerals affect the blasting mechanisms; working in a model material such as mortar will not bring us closer to the truth about this. For studying specific mechanisms, however, where as many parameters as possible are held constant, mortar in specimens of various shapes is an acceptable choice.

6.1.5 Crack propagation

The thin sections of the mortar shown in Chapter 5 revealed how the cracks inside the cement matrix had propagated. In the areas studied, the cracks had run exclusively through the cement paste and not through any of the aggregates, quartz grains of maximum size 0.5 mm. This means that the cracks followed the path of least resistance, which is probably in agreement with most other materials. However, even if crystalline rock material is a matrix of different aggregates, they often have more than two strengths; mortar has only two (cement and quartz grains). Thus, the mortar is closer to a sandstone, consisting of

well-sorted quartz grains cemented together, than to a magmatic rock. Another aspect is whether the grains play a role or not. The crack propagation in concrete is highly dependent on the rate of loading. The path of a single crack varies with increasing stress rate in such way that fewer bond fractures occur and more aggregate patricles fracture (Zielinski 1982). Hence, where the aggregates are large, the crack pattern differs widely for static loading and impact loading: for the latter the cracks propagate right through the cement matrix as well as the aggregates. This was true for mortar; perhaps the same goes for the rock material. Maybe the loading rate is enough for the cracks to develop in the same way in granite and gabbro as in mortar. If this is true, then studying the crack propagation is of minor importance when it comes to fines generation, while taking into account the different minerals and their characteristics becomes more important.

Kutter studied crack patterns in both rock and a model material, Plexiglas (Naarttijärvi 1978). He found that the pattern looked the same, but the length of the cracks varied. This supports the previous statement. Another finding was that the propagation in rock is affected by cracks, foliation and discontinuites. In the close vicinity of existing cracks no new cracks are formed, although formation does seem to continue in the weaknesses. It is difficult for cracks to pass through old cracks: they seem instead to propagate parallel with and close to the old ones, as the strength is locally decreased there. This is something few researchers have taken into account (Naarttijärvi 1978). Cracks in general seem to propagate in the direction of greatest stress. Kutter (Naarttijärvi 1978) found this to be a very dominant factor which could even eliminate the effect of existing cracks.

6.2 MODEL-SCALE BLASTS

The results from the model-scale blasts, presented in the previous chapter, indicate that the crushing near a borehole is a major source of fines, no matter what sizes are considered (0 - 2, 0 - 4 or 0 - 8 mm). The unbroken line, in Figures 6.1 – 6.3, is a regression curve fitted to the data (Appendix II). From studying this curve, one can suppose that two fragmentation mechanisms are involved; one constant part, represented by the first term in the regression curve equation, and one varying with the distance to the borehole (the second term).

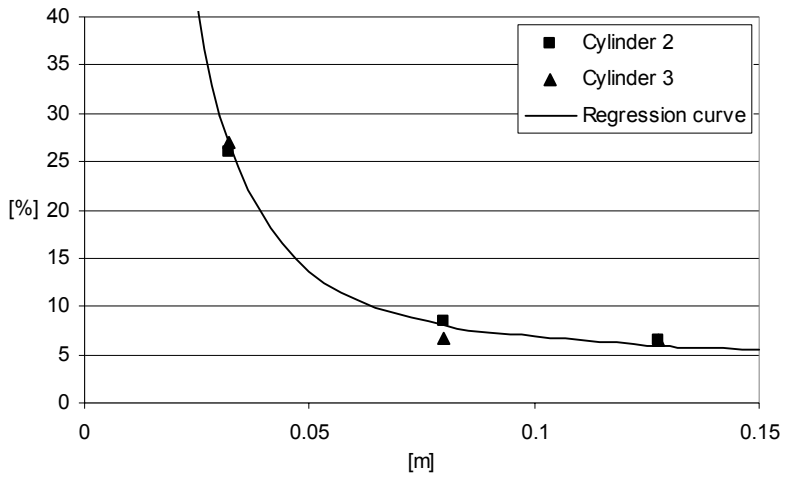

Figure 6.1 The percentage of fines, < 8 mm, as a function of the distance from the charged borehole, for cylinders 2 and 3. The curve is the calculated regression curve, $y = 4.56 + 0.023(1/x^2)$ (Appendix II). R^2 for the regression line is 99.7.

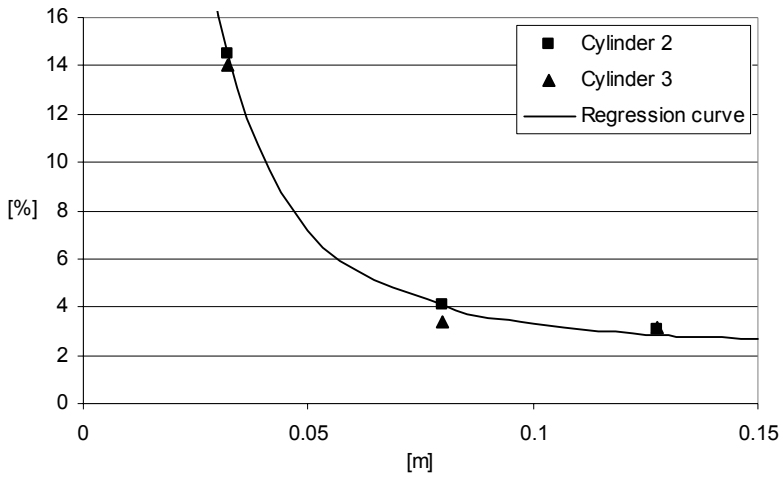

Figure 6.2 The percentage of fines, < 4 mm, as a function of the distance from the charged borehole, for cylinders 2 and 3. The curve is the calculated regression curve, $y = 2.09 + 0.013(1 / x^2)$ (Appendix II). R^2 for the regression line is 99.8.

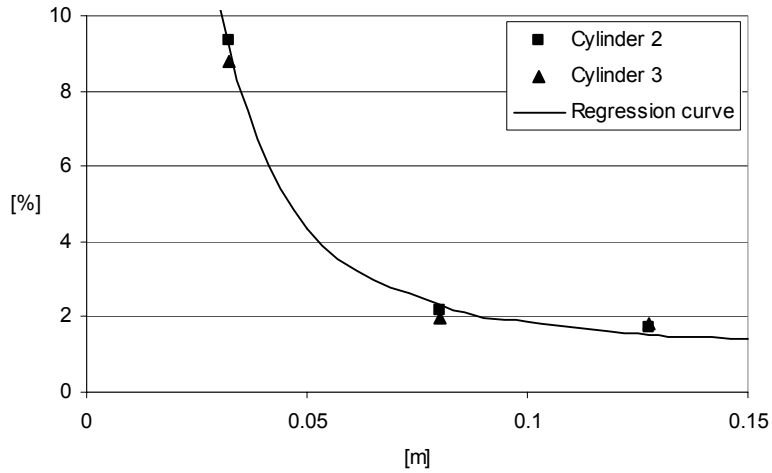

Figure 6.3 The percentage of fines, < 2 mm, as a function of the distance from the charged borehole, for cylinders 2 and 3. The curve is the calculated regression curve, $y = 1.02 + 0.008(1 / x^2)$ (Appendix II). R^2 for the regression line is 99.6.

The first term would represent a "general" fragmentation that could have occurred anywhere between the borehole and the material surrounding it. Possibly this could be an effect of crack propagation and movement of the material. The amount represented by the variable is, then, the fines caused by the crushing in the vicinity of the borehole. However, this hypothesis is based on only three layers within a 600 mm diameter mortar cylinder, which makes it speculative. Nevertheless, it is an interesting observation, since it would mean that the crushing mechanism does not cause all of the fines and another source needs to be identified to account for the rest.

6.3 HALF-SCALE BLASTS

6.3.1 Correlation analysis

A correlation analysis was made between the amount of fines (0 - 8 mm) and several blasting parameters for the six rounds at Bårarp (Table 6.2). The correlation coefficients were calculated as follows:

$$\rho_{x,y} = \frac{Cov(X,Y)}{\sigma_x \cdot \sigma_y} \qquad -1 \le \rho_{x,y} \le 1 \tag{6.1}$$

$$Cov(X,Y) = \frac{1}{n} \sum_{j=1}^{n} (x_j - \bar{x})(y_j - \bar{y}) \tag{6.2}$$

where $\rho_{x,y}$ = correlation coefficient
σ_x = standard deviation for sample series x
σ_y = standard deviation for sample series y
n = number of samples
$\bar{x}$ = mean value for sample series x
$\bar{y}$ = mean value for sample series y

Table 6.2 Correlation coefficients for the amount of fines (0 - 8 mm) and several blasting parameters, at Bårarp

Parameter	$\rho_{x,y}$	**Parameter**	$\rho_{x,y}$
Burden	-0.53	Total charge length	0.54
Spacing	-0.52	Number of cartridges	0.53
Bench height	0.47	Charge weight per hole	-0.51
Hole depth (real)	0.09	Total charge weight	-0.43
Hole diameter	**-0.87**	Theoretical hole volume	-0.54
Number of holes	0.50	Linear charge concentration	-0.56
Theoretical volume	-0.38	Percentage of filling	-0.31
Cartridge diameter	-0.52	Stemming length	-0.67
Cartridge weight	-0.53	Number of detonating holes	0.34
Charged diameter	-0.52	Detonated charge weight	-0.51
Coupling ratio	0.60	Specific charge per hole	0.40
Charge length of hole	0.56	Specific charge	-0.50
Cartridges per hole	0.35	Charge weight / area charged borehole	-0.21

No clear correlation can be found, except perhaps for the borehole diameter. However, when this coefficient was calculated, the second decoupled round was included, which is not entirely correct to do. With this round removed, the correlation coefficient becomes - 0.80, which makes the relationship weaker; a stronger relationship would have been more understandable. Appendix III contains all the tested parameters and their values.

6.3.2 The amount of fines as a function of the distance from the borehole

When making the regression analysis on the data from the model-scale tests (Appendix II), it was found that the amount of fines is inversely proportional to the square of the distance from the borehole.

$$M_f = M_0 + c \cdot \frac{1}{x^2} \tag{6.3}$$

where M_f = amount of fines from the area surrounding a borehole [%]
M_0 = amount of fines from a "general" fragmentation [%]
c = constant [m^2]
x = distance from the centre of the borehole [m]

M_0 is a general fragmentation, that occurs anywhere in the material, and it depends only on the size of the rock mass to be blasted. In the search for a more detailed relation between the amount of fines and the distance from the borehole this term is therefore not included in the following equations.

The mass of fines generated between the borehole, and half the borehole spacing or the burden (the mass to be fragmented) depends on the mass of the rock mass.

$$m_{fines} = M_f \cdot m_{rock} \tag{6.4}$$

where m_{fines} = mass of fines [kg]
m_{rock} = mass of rock mass [kg]

The rock mass to be fragmented is decided by the density of the rock and the distance from the borehole.

$$m_{rock} = \rho \cdot 2\pi \cdot x \cdot dx \tag{6.5}$$

where ρ = density of rock material [kg/m^3]

Equations 6.3 - 6.5 give the mass of fines.

$$m_{fines} = \frac{c}{x^2} \cdot \rho \cdot 2\pi \cdot x \cdot dx \tag{6.6}$$

The amount of fines is the proportion of the rock mass that is below a given fraction, e.g. < 8 mm.

$$M_f = \frac{m_{fines}}{m_{rock}} = \frac{\frac{c}{x^2} \cdot \rho \cdot 2\pi \cdot x \cdot dx}{\rho \cdot \pi \cdot R_0^{\,2}} \qquad r_b << R_0 \tag{6.7}$$

where r_b = radius of borehole [m]
R_0 = the distance from the borehole (to be fragmented), i.e. the burden or half of the borehole spacing

Integration gives the amount of fines as a function of the borehole radius.

$$M_f = \frac{2 \cdot c}{R_0^{\,2}} \cdot \int_{r_b}^{R_0} \frac{1}{x} dx = \frac{2 \cdot c}{R_0^{\,2}} \cdot \ln \frac{R_0}{r_b} \tag{6.8}$$

If the amount of fines is assumed to be approximately proportional to the energy in the borehole, then the fines are also proportional to the size of the borehole, i.e. the squared radius.

$$M_f \propto E_0 \qquad E_0 \propto c_1 \cdot r_b^{\,2} \tag{6.9}$$

where E_0 = energy [J]
c_1 = constant [J/m^2]

$$M_f = \frac{c_2 \cdot r_b^{\,2}}{R_0^{\,2}} \cdot \ln \frac{R_o}{r_b} \tag{6.10}$$

where c_2 = constant [-]

The amount of fines depend on both the borehole radius and the distance that needs to be fragmented. Also, the constant c_2 is related to site-specific parameters such as geometrical, detonic and material properties. It is, however, not possible to further investigate what the constant looks like in detail from the tests conducted in this project.

The constant c_2 can be assumed to be the same for all the Bårarp round as these were performed under similar conditions. It is therefore of interest to study the rest of equation 6.10. By summarising the borehole diameters ($2r_b$) and the borehole spacings ($2R_0$) for the six Bårarp rounds (Table 6.3) and entering them into equation 6.10, it can be seen that the final values are quite similar for all blasts. The second round is not easily evaluated as the conditions are slightly different due to decoupling. According to the model above, this would mean that no difference in the amount of fines should be expected. Looking back at Figure 5.20 this explains why there is no difference in the fines generation between the last three rounds. If the first three rounds are examined (Figure 5.19), and the second decoupled round is excluded, there is, however, a difference in the fines generation.

Table 6.3 The parameters r_b and R_0 for the six Bårarp rounds

Blast	**Borehole diameter ($2r_b$) [mm]**	**Hole spacing ($2R_0$) [mm]**	$\frac{r_b^{\,2}}{R_0^{\,2}} \cdot \ln \frac{R_0}{r_b}$	**Amount of fines (0 – 8 mm) [%]**
1	51	2100	0.0022	4.3
2	51/76	2100	0.0022/0.0043	1.3
3	76	3400	0.0019	1.3
4	51	2200	0.0020	3.6
5	38	1650	0.0020	3.3
6	64	2850	0.0019	3.1

The indication that there should not be any difference in the fines generation can perhaps be explained with the specific charge. The specific charge was kept constant in all of the Bårarp rounds and consequently this makes equation 6.10 constant.

$$q = \frac{m_{ex}}{V_{rock}} = \frac{\rho_{ex} \cdot V_{ex}}{V_{rock}} = \frac{c_3 \cdot \pi \cdot r_b^{\,2}}{\pi \cdot R_0^{\,2}} = c_3 \cdot \frac{r_b^{\,2}}{R_0^{\,2}} = c_4 \tag{6.11}$$

where q = specific charge [kg/m^3]
m_{ex} = mass of explosive [kg]
V_{rock} = volume of rock [m^3]
ρ_{ex} = density of explosive [kg/m^3]
V_{ex} = volume of explosive [m^3]

The amount of fines from the fully coupled Bårarp rounds is approximately the same for the two sites.

$$M_f = c_5$$

where c_5 = constant [-] (6.12)

The model presented above is a way of looking at the crushing phenomenon; however, it does not take into account properties of the explosive, such as the VOD, or geological conditions. These are properties that should be included in the site-specific constants. The VOD for example, most likely affects the crushing of the rock, and the generation of fines, since it controls the loading rate. Also, the pressure is not as high with a lower VOD which generates a smaller shock wave. Although the same amount of energy might be generated by two different explosives, the way it is distributed within the rock mass is also important.

6.3.3 From *in situ* rock mass to fragmented muckpile

The specific surface of the *in situ* rock mass was established in two ways. The first, and perhaps most reliable, was the surface area of all cracks that had been identified during the mapping process, which was easily calculated since the length and dip had been measured. The difficult part was to know how deep into the bench the cracks went; after studying the data from the five drilled rock cores, the cracks were divided into three groups: one was cracks going through the entire rock mass, another was the depth of half the bench height (2.5 m) and the third was the cracks considered to be shallow (1 m). Appendix IV gives the calculations. The second way to calculate the surface area is by using the sieving curve. Since an *in situ* distribution curve was determined by modelling, it could be used for this. For the modelling, however, some simplifications were made; hence, the resulting surface calculation cannot be considered as reliable as the previously described one. The calculations were made by using a technique developed by Gustafson (1983).

The specific surface is defined as the ratio of the area of a particle and its volume.

$$S_{spec} = \frac{A_{particle}}{V_{particle}} \tag{6.13}$$

where S_{spec} = specific surface for a particle [m^2/m^3]
$A_{particle}$ = surface area of the particle [m^2]
$V_{particle}$ = volume of the particle [m^3]

It is essential to know the particle shape to be able to conduct this calculation. The particle is assumed to be spherical.

$$S_{spec,sphere} = \frac{4 \cdot \pi \cdot d^2 \cdot 3 \cdot 8}{4 \cdot 4 \cdot \pi \cdot d^3} = \frac{6}{d} = \frac{\alpha}{d} \tag{6.14}$$

where $S_{spec,sphere}$ = specific surface for a particle of spherical shape [m^2/m^3]
d = diameter of the sphere [m]
α = particle shape factor [-]

The mass of a fraction from a sample of particles can be expressed with the aid of an accumulated sieving curve (Figure 6.4).

$$dM = M \cdot f(d) \cdot dd \tag{6.15}$$

where dM = the mass of a fraction [kg]
M = mass of the entire sample [kg]
$f(d)$ = frequency function for the sample
dd = the considered fraction [mm]

The number of particles in the fraction and their volume can be calculated by means of the mass and the density.

$$dN = \frac{dM}{\rho \cdot dV_{sphere}} = \frac{M \cdot f(d) \cdot dd}{\rho \cdot \frac{4 \cdot \pi \cdot d^3}{3 \cdot 8}} = \frac{M}{\rho} \cdot \frac{6}{\pi \cdot d^3} \cdot f(d) \cdot dd \tag{6.16}$$

where dN = number of particles within the fraction [-]
dV_{sphere} = volume of one spherical particle [m^3]
ρ = density of the material [kg/m^3]

The surface of the particles within the fraction as well as the area of the whole sample can then be calculated.

$$dA = dN \cdot \frac{4 \cdot \pi \cdot d^2}{4} = \frac{M}{\rho} \cdot \frac{6}{d} \cdot f(d) \cdot dd \tag{6.17}$$

$$A_{sample} = \frac{M}{\rho} \cdot \int_0^\infty \frac{6 \cdot f(d)}{d} \cdot dd = \frac{M}{\rho} \cdot S_{spec,sample} \tag{6.18}$$

where dA = surface area of particles within the fraction [m^2]
A_{sample} = surface area of the entire sample [m^2]
$S_{spec,sample}$ = specific surface of the sample [m^2/m^3]

The specific surface for the sample, which depends on the size distribution curve, can be determined by numerical integration of the frequency function (6.18).

$$f(d) = \frac{dF(d)}{dd} \tag{6.19}$$

where $f(d)$ = frequency function
$F(d)$ = distribution curve

The distribution curve (in a lin-log diagram) is assumed to consist of straight lines between given values, in this instance the screen sizes.

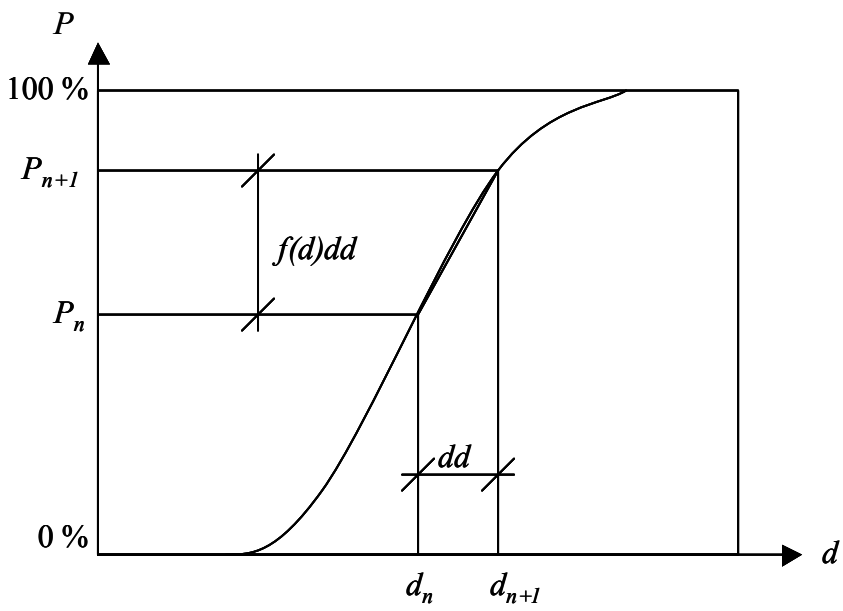

Figure 6.4 The specific surface for the sample depends on the size distribution curve.

The equation for these straight lines is as follows.

$$F(d) = P_n + (P_{n+1} - P_n) \cdot \frac{\log \frac{d}{d_n}}{\log \frac{d_{n+1}}{d_n}} = P_n + (P_{n+1} - P_n) \frac{\ln \frac{d}{d_n}}{\ln \frac{d_{n+1}}{d_n}} \tag{6.20}$$

Deriving the distribution curve (6.20) gives the frequency function needed to determine the specific surface.

$$f(d) = \frac{P_{n+1} - P_n}{\ln \frac{d_{n+1}}{d_n}} \cdot \frac{1}{d} \tag{6.21}$$

According to equation 6.18, the specific surface for a fraction can be established.

$$S_{spec,n-(n+1)} = 6 \cdot \frac{P_{n+1} - P_n}{\ln \frac{d_{n+1}}{d_n}} \cdot \int_{d_n}^{d_{n+1}} \frac{1}{d^2} \cdot dd = 6 \cdot \frac{P_{n+1} - P_n}{\ln \frac{d_{n+1}}{d_n}} \cdot \left(\frac{1}{d_n} - \frac{1}{d_{n+1}} \right) \tag{6.22}$$

$$S_{spec,n-(n+1)} = \frac{6 \cdot (P_{n+1} - P_n)}{\ln \frac{d_{n+1}}{d_n}} \cdot (\frac{1}{d_n} - \frac{1}{d_{n+1}}) = \alpha \cdot \frac{(P_{n+1} - P_n) \cdot (\frac{1}{d_n} - \frac{1}{d_{n+1}})}{\ln \frac{d_{n+1}}{d_n}} \tag{6.23}$$

By adding each specific surface for all of the fractions, the total specific surface for the sample can be determined.

$$S_{spec} = \sum S_{spec,n-(n+1)} \tag{6.24}$$

The particle shape for the six Bårarp rounds is assumed to be cubical because, when the material was studied during the sieving process, it appeared to be more nearly cubical than either spherical or elongated. Moreover, the flakiness index is quite normal, which supports the assumption. As it happens, the particle shape factor, α, is the same for both the spherical and cubical shape.

$$S_{spec,cube} = \frac{A_{cube}}{V_{cube}} = \frac{6 \cdot l^2}{l^3} = \frac{6}{l} = \frac{\alpha}{l} \tag{6.25}$$

where l = the side length of the cubical particle [m]

Equations 6.23 and 6.24 were used to calculate the specific surface for the modelled *in situ* block size distribution, as well as for the six rounds at Bårarp. The results are given in Table 6.4.

Table 6.4 Specific surface for the in situ *distribution, and after fragmentation, at Bårarp*

	In situ* 1	***In situ* 2****	**Round 1**	**Round 2**	**Round 3**	**Round 4**	**Round 5**	**Round 6**
Specific surface [m²/m³]	2.1	1.7	65 042	23 640	24 707	50 373	51 117	55 355

**In situ* distribution calculated directly from the mapping information. ***In situ* distribution from modelling.

When the specific surface has been calculated, it could then be related to the energy from the explosive. The explosive Emulite 100 contains 2.7 MJ/kg and Kemix 3.2 MJ/kg. The amount of energy per volume of rock for each round is presented in Table 6.5.

Table 6.5 Energy content per volume of rock in each round

	Round 1	**Round 2**	**Round 3**	**Round 4**	**Round 5**	**Round 6**
Energy [MJ/m³]	1.54	1.54	1.49	1.75	1.67	1.76

Plotting the amount of energy per volume of rock against the newly formed specific surface for each round gives the following picture (Figure 6.5).

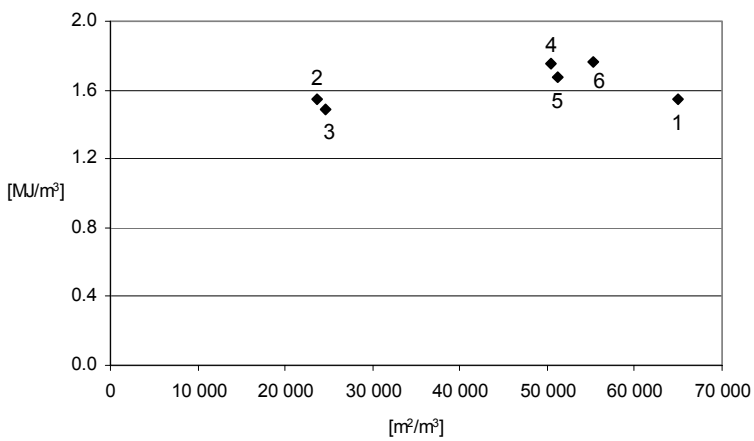

Figure 6.5 Amount of energy per volume of rock plotted against newly formed specific surface.

What can be seen is that there is a clustering effect for the last three rounds; this is not a surprise, since the same explosive was used, as well as the same specific charge, and the fragmentation was very similar. In comparison with the model proposed in Section 6.3.2, these blasts were performed under similar conditions and would thereby be expected to give the same amount of fines. Since the fragmentation was the same, so is also the newly generated specific surface. For the first three rounds, it can be seen that the 51 mm round has been fragmented to a much greater extent than the 76 mm and 51/76 mm rounds. That can be observed in the sieving curves as well, but this visualization is much clearer. Consequently, it is difficult to interpret the results. Is it the first round (51 mm), with a fine fragmentation, that stands out from the others, or is it the third (76 mm), with an unexpectedly coarse fragmentation? Is it the geological conditions that cause the clustering effect, or is it perhaps the change in explosive? Is it possible that the failure of one detonation in a borehole, in the first blast, could have affected the final fragmentation result?

Taking all the blasts together, and assuming that it is the fragmentation result from the first round (51 mm) which deviates, then the theory that the same blasting conditions (except for the diameter of the borehole) give the same amount of fines can be illustrated by a straight line between the values (Figure 6.6).

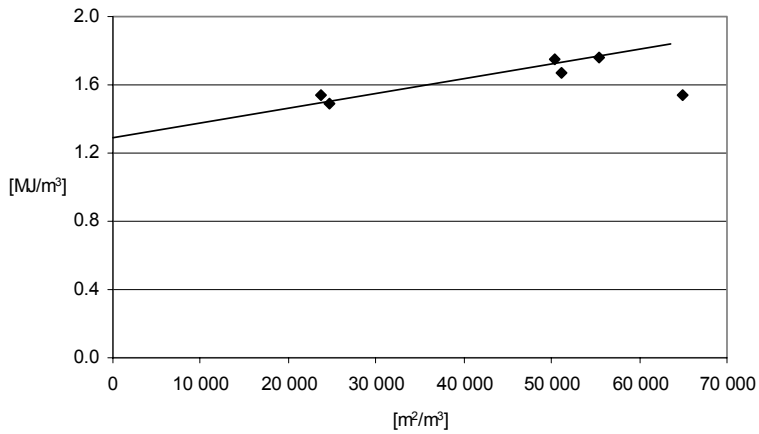

Figure 6.6 The straight line illustrates the idea of a linear function between the specific energy and the newly generated specific surface.

An alternative approach would be to assume a relationship similar to a square root function (Figure 6.7).

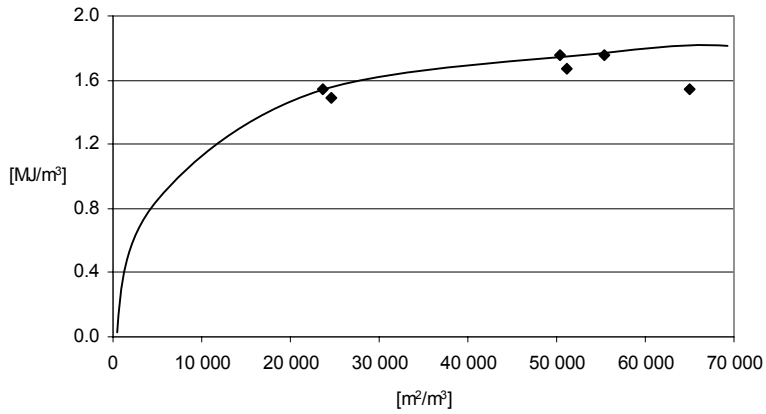

Figure 6.7 The curve illustrates an alternative approach to explain the relation between specific energy and newly formed specific surface.

Kristiansen (1995a) managed to find a correlation between the amount of fines (0 - 4 mm) and the amount of explosive per borehole area. Although this was also tested for the Bårarp rounds, no such indications could be found.

6.3.4 Design analysis

The half-scale blasts conducted at the Bårarp test site are rather difficult to evaluate. The result most anticipated when designing the first three rounds was that the decoupled charge would give a very small amount of fines. This is explained by the decreased borehole pressure, which is due to the empty space left between the charge and the borehole wall. The unexpected result when evaluating these three rounds was that the largest borehole diameter, 76 mm, also give a very small amount of fines, even lower than the decoupled round. These two rounds stand out from the other ones when looking at the sieving curves given in Figures 5.17 and 5.18. Studying the amount of energy versus newly formed specific surface changes the picture. Here (Figure 6.5), it is the first round (51 mm) that stands out from the rest. For the last three rounds the results are much more coherent. For either way of looking at the results, we can see that no matter which borehole diameter is used, as long as all other conditions are kept the same, the amount of fines generated is the same. A fair question is: What makes the results so hard to interpret?

Analysing possible sources of difficulty reveals some parameters that could have affected the result. Although the geology was investigated thoroughly for the first three rounds, when the bench was changed for the last three rounds it was assumed, after visually studying the area, that the properties of the rock mass were the same. This bench was located only a few tens of metres from the previous site, which is why the assumption seemed reasonable. However, since this was never established, the geological conditions could be an explanation. Even if the rock material itself was quite similar, the structure of it was probably not. In the first bench, there were a couple of large open joints filled with sand. These kinds of large structures in the bench affect greatly the fragmentation result in a bench as small as the ones used in the tests. A joint will absorb energy and hinder any fragmentation beyond itself. The joints were large even for production-size blasts. There were not as many of these in the second bench, which could explain why the three last rounds have a finer and similar fragmentation. It is also possible to explain the crossing behaviour of the sieving curves (Figure 5.18), between the first three rounds and last three, by the geological conditions. The crossing does not take place when considering only the

fully coupled rounds and separating the two benches; however, this might just as well be an effect of the change in sieving process, i.e. from field screening to laboratory sieving.

It is difficult to say how much the scale of the blast tests influenced the fragmentation result. First of all, the stemming part of the boreholes is quite large, even though it is very well comparable with the production-size blast recommendation for stemming: this should be approximately equal to the burden. However, the size of the largest borehole, 76 mm, is very seldom found in such small benches as the ones at Bårarp. This could give an erroneous idea about the fragmentation. Also, the stemming is larger for the 76 mm round, in relation to the height of the bench, which could have affected the outcome and given a coarser fragmentation than in the other rounds.

For all of the rounds fired, a certain amount of overbreak almost always occurred. This amount of additional rock mass is impossible to trace and remove from the sieving curves. It is also difficult to say whether this adds large pieces or mostly finer ones to the muckpile. Both cases have been observed. Another aspect is the loading of the muckpile and how it was done. The correct way to load the muckpile would have been for the excavator to dig to the same level every time. This would have assured that the floor in front of the bench was always kept at the same level and that all of the material, no more or less, was taken to the drum sizer. At the beginning of the project, the idea was to pave the floor to avoid this problem, but since that would have been too costly the idea was abandoned.

The initiation of the rounds is also worth considering. First, it must be pointed out that in the first 51 mm round, one out of the six boreholes did not detonate, which could have affected the resulting composition of the muckpile. To make the best of the situation, the rock that should have been fragmented by this hole was not regarded as a part of the blast. A new theoretical volume (75.6 m^3 instead of 94.5 m^3) was calculated, which in the end also meant a new specific charge (0.57 kg/m^3), slightly different from the one planned (0.55 kg/m^3). This was the best that could be done under the circumstances, and since the difference in specific charge was small, it seemed an appropriate solution. The initiation sequence was not quite the same for the first three rounds as for the last. The first rounds were initiated with the two boreholes in the middle going off at the same time (321123), while in the last three the blast was opened with one borehole in the middle (321234). What kind of effect this could have on the fragmentation result is hard to say. The reason for changing the design is that when the charges in two neighbouring boreholes go off at the same time, it is very likely that a crack forms between them, and a large piece of rock falls out without being fragmented. Since the initiators were electronic, it is rather safe to say that they were initiated at the same time. To avoid this, the design was changed so that no boreholes were initiated simultaneously.

Due to the constant specific charge, the number of boreholes had to vary in order to have different borehole diameters. The number of boreholes ranged from four to eight. If the fragmentation is to any extent related to this, it should have been visible in the correlation analysis in Section 6.3.1. However, the correlation is very weak both for the number of boreholes and for the number of detonating boreholes.

6.3.5 Rock quality parameters

Since only a few rock quality parameters were evaluated for all six blasts, it is difficult to draw conclusions from them. What can be observed though, is that the parameters behave as expected in relation to each other. When the average flakiness decreases, so does the abrasion value. This is a normal behaviour, since long particles break more easily than more cubical ones; hence, cubical particles give a much better abrasion value. However,

when the values for the average flakiness were arranged in order of increasing borehole diameter, no trends could be observed (Table 6.6).

Table 6.6 Average flakiness in the order of increasing borehole diameter

Diameter [mm]	**38**	**51**	**51**	**64**	**76**	**51/76**
Average flakiness [weight - %]	1.37	1.46	1.42	1.36	1.42	1.41

The difference between the two 51 mm rounds is as great as the difference between the first 51 mm round and the 76 mm one. As for the abrasion and the impact values, there is no trend found for them either. The values vary little and the spread among them is no more than would be expected between production blasts in a quarry, even though they have the same design. This is due to the variations in geological conditions within the excavation site.

7 CONCLUSIONS

When summarising the results from the model-scale blasts performed in mortar cylinders, it is clear that most of the fines originate from the close vicinity of the borehole.

To investigate whether the results can be applied to rock, the material, the shape of the specimen, loading rate, confinement and crack propagation were examined. The material seems to be a good alternative to rock, with the assumption that the results are interpreted as trends rather than as absolute values. Since mortar and rock have many properties in common, it should be possible to draw conclusions applicable to rock, even if not for an entire rock mass.

Evidence of two fines generation mechanisms is suggested by studying the results from the model-scale tests. One is the crushing of the material closest to the borehole, while the other is general, and occurs anywhere in the material. When fitting a regression curve to the data, it was found that the amount of fines is a function of the inverse square of the distance from the borehole. A simplified model was developed to show how this relationship could be described in detail. The model suggests that the amount of fines is linked to a constant, the distance to a free face and the borehole radius. The constant must be related to several site-specific properties: geometrical, detonic and material, however, it is unfortunately not possible to further investigate the constant in this project. By using the model equation on the Bårarp half-scale blasts, it was found that the amount of fines generated should be equal for all blasts. This is the case for the last three rounds, but not for the first three.

The newly generated specific surface was calculated for the Bårarp rounds. When comparing these to the explosive energy per volume of rock, it is shown that the greater the specific energy (MJ/m^3) is, the finer the fragmentation (larger specific surface). The correct relationship is difficult to define because there are only two clusters of points to evaluate and the range of specific energies is very small, since the intention of the design was to keep the specific charge constant. However, the clustering indicates that the size of the borehole does not affect the final fragmentation result, provided, the blasting conditions, the specific energy, and the relation between the distance to a free face and the borehole radius are the same. Hopefully, this will give some guidance for quarries that has difficulties with excessive fines and want to experiment with the design.

8 FUTURE WORK

As with many other research projects, this one began with questions and ended with even more. Even if the model-scale tests have shown that the crushing near the borehole is a large source of fines, it is still a fact that these tests were not performed in rock. The next interesting step would be to repeat the blasting procedure of the same model but in a variety of rock materials. Although the colouring would not be possible, a study of the general fragmentation would offer much additional information. It would be possible to study the effect of mineralogy, and by looking more closely at the fracture surfaces, perhaps to say something about how different individual minerals give rise to weaknesses or make the rock stronger. Can weak porous minerals such as mica, for example, act as small free surfaces within the rock, interfering with the stress waves? Selmer-Olsen (1966) related a drillability index to the mechanical properties of rock and discovered that rock containing mica behaved differently: it needed to be dealt with separately from the other rock types. Perhaps such an index could be of help to estimate the amount of mica in the rock at a specific blast site. If it were possible to relate a drillability index to the blastability, this would be of great importance to the design of blasting. Since the drilling always occurs before the blasting, no extra effort would be necessary.

Another interesting question is whether there is a difference in mineral content between the fines generated in blasting and the fines originating from the crushing procedure, which could be attributed to breakage mechanisms? This proposed investigation could also be supported by information from different quarries. Every quarry collects an enormous amount of information during the stages of aggregate production. There must be a lot that can be learned by studying the rock and the fragmentation, as well as the charging techniqes and explosives. Collecting and analysing this data would be an enormous task but a better data source cannot be found.

Another natural way to proceed would be to start working on a slightly larger scale to permit the firing of more than one borehole. Doing this work in mortar would make it possible to continue with the same coloured zones around each borehole and, once again, study from where inside the specimens each fraction originates (Figure 8.1).

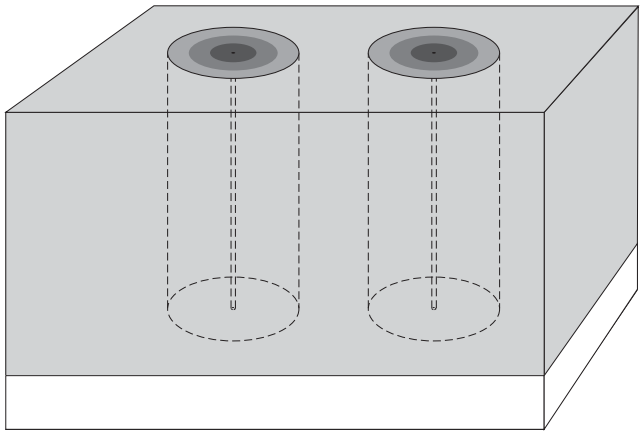

Figure 8.1 Example of a test specimen where, for example, the effect of stemming and bottom charge could be investigated.

These kinds of tests would answer questions such as: Are there any boundary effects in the cylinder tests? Is the amount of fines from the borehole the same? What are the effects of

different bottom charges or stemming lengths? As concrete, or mortar, appears to be a suitable model material, there is much to be gained by using it within the field of rock blasting.

REFERENCES

Adhikari, G. R., Barman, B. K. & Singh, B., 1990: Control of fines through blasting design at a limestone quarry. Mining Science and Technology, No. 11, pp. 173-177.

Alm, O., Jaktlund, L.-L. & Shaoquan, K., 1985: The influence of microcrack density on the elastic and fracture mechanical properties of Stripa granite. Physics of the Earth and Planetary Interiors, Vol. 40, pp. 161-179.

Anderson, D. A., Winzer, S. R. & Ritter, A. P., 1985: The relationships between rock structures and delay time, and fragment size and distribution in explosively-loaded rock. Fragmentation by Blasting. Society for Experimental Mechanics, Brookfield, USA. pp. 41-62.

Armstrong, L. W., Moxon, N. T. & Sen, G. C., 1993: The effects of confinement on fragmentation and movement. Proceedings of the Fourth International Symposium on Rock Fragmentation by Blasting, FRAGBLAST 4, Vienna, Austria, pp. 353-360.

Badal, R., 1995: Rock Blasting with Discontinuities. International Book Traders, New Dehli, India.

Belland, J. M., 1966: Structure as a control in rock fragmentation. Canadian Mining and Metallurgical Bulletin, Vol. 59, No. 647, pp. 323-328.

Bhandari, S., 1983: Influence of Joint Directions in Blasting. Proceedings of the Ninth Conference on Explosives and Blasting Technique, Dallas, Texas, USA, pp. 359-369.

Bhandari, S., 1996: Changes in fragmentation processes with blasting conditions. Proceedings of the Fifth International Symposium on Rock Fragmentation by Blasting, FRAGBLAST 5, Montreal, Canada, pp. 301-309.

Bhandari, S. & Badal, R., 1990: Relationship of Joint Orientation with Hole Spacing Parameter in Multihole Blasting. Proceedings of the Third International Symposium on Rock Fragmentation by Blasting, FRAGBLAST-3, Brisbane, Australia, pp. 225-231.

Bieniawski, Z. T., 1989: Engineering Rock Mass Classification: A complete Manual for Engineers and Geologists in Mining, Civil and Petroleum Engineering. Wiley, New York, USA.

Bohloli, B., 1997: Effects of the Geological Parameters on Rock Blasting Using the Hopkinson Split Bar. International Journal of Rock Mechanics and Mining Science, Vol. 34, No. 3-4, pp. 630-637.

Bohloli, B., Gustafson, G. & Ronge, B., 2001: A laboratory study on reducing the quantity of rock fines at failure: Application to rock blasting and crushing. Bulletin of Engineering Geology and the Environment, Vol. 60, No. 4, pp. 271-276.

Bohloli, B. & Ronge, B., 1999: Investigating tensile strength and fragmentation of anisotropic rocks in 3D using the Brazilian test. International Journal of Blasting and Fragmentation, No. 3, pp. 155-164.

Bolger, J. M. & McMaster, K. E., 1996: Fines Reduction Program at the Canadian Salt Company. Proceedings of the 22nd Conference on Explosives and Blasting Technique, Orlando, Florida, USA, pp. 282-285.

Bond, F. C., 1952: The Third Theory of Comminution. Mining Engineering Trans. AIME, Vol. 193, pp. 484-494.

Bond, F. C., 1959: The Work Index in Blasting. Quaterly of the Colorado School of Mines, Vol. 54, No. 3, pp. 77-82.

Brinkmann, J. R., 1987: Separating shock wave and gas expansion breakage mechanisms. Proceedings of the Second International Symposium on Rock Fragmentation by Blasting, FRAGBLAST-2, Keystone, Colorado, USA, pp. 6-15.

Brinkmann, J. R., 1990: An Experimental Study of the Effects of Shock and Gas Penetration in Blasting. Proceedings of the Third International Symposium on Rock Fragmentation by Blasting, FRAGBLAST-3, Brisbane, Australia, pp. 55-66.

Brook, N., 1993: The Measurement and Estimation of Basic Rock Strength. Comprehensive Rock Engineering: Principles, Practice and Projects. Rock Testing and Site Characterization. Vol. 3. Pergamon Press Ltd., Oxford, England. pp. 982.

Cunningham, C. V. B., 1983: The Kuz-Ram Model for Predicition of Fragmentation from Blasting. Proceedings of the First International Symposium on Rock Fragmentation by Blasting, FRAGBLAST-1, Luleå, Sweden, Vol. 2 (3), pp. 439-453.

Cunningham, C. V. B., 1987: Fragmentation estimations and the Kuz-Ram model - Four years on. Proceedings of the Second Symposium on Rock Fragmentation by Blasting, FRAGBLAST-2, Keystone, Colorado, USA, pp. 475-483.

Da Gama, D. C., 1971: Size Distribution General Law of Fragments Resulting from Rock Blasting. Transactions SME/AIME, Vol. 250, Dec., pp. 314-316.

Da Gama, D. C., 1983: Use of Comminution Theory to Predict Fragmentation of Jointed Rock Masses Subjected to Blasting. Proceedings of the First International Symposium on Rock Fragmentation by Blasting, FRAGBLAST-1, Luleå, Sweden, Vol. 2 (3), pp. 565-580.

Daehnke, A., Rossmanith, H.-P. & Knasmillner, R. E., 1996: Blast-induced dynamic fracture propagation. Proceedings of the Fifth International Symposium on Rock Fragmentation by Blasting, FRAGBLAST-5, Montreal, Canada, pp. 13-18.

Dershowitz, W., Lee, G., Geier, J. E., Foxford, T., La Pointe, P. & Thomas, A., 1998: FracMan. Interactive discrete feature data analysis geometric modeling and exploration simulation. User documentation version 2.6. Golder Assoc. Inc., Seattle, USA.

Djordjevic, N., 1999: A Two-Component Model of Blast Fragmentation. Proceedings of the Sixth International Symposium on Rock Fragmentation by Blasting, FRAGBLAST-6, Johannesburg, South Africa, pp. 213-219.

Eberhardt, E., Stimpson, B. & Stead, D., 1999: Effects of Grain Size on the Initiation and Propagation Thresholds of Stress-induced Brittle Fractures. Rock Mechanics and Rock Engineering, Vol. 32, No. 2, pp. 81-99.

FAS, 1995: FAS Metoder (In Swedish). FAS (Föreningen för asfaltbeläggningar i Sverige) Service AB, Stockholm, Sweden.

Field, J. E. & Ladegaard-Pedersen, A., 1971: The importance of the reflected stress wave in rock blasting. International Journal of Rock Mechanics and Mining Sciences, Vol. 8, pp. 213-226.

Fordyce, D. L., Fourney, W. L., Dick, R. D. & Wang, X. J., 1993: Effect of joints on stress wave transmission. Proceedings of the Fourth International Symposium on Rock Fragmentation by Blasting, FRAGBLAST-4, Vienna, Austria, pp. 211-219.

Fourney, W. L., Barker, D. B. & Holloway, D. C., 1983: Fragmentation in Jointed Rock Material. Proceedings of the First International Symposium on Rock Fragmentation by Blasting, FRAGBLAST-1, Luleå, Sweden, Vol. 2 (3), pp. 505-531.

Fourney, W. L., Dick, R. D., Wang, X. J. & Weaver, T. A., 1997: Effects of Weak Layers on Particle Velocity Measurements. Rock Mechanics and Rock Engineering, Vol. 30, No. 1, pp. 1-18.

Fourney, W. L., Holloway, D. C., Wilson, W. H. & Barker, D. B., 1985: Fragmentation studies in jointed brittle material. Fragmentation by Blasting. Society for Experimental Mechanics, Brookfield, USA. pp. 73-87.

Glatolenkov, A. I. & Ivanov, V. I., 1991: Mechanism of breakdown of rock masses and formation of fines by blasting. Translated from Fiziko-Tekhnicheskie Problemy Razrabotki Poleznykh Iskopaemykh, No. 5, pp. 78-86.

Gustafson, G., 1983: Brunnsystem för värmelagring och värmeutvinning i akviferer (in Swedish). Byggforskningsrådet, Report R39:1983, Göteborg, Sweden.

Gynnemo, M., 1995: The importance of velocity of detonation in rock blasting (In Swedish). Sprängnytt (Nitro Nobel), No. 3, pp. 32-35.

Gynnemo, M., 1997: Undersökning av styrande faktorer vid pallsprängning - Fullskaleförsök i Kållered och Billingsryd (In Swedish). Licentiate thesis, Chalmers University of Technology, Department of Geology. Göteborg, Sweden.

Hagan, T. N., 1973: Rock Breakage by Explosives. Proceedings of the National Symposium on Rock Fragmentation, Adelaide, Australia, pp. 1-17.

Hagan, T. N., 1979: The Control of Fines through Improved Blast Design. Proc. Australas. Inst. Min-Metall., No. 271, pp. 9-20.

Hall, J. & Brunton, I., 2001: Critical Comparison of Julius Kruttschnitt Mineral Research Centre (JKMRC) Blast Fragmentation Models. Proceedings of the EXPLO'2001, Hunter Valley, NSW, Australia, pp. 207-212.

Hoek, E. & Bray, J. W., 1981: Rock Slope Engineering. Elsevier Science Publishers Ltd., London, England.

Honma, H., 1990: Properties of rock blasting. Proceedings of the Third International Symposium on Rock Fragmentation by Blasting, FRAGBLAST-3, Brisbane, Australia, pp. 265-271.

Jern, M., 2001: Determination of the damaged zone in quarries, related to aggregate production. Bulletin of Engineering Geology and the Environment, Vol. 60, No. 2, pp. 157-166.

Jimeno, C. L., Jimeno, E. L. & Carcedo, F. J. A., 1987: Drilling and Blasting of Rocks. A.A. Balkema, Rotterdam, the Netherlands.

JKMRC, 1996: Open Pit Blast Design - Analysis and Optimisation. Julius Kruttschnitt Mineral Research Centre, Indooroopilly, Australia.

Johansson, C. H. & Persson, P. A., 1970: Detonics of high explosives. Academic Press Inc. Ltd, London, England.

Johnson, R. B. & DeGraff, J. V., 1988: Principles of Engineering Geology. John Wiley & Sons, Inc, New York, USA.

Kim, D. S. & McCarter, M. K., 1998: Quantative Assessment of Extrinsic Damage in Rock Material. Rock Mechanics and Rock Engineering, Vol. 31, No. 1, pp. 43-62.

Kojovic, T., Michaux, S. & McKenzie, C., 1995: Impact of Blast Fragmentation on Crushing and Screening Operations in Quarrying. Proceedings of the EXPLO'95, Brisbane, Australia, pp. 427-436.

Konya, C. J. & Walter, E. J., 1990: Surface Blast Design. Prentice Hall, Englewood Cliffs, N.J., USA.

Kristiansen, J., 1987: Utvikling av en ny parameter for å karakterisere sprengstoffers evne til å fragmentere fjell - Belyst ved sprengningsforsøk i betong (in Norwegian). Master thesis, University of Oslo, Department of Geology. Oslo, Norway.

Kristiansen, J., 1994a: Rock blastability. A project to optimize the quality of fragmented rock for the Norwegian aggregate industry (In Norwegian). Proceedings of the Nitro Nobel Sprängteknisk konferens, Stockholm-Helsinki, pp. 1-12.

Kristiansen, J., 1994b: Sprengbarhet av berg, Fullskaleforsøk i Åndalen Pukkverk (In Norwegian). Norges Geotekniske Institutt (NGI), 548095-3, Oslo, Norway.

Kristiansen, J., 1995a: Finandelens beroende av håldimensionen (In Swedish). Sprängnytt (Nitro Nobel), No. 3, pp. 20-23.

Kristiansen, J., 1995b: A Study of How the Velocity of Detonation Affects Fragmentation and the Quality of Fragments in a Muckpile. Proceedings of the EXPLO'95, Brisbane, Australia, pp. 437-444.

Kristiansen, J., Kure, K., Vestre, J. & Bergqvist, I., 1990: An Investigation of Heave and Fragmentation Related to Explosive Properties. Proceedings of the EXPLO'90, Brisbane, Australia, pp. 83-90.

Kuznetsov, V. M., 1973: The mean diameter of the fragments formed by blasting rock. Translated from Fiziko-Tekhnicheskie Problemy Razrabotki Poleznykh Iskopaemykh, No. 2, pp. 39-43.

Lande, G., 1983: Influence of structural geology on controlled blasting in sedimentary rocks: Case history. Proceedings of the First International Symposium on Rock Fragmentation by Blasting, FRAGBLAST-1, Luleå, Sweden, Vol. 2 (3), pp. 555-563.

Langefors, U. & Kihlström, B., 1963: The Modern Technique of Rock Blasting. Almqvist & Wiksells/Gebers Förlag, Stockholm, Sweden.

Lewandowski, T., Luan Mai, V. K. & Danell, R. E., 1996: Influence of discontinuties on presplitting effectiveness. Proceedings of the Fifth Symposium on Rock Fragmentation by Blasting, FRAGBLAST-5, Montreal, Canada, pp. 217-225.

Liu, Q. & Katsabanis, P. D., 1993: A theoretical approach to the stress waves around a borehole and their effect on rock crushing. Proceedings of the Fourth International Symposium on Rock Fragmentation by Blasting, FRAGBLAST-4, Vienna, Austria, pp. 9-16.

Lizotte, Y. C. & Scoble, M. J., 1994: Geological control over blast fragmentation. CIM Bulletin, Vol. 87, No. 983, pp. 57-71.

Lundqvist, I. & Wik, N.-G., 1998: Industriella mineral och bergarter i Hallands län (In Swedish). Geological Survey of Sweden, Report 96, Uppsala, Sweden.

Masuda, K., 2001: Effects of water on rock strength in a brittle regime. Journal of Structural Geology, Vol. 23, No. 11, pp. 1653-1657.

Mohanty, B., 1987: Strength of rock under high strain rate loading conditions applicable to blasting. Proceedings of the Second International Symposium on Rock Fragmentation by Blasting, FRAGBLAST-2, Keystone, Colorado, USA, pp. 72-79.

Moser, P., Cheimanoff, N., Ortiz, R. & Hochholdinger, R., 2000: Breakage characteristics in rock blasting. Proceedings of the 1st World Conference on Explosives & Blasting Technique, Munich, Germany, pp. 165-170.

Mäki, K., 1983: On the Applicability of the Tensile Strength as an Index to Rock Fragmentation. Proceedings of the First International Symposium on Rock Fragmentation by Blasting, FRAGBLAST-1, Luleå, Sweden, Vol. 1 3, pp. 79-95.

Naarttijärvi, T., 1978: Modellförsök i försiktig sprängning, delrapport nr. 4 (In Swedish). Tekniska högskolan i Luleå, Avdelningen för bergteknik, Report 1978:65T, Luleå, Sweden.

Naarttijärvi, T., Rustan, A., Öqvist, J. & Ludvig, B., 1980: Laboratorieförsök i försiktig sprängning, delrapport 7 (In Swedish). Luleå University of Technology, Research report 1980:22, Luleå, Sweden.

Olofsson, S. O., 1999: Modern bergsprängningsteknik (In Swedish). APPLEX, Ärla, Sweden.

Olsson, M., 1995: Faktorer som styr oönskad sprickbildning vid sprängning (In Swedish). Sprängnytt (Nitro Nobel), No. 3, pp. 9-11 and 31.

Olsson, M., 1999: Projektplan-Fragmentering i bergtäkter (In Swedish). SveBeFo (Swedish Rock Engineering Research), Stockholm, Sweden.

Olsson, M., 2002: Fragmentering i bergtäkter (In Swedish). Bergsprängningskommittén, Stockholm, Sweden.

Olsson, M., Nie, S., Bergqvist, I. & Ouchterlony, F., 2001: What Causes Cracks in Rock Blasting? Proceedings of the EXPLO'2001, Hunter Valley, Australia, pp. 191-196.

Ouchterlony, F., 1974: Fracture Mechanics Applied to Rock Blasting. Proceedings of the Third Congress of the International Society for Rock Mechanics, Denver, USA, Vol. 2 Part B, pp. 1377-1383.

Ouchterlony, F., Niklasson, B. & Abrahamsson, S., 1990: Fragmentation Monitoring of Production Blasts at MRICA. Proceedings of the Third International Symposium on Rock Fragmentation by Blasting, FRAGBLAST-3, Brisbane, Australia, pp. 283-289.

Pells, P. J. N., 1993: Uniaxial Strength Testing. Comprehensive Rock Engineering - Principles, Practice and Projects. Rock Testing and Site Characterization. Vol. 3. Pergamon Press Ltd., Oxford, England. pp. 982.

Persson, P.-A., 1990: Fragmentation Mechanics. Proceedings of the Third International Symposium on Rock Fragmentation by Blasting, FRAGBLAST-3, Brisbane, Australia, pp. 101-108.

Persson, P.-A., Holmberg, R. & Lee, J., 1994: Rock Blasting and Explosives Engineering. CRC Press Inc., Boca Raton, USA.

Persson, P.-A., Lundborg, N. & Johansson, C. H., 1970: The Basic Mechanisms in Rock Blasting. Proceedings of the 2nd Congress, International Society of Rock Mechanics, Beograd, pp. 19-33.

Rakishev, B. R., 1982: A New Characteristic of the Blastability of Rock in Quarries. Soviet Mining Science, No. 17, pp. 248-251.

Ronge, B., 2000: Lokalisering av försökstäkter SveBeFo-projekt 636 (In Swedish). Department of Geology, Chalmers University of Technology, Göteborg, Sweden.
Ross, C. A., Jerome, D. M., Tedesco, J. W. & Hughes, M. L., 1996: Moisture and Strain Rate Effects on Concrete Strength. ACI Materials Journal, Vol. 93, No. 3, pp. 293-300.

Rustan, A., 1981: Styckefallspåverkande faktorer vid bergsprängning (In Swedish). Tekniska högskolan i Luleå, Avdelningen för bergteknik, 1981:38T, Luleå, Sweden.

Rustan, A., Bergqvist, I. & Persson, A., 1988: Bergets rörelse och uppsprickning vid pallsprängning (In Swedish). Tekniska högskolan i Luleå, Avdelningen för bergteknik, 1988:21T, Luleå, Sweden.

Rustan, A. & Naarttijärvi, T., 1983b: The influence from specific charge and geometric scale on fragmentation. Div. of Mining and Rock Excavation, FG 8322, Luleå, Sweden.

Rustan, A., Vutukuri, V. S. & Naarttijärvi, T., 1983a: The influence from specific charge, geometric scale and physical properties of homogenous rock on fragmentation. Proceedings of the First International Symposium on Rock Fragmentation by Blasting, FRAGBLAST-1, Luleå, Sweden, Vol. 1 (3), pp. 115-142.

Schön, J. H., 1996: Physical properties of rocks - fundamentals and principles of petrophysics. Pergamon, New York, USA.

Scott, A., 1996: "Blastability" and blast design. Proceedings of the Fifth International Symposium on Rock Fragmentation by Blasting, FRAGBLAST-5, Montreal, Canada, pp. 27-36.

Seinov, N. P. & Chevkin, A. I., 1968: Effect of fissure on fragmentation of a medium by blasting. Soviet Mining Science, No. 3, pp. 254-259.

Selmer-Olsen, R., 1966: Alminnelig Geologi og Ingeniørgeologi (in Norwegian). Tapirs forlag, Trondheim, Norway.

Senyur, M. G., 1998: A Statistical Analysis of Fragmentation after Single Hole Bench Blasting. Rock Mechanics and Rock Engineering, Vol. 31, No. 3, pp. 181-196.

SGU, 1997: Bestämning av punktlastindex (In Swedish). Geological Survey of Sweden, Report 08-858/97, Uppsala, Sweden.

Sheahan, R. M. & Beattie, T. A., 1990: Effect of Explosive Type on Fines Generation in Blasting. Proceedings of the Third International Symposium on Rock Fragmentation by Blasting, FRAGBLAST-3, Brisbane, Australia, pp. 413-415.

Singh, D. P. & Sarma, K. S., 1983: Influence of joints on rock blasting - a model scale study. Proceedings of the First International Symposium on Rock Fragmentation by Blasting, FRAGBLAST-1, Luleå, Sweden, Vol. 2 (3), pp. 533-554.

Singh, D. P. & Sastry, V. R., 1987: Role of weakness planes in bench blasting - a critical study. Proceedings of the Second International Symposium on Rock Fragmentation by Blasting, FRAGBLAST-2, Keystone, Colorado, USA, pp. 135-146.

Smith, M. R. & Collis, L., 1993: Aggregates - Sand, gravel and crushed rock aggregates for construction purposes. The Geological Society, London, England.
SP, 1996: Swedish National Testing and Research Institute, Report 96B3,3352, Borås, Sweden.

SP, 1997: Petrographic description of Armour stone from Bårarp. Swedish National Testing and Research Institute, Report 97B3.3413, Borås, Sweden.

Stagg, M. S., Rholl, S. A., Otterness, R. E. & Smith, N. S., 1990: Influence of shot design parameters on fragmentation. Proceedings of the Third International Symposium on Rock Fragmentation by Blasting, FRAGBLAST-3, Brisbane, Australia, pp. 311-317.

Tarbuck, E. J. & Lutgens, F. K., 1993: The Earth - An Introduction to Physical Geology. Macmillan Publishing Company, New York, USA.

Tepfers, R., 1995: Byggnadsmaterial-Allmän kurs (in Swedish). Department of Building Materials, Chalmers University of Technology, Göteborg, Sweden.

Tien, Y. M. & Tsao, P. F., 2000: Preparation and mechanical properties of artificial transversely isotropic rock. International Journal of Rock Mechanics and Mining Sciences, Vol. 37, pp. 1001-1012.

Vestre, J., 1992: Korrelasjon mellom resultat fra sprengning i liten skala og feltforsøk (In Norwegian). Sprängteknisk konferens Nitro Nobel AB, Göteborg-Kiel, Jan 15-16. pp. 1-35.

Winzer, S. R., Anderson, D. A. & Ritter, A. P., 1983: Rock Fragmentation by Explosives. Proceedings of the First International Symposium on Rock Fragmentation by Blasting, FRAGBLAST-1, Luleå, Sweden, Vol. 1 (3), pp. 225-249.

Winzer, S. R. & Ritter, A. P., 1980: The Role of Stress Waves and Discontinuities in Rock Fragmentation: A Study of Fragmentation in Large Limestone Blocks. Proceedings of the 21st U.S. Symposium - The State of the Art in Rock Mechanics, Rolla, USA, pp. 362-370.

Yang, Z. G. & Rustan, A., 1983: The Influence from Primary Structure on Fragmentation. Proceedings of the First International Symposium on Rock Fragmentation by Blasting, FRAGBLAST-1, Luleå, Sweden, Vol. 2 (3), pp. 581-604.

Zhang, Z. X., Kao, S. Q., Yu, Y., Jiang, L. G. & Lindqvist, P.-A., 1999: Effects of loading rate on rock fracture. International Journal of Rock Mechanics and Mining Sciences, Vol. 36, No. 5, pp. 597-611.

Zielinski, A. J., 1982: Fracture of concrete and mortar under uniaxial impact tensile loading. Doctoral Thesis, Delft University of Technology, Delft, the Netherlands.

Öqvist, J., 1982: Jämförelse preliminära styckefallsmetoder vid fullskaleförsök i Fabianmalmen, Malmberget (In Swedish). Tekniska högskolan i Luleå, Avdelningen för bergteknik, fg 8213, Luleå, Sweden.

APPENDIX I -V

APPENDIX I: ERROR ANALYSIS IN THE SIEVING PROCESS

Standard deviation (σ) $= \sqrt{\dfrac{n\sum x^2 - (\sum x^2)^2}{n(n-1)}}$ Confidence limits $= 1.96 \cdot \left(\dfrac{\sigma}{\sqrt{n}}\right)$ with 95 % confidence interval

where n = number of tests
x = mean value for every test

Cylinder	Fraction [mm]	Number of tests	Layer	Number of fragments	Mean value [%]	Standard deviation	Confidence limits [%]
1	4 - 8	5	Green	3283	50.2	2.0	1.7
			Yellow		14.6	1.7	1.5
			Black		35.2	0.8	0.7
2	4 - 8	5	Green	2998	45.6	0.3	0.4
			Yellow		24.2	0.4	0.5
			Black		30.3	0.7	0.8
3	4 - 8	5	Green	3004	48.7	1.6	1.9
			Yellow		19.9	0.4	0.4
			Black		31.4	1.6	1.8
1	2 - 4	5	Green	11546	45.2	2.0	1.8
			Yellow		16.1	0.9	0.8
			Black		38.8	1.8	1.6
2	2 - 4	5	Green	11309	37.9	0.6	0.5
			Yellow		25.4	1.1	0.9
			Black		36.7	0.5	0.4
3	2 - 4	5	Green	10627	38.9	0.8	0.7
			Yellow		21.6	1.0	0.9
			Black		39.6	0.4	0.3
1	1 - 2	7	Green	7178	50.6	2.0	1.5
			Yellow		14.5	1.0	0.8
			Black		34.9	1.4	1.0
2	1 - 2	7	Green	6347	38.2	1.1	1.1
			Yellow		22.0	1.6	1.5
			Black		39.8	1.1	1.1

Cylinder	Fraction [mm]	Number of tests	Layer	Number of fragments	Mean value [%]	Standard deviation	Confidence limits [%]
3	1 - 2	12	Green	15387	38.2	1.4	0.8
			Yellow		20.7	1.1	0.6
			Black		41.1	1.4	0.8
1	0.5 - 1	5	Green	3949	44.0	1.7	1.9
			Yellow		14.3	0.6	0.7
			Black		41.7	1.1	1.2
2	0.5 - 1	5	Green	5116	36.1	1.6	1.4
			Yellow		19.8	1.1	1.0
			Black		44.1	1.7	1.5
3	0.5 - 1	5	Green	2368	37.5	1.0	0.9
			Yellow		16.9	1.5	1.3
			Black		45.7	1.8	1.5
1	0.25 - 0.5	5	Green	6039	43.6	0.5	0.6
			Yellow		16.6	0.5	0.6
			Black		39.8	0.5	0.6
2	0.25 - 0.5	5	Green	4403	34.0	1.0	1.1
			Yellow		19.4	1.6	1.8
			Black		46.6	0.7	0.8
3	0.25 - 0.5	5	Green	6761	33.1	1.5	1.3
			Yellow		18.4	1.8	1.6
			Black		48.5	2.1	1.8
1	0.125 - 0.25	5	Green	6192	39.5	1.6	1.8
			Yellow		18.1	1.0	1.1
			Black		42.4	1.0	1.1
2	0.125 - 0.25	5	Green	6075	29.2	1.6	1.6
			Yellow		18.3	1.1	1.1
			Black		52.5	1.4	1.4
3	0.125 - 0.25	5	Green	6561	30.5	1.7	1.5
			Yellow		17.8	1.0	0.9
			Black		51.7	2.0	1.8
1	0.075 - 0.125	5	Green	6568	38.9	1.2	1.2
			Yellow		14.6	1.8	1.7
			Black		46.5	1.9	1.9

Cylinder	Fraction [mm]	Number of tests	Layer	Number of fragments	Mean value [%]	Standard deviation	Confidence limits [%]
2	0.075 - 0.125	5	Green	7366	26.7	0.8	0.9
			Yellow		18.1	0.7	0.8
			Black		55.3	0.8	0.9
3	0.075 - 0.125	5	Green	6098	25.8	0.5	0.5
			Yellow		16.5	0.8	0.8
			Black		57.7	1.0	1.2
1	< 0.075	5	Green	3137	35.0	1.0	1.1
			Yellow		18.4	0.7	0.8
			Black		46.7	1.1	1.2
2	< 0.075	5	Green	3846	21.7	0.2	0.3
			Yellow		21.8	1.0	1.1
			Black		56.5	0.8	0.9
3	< 0.075	5	Green	3066	25.7	1.0	1.2
			Yellow		19.6	1.0	1.1
			Black		54.7	1.1	1.3

APPENDIX II: REGRESSION ANALYSIS

$C1 = k_1 + k_2 * C2$ where C1 = amount of fines (0 - 8 mm)
k_1, k_2 = constants
C2 = distance from the borehole

C1 [%]	C2 [m]
26.45	0.03
7.49	0.08
6.50	0.13

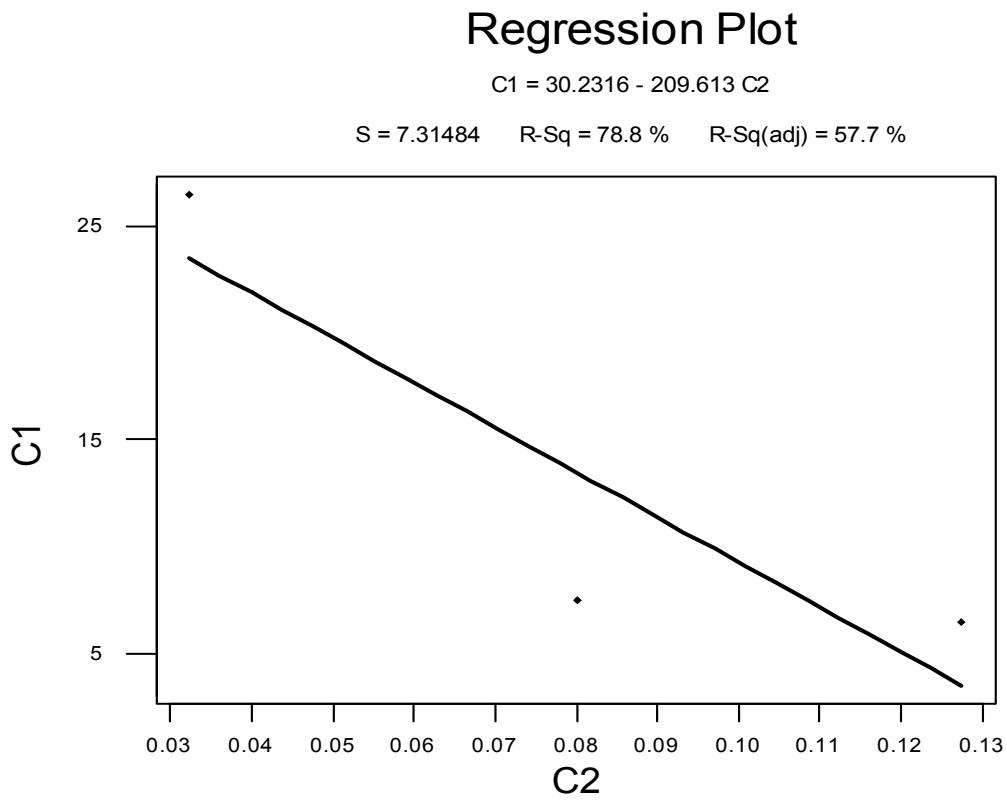

The regression equation is
C1 = 30.2316 - 209.613 C2

S = 7.31484 R-Sq = 78.8 % R-Sq(adj) = 57.7 %

$C1 = k_1 + k_2 * C3$ where C1 = amount of fines (0-8 mm)
k_1, k_2 = constants
C3 = (distance from the borehole)^2

C1 [%]	C3 [m]
26.45	0.00104
7.49	0.00640
6.50	0.01625

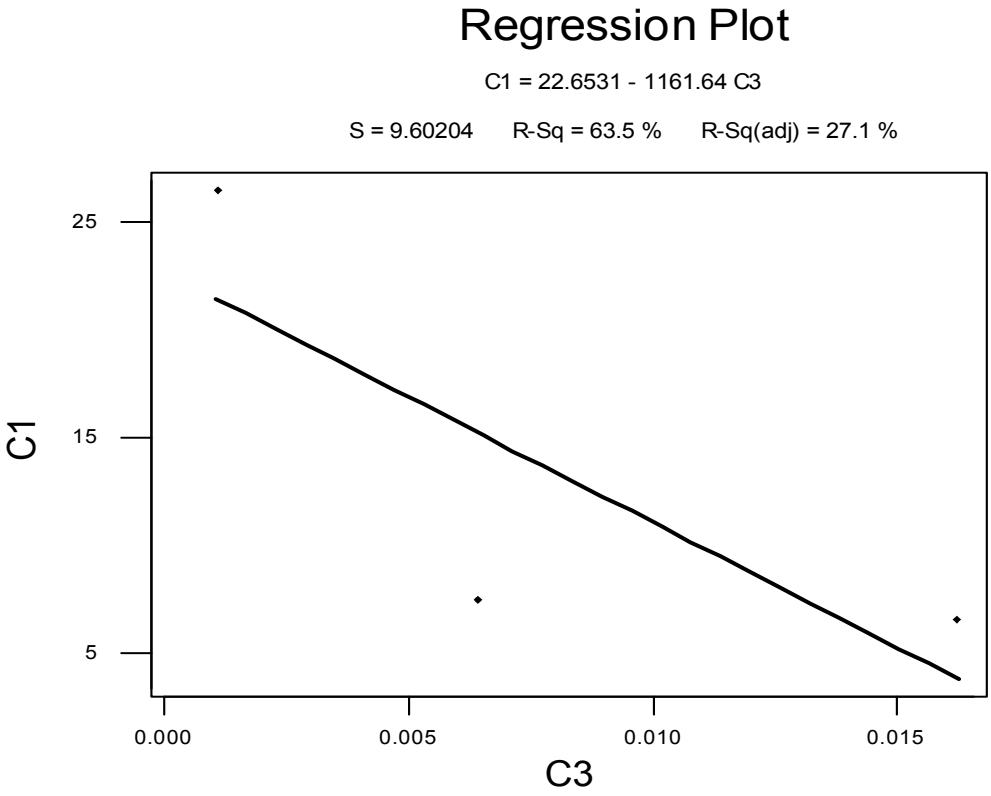

The regression equation is
C1 = 22.6531 - 1161.64 C3

S = 9.60204 R-Sq = 63.5 % R-Sq(adj) = 27.1 %

$C1 = k_1 + k_2 * C4$ where C1 = amount of fines (0-8 mm)
k_1, k_2 = constants
C4 = (distance from the borehole)$^{-2}$

C1 [%]	C4 [m]
26.45	961.48
7.49	156.25
6.50	61.51

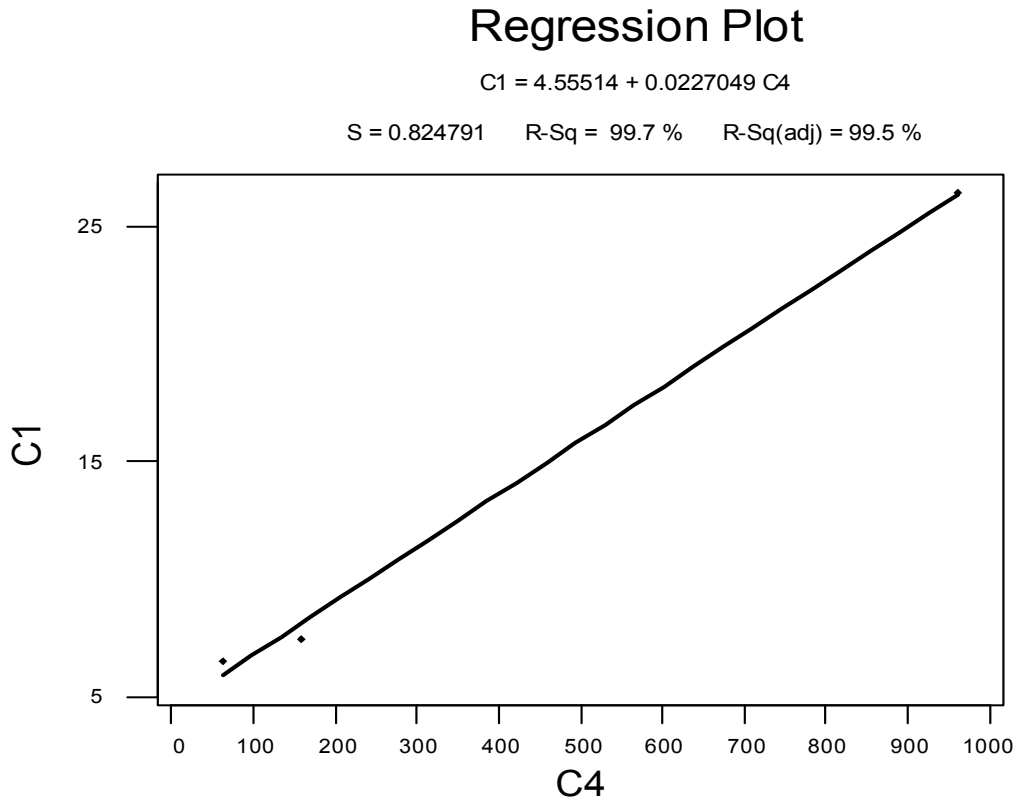

The regression equation is
C1 = 4.55514 + 0.0227049 C4

S = 0.824791 R-Sq = 99.7 % R-Sq(adj) = 99.5 %

$C5 = k_1 + k_2 * C4$ where C5 = amount of fines (0-4 mm)
k_1, k_2 = constants
C4 = (distance from the borehole)$^{-2}$

C5 [%]	C4 [m]
14.26	961.48
3.74	156.25
3.15	61.51

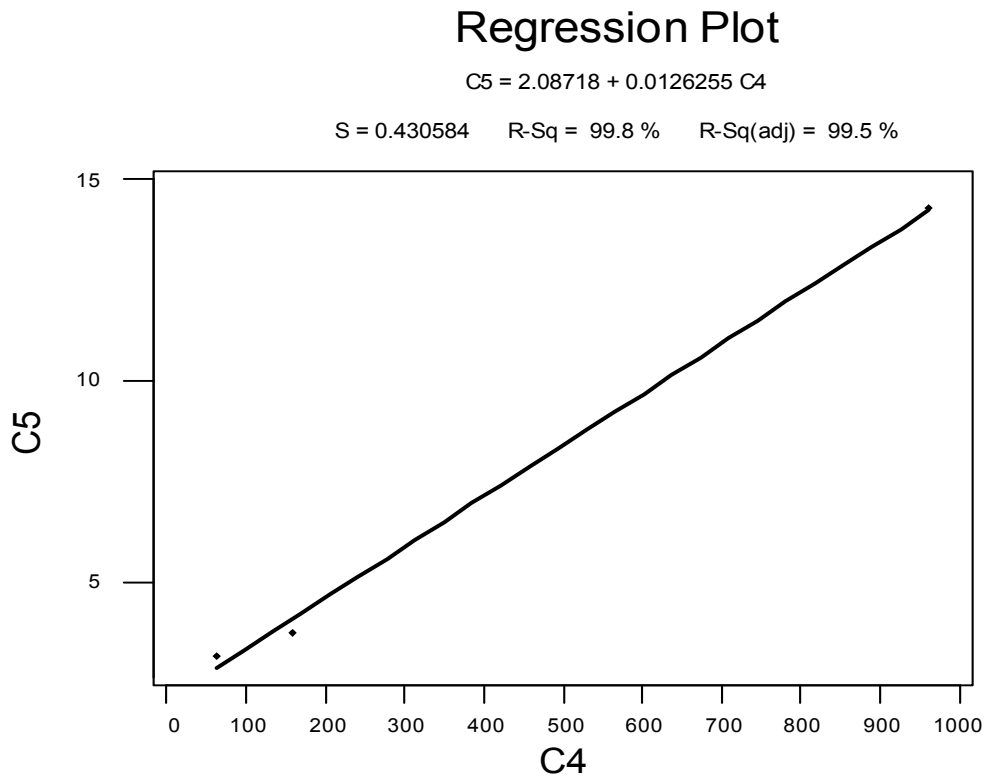

The regression equation is
C5 = 2.08718 + 0.0126255 C4

S = 0.430584 R-Sq = 99.8 % R-Sq(adj) = 99.5 %

$C6 = k_1 + k_2 * C4$ where C6 = amount of fines (0-2 mm)
k_1, k_2 = constants
C4 = (distance from the borehole)$^{-2}$

C6 [%]	C4 [m]
9.055	961.48
2.066	156.25
1.769	61.51

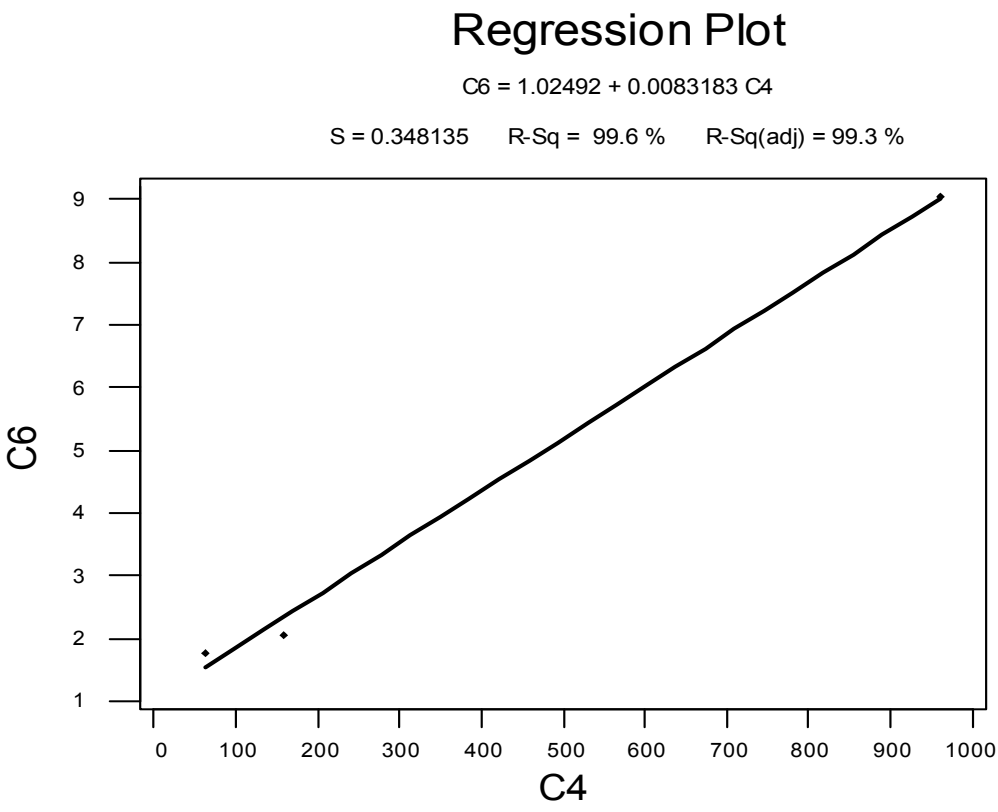

The regression equation is
C6 = 1.02492 + 0.0083183 C4

S = 0.348135 R-Sq = 99.6 % R-Sq(adj) = 99.3 %

APPENDIX III: DATA FROM FIELD TESTS AT BÅRARP

Mats Olsson, SveBeFo

	Round 1	Round 2	Round 3	Round 4	Round 5	Round 6
Burden (m)	1.8	1.8	2.7	1.8	1.35	2.3
Spacing (m)	2.1	2.1	3.4	2.2	1.65	2.85
Bench height (m)	5.0	5.0	5.0	5.2	5.2	5.3
Hole depth (m)-real	5.6	5.5	5.5	5.5	5.35	5.6
Hole diameter (mm)	51	76	76	51	38	64
Number of holes	6	6	4	6	8	5
Theoretical volume (m^3)	94.5	94.5	137.7	103	81.1	139
Theoretical tonnage (ton)	283.5	283.5	413.1	309	243.3	417
Caps	EPD	EPD	EPD	EPD	EPD	EPD
Intiation (interval no. in 25 ms steps)	321123	321123	2112	321234	32101234	32123
Explosive	Emulite	Emulite	Emulite	Kemix	Kemix	Kemix
Density (kg/dm^3)	1.2	1.2	1.2	1.2	1.2	1.2
Cartridge diameter (mm)	43	43	60	40	32	55
Cartridge weight (kg/unit)	0.90	0.90	1.90	0.83	0.53	1.56
Charged diameter (mm)	51	50	76	51	38	64
Coupling factor (1.0 = slit cartridges)	1.0	0.66	1.0	1.0	1.0	1.0
Charge length in hole (m)	4.2	4.2	3.7	4.2	4.2	4.4
Number of cartridges/hole	10	10	10	11.3	10	9.8
Total charge length (m)	25.0	25.2	14.7	25.3	33.9	21.9
Total number of cartridges	58	60	40	68	80	49
Charge weight/hole (kg)	9	9	19	9.4	5.3	15.3
Total charge weight (kg)	52.2	54.0	76.0	56.4	42.4	76.4
Theoretical hole volume	2.04	1.96	4.54	2.04	1.13	3.22
Theoretical charge volume	2.45	2.35	5.45	2.45	1.36	3.86
Linear charge concentration (kg/m)	2.1	2.1	5.2	2.2	1.3	3.5
Percentage of filling	0.86	0.89	0.95	0.90	0.96	0.91
Stemming (m)	1.4	1.4	1.8	1.2	1.1	1.2
No. of detonating holes (1 misfire in round 1)	5	6	4	6	8	5
Measured VOD (m/s)		5491			5851	
Detonated charge weight (kg)	43.2	54.0	76.0	56.4	42.4	76.4
Specific charge/hole ($kg/m/m^3$)	0.48	0.48	0.41	0.46	0.46	0.44
Specific charge (kg/m^3)	0.55	0.57	0.55	0.55	0.52	0.55
Charge weight/area charged borehole (g/cm^2)	13.4	9	21.5	14	10.6	17.3

APPENDIX IV: CALCULATIONS OF SPECIFIC SURFACE

Bårarp

Fraction [m]	Round 1	Round 2	Round 3	Round 4	Round 5	Round 6	Spec. surface 1	Spec. surface 2	Spec. surface 3
0.000075	0.6	0.2	0.1	0.4	0.4	0.4	18793.11	6264.37	6264.37
0.000125	0.9	0.3	0.2	0.6	0.6	0.6	20774.81	6924.94	6924.94
0.00025	1.5	0.5	0.4	1.0	1.0	1.0	10387.40	3462.47	1731.23
0.0005	2.1	0.7	0.5	1.4	1.4	1.4	3462.47	865.62	865.62
0.001	2.5	0.8	0.6	1.7	1.7	1.7	2164.04	432.81	432.81
0.002	3.0	0.9	0.7	2.0	2.0	2.0	1298.43	432.81	432.81
0.004	3.6	1.1	0.9	2.4	2.5	2.4	509.49	127.37	254.74
0.0056	4.0	1.2	1.1	2.9	2.9	2.7	270.35	90.12	180.24
0.008	4.3	1.3	1.3	3.6	3.3	3.1	68.91	68.91	137.82
0.0095	4.4	1.4	1.5	4.1	3.8	3.8	221.03	221.03	221.03
0.00112	4.5	1.5	1.6	4.1	3.8	3.8	450.59	450.59	1351.77
0.0016	4.6	1.6	1.9	4.8	4.5	4.9	0.00	318.43	955.29
0.00224	4.6	1.7	2.2	5.5	5.2	6.3	5233.24	2758.06	3606.69
0.09	12.0	5.6	7.3	10.8	11.8	13.5	249.12	196.98	254.91
0.12	16.3	9.0	11.7	17.3	18.9	19.8	234.91	164.44	176.19
0.2	22.3	13.2	16.2	22.8	25.1	26.0	349.22	266.51	307.86
0.35	37.5	24.8	29.6	38.1	42.5	41.3	118.75	78.63	141.22
0.4	44.9	29.7	38.4	45.3	49.4	48.0	91.42	100.83	114.28
0.5	51.7	37.2	46.9	53.6	58.6	58.1	310.76	287.38	246.70
1.0	87.6	70.4	75.4	98.3	82.6	98.7	53.67	128.11	106.47
2.0	100.0	100.0	100.0	100.0	100.0	100.0			
Specific surface		**[m^2/m^3]**					65041.71	23640.40	24706.98

Spec. surface 4	Spec. surface 5	Spec. surface 6
12528.74	12528.74	12528.74
13849.87	13849.87	13849.87
6924.94	6924.94	6924.94
2596.85	2596.85	2596.85
1298.43	1298.43	1298.43
865.62	1082.02	865.62
636.86	509.49	382.12
630.83	360.47	360.47
344.55	344.55	482.37
0.00	0.00	0.00
3154.13	3154.13	4956.49
2229.01	2229.01	4458.02
3748.13	4667.48	5091.80
376.57	411.33	364.99
215.34	242.74	242.74
351.52	399.76	351.52
115.54	110.73	107.52
111.59	123.69	135.79
386.93	207.75	351.44
7.36	75.31	5.63
50372.79	51117.29	55355.33

In situ (modelled)

Fractions [m]	Modelled	Spec. surface
0.025	0.0000	4.89206E-07
0.09	0.0000	3.18274E-06
0.12	0.0000	2.03453E-05
0.2	0.0001	0.000349261
0.35	0.0016	0.000296086
0.4	0.0034	0.000392397
0.45	0.0062	0.000464839
0.5	0.0099	0.006363347
0.75	0.0744	0.018252083
1.0	0.3369	0.265186058
2.0	6.4640	0.465317249
3.0	25.3310	0.872178585
6.0	85.7858	0.095945337
9.0	97.4566	0.009610238
12.0	99.1154	0.003964371
15.0	100.0000	
Specific surface [m^2/m^3]		**1.73834387**

In situ (calculated from mapping information)

Joint	Length [m]	Dip	Depth [m]	Width [m]	Surface area [m^2]
A1	3.64	90	5.0	5.59	20.3643
	2.48	75	5.0	-12.89	31.9419
	5.35	90	5.0	5.59	29.9432
A2	1.81	90	5.0	5.59	10.0951
	10.53	90	5.0	5.59	58.8935
A3	10.32	90	5.0	5.59	57.7408
A6	3.83	65	2.5	3.02	11.5791
A7	1.80	70	2.5	3.23	5.8087
A8	1.19	65	2.5	3.02	3.6020
A9	2.00	80	2.5	-2.52	5.0409
	1.49	80	2.5	-2.52	3.7403
A10	0.88	80	1.0	-1.01	0.8812
A11	0.41	55	1.0	-1.00	0.4059
A12	1.31	90	2.5	2.80	3.6546
A13	0.89	90	1.0	1.12	0.9926
A14	0.84	60	1.0	-3.28	2.7570
A15	3.04	70	2.5	3.23	9.8253
A16	1.38	90	1.0	1.12	1.5445
A17	5.86	90	2.5	2.80	16.3856
A18	0.74	60	1.0	-3.28	2.4342
A19	2.84	90	2.5	2.80	7.9488
A20	5.98	90	2.5	2.80	16.7271
B1	2.06	60	2.5	-8.20	16.8561
A21	2.93	60	2.5	-8.20	24.0031
A22	4.43	60	2.5	-8.20	36.3465
A23	0.99	60	1.0	-3.28	3.2427
A24	4.94	70	2.5	3.23	15.9591
A25	3.28	60	2.5	-8.20	26.9125
	4.09	60	2.5	-8.20	33.5248
A26	0.34	60	2.5	-8.20	2.8093
A27	0.79	60	1.0	-3.28	2.5936
A28	0.85	60	1.0	-3.28	2.7877
A29	0.89	90	1.0	1.12	0.9926
A30	2.21	60	2.5	-8.20	18.1231
A31	3.95	90	2.5	2.80	11.0497
A32	2.62	90	2.5	2.80	7.3262
A33	1.96	80	2.5	-2.52	4.9205
A34	1.57	80	2.5	-2.52	3.9555
A38	2.42	70	2.5	3.23	7.8120
A39	4.70	90	2.5	2.80	13.1309
A40	1.25	90	2.5	2.80	3.4838
A41	2.01	90	2.5	2.80	5.6226
A42	1.63	70	1.0	1.29	2.1104
A43	0.85	60	1.0	-3.28	2.7727
A44	1.51	60	2.5	-8.20	12.3966
	2.09	60	2.5	-8.20	17.1390
A45	1.00	90	2.5	2.80	2.8087
A46	2.51	90	2.5	2.80	7.0057
A47	0.91	70	1.0	1.29	1.1787
A48	0.48	70	1.0	1.29	0.6181
A52	0.34	90	1.0	1.12	0.3839
A53	1.14	90	1.0	1.12	1.2779

Joint	Length [m]	Dip	Depth [m]	Width [m]	Surface area [m^2]
A55	0.57	90	1.0	1.12	0.6411
	0.77	90	1.0	1.12	0.8668
A56	0.25	80	1.0	-1.01	0.2465
A57	0.81	80	1.0	-1.01	0.8131
A58	0.62	90	1.0	1.12	0.6922
A59	4.61	70	2.5	3.23	14.8896
Vertical joints			Surface area [m^2]		1220.85
Horizontal joints			Surface area [m^2]		381.96
			Total surface area [m^2]		1602.82
			Volume of bench [m^3]		780.00
			Specific surface [m^2/ m^3]		**2.05**

APPENDIX V: SIEVING DATA CYLINDERS 1-3

Cylinder 1

Fraction	On screen [g]	Passing [g]	Passing [%]	Green* [%]	Yellow* [%]	Black* [%]
128 - 256	0.00	88028	100.00	0.00	0.00	0.00
64 - 128	8824.00	79204	89.98	43.15	40.19	16.67
32 - 64	37524.00	41680	47.35	61.62	29.54	8.84
16 - 32	19753.00	21927	24.91	56.55	22.00	21.44
8 - 16	11178.00	10749	12.21	56.35	13.90	29.75
4 - 8	5333.00	5416	6.15	50.20	14.60	35.20
2 - 4	2253.00	3163	3.59	45.20	16.10	38.80
1 - 2	915.00	2248	2.55	50.60	14.50	34.90
0.5 - 1	621.00	1627	1.85	44.00	14.30	41.70
0.25 - 0.5	711.00	916	1.04	43.60	16.60	39.80
0.125 - 0.25	660.00	256	0.29	39.50	18.10	42.40
0.075 - 0.125	110.00	146	0.17	38.90	14.60	46.50
< 0.075	146.00	0	0.00	35.00	18.40	46.70

Cylinder 2

Fraction	On screen [g]	Passing [g]	Passing [%]	Green* [%]	Yellow* [%]	Black* [%]
128 - 256	0.00	96995	100.00	0.00	0.00	0.00
64 - 128	14763.00	82232	84.78	47.26	34.19	18.55
32 - 64	39912.00	42320	43.63	65.11	24.38	10.51
16 - 32	22438.00	19882	20.50	49.51	26.54	23.95
8 - 16	10205.00	9677	9.98	47.10	22.85	30.05
4 - 8	4737.00	4940	5.09	45.60	24.20	30.30
2 - 4	2055.00	2885	2.97	37.90	25.40	36.70
1 - 2	908.00	1977	2.04	38.20	22.00	39.80
0.5 - 1	567.00	1410	1.45	36.10	19.80	44.10
0.25 - 0.5	692.00	718	0.74	34.00	19.40	46.60
0.125 - 0.25	559.00	159	0.16	29.20	18.30	52.50
0.075 - 0.125	59.00	100	0.10	26.70	18.10	55.30
< 0.075	100.00	0	0.00	21.70	21.80	56.50

Cylinder 3

Fraction	On screen [g]	Passing [g]	Passing [%]	Green* [%]	Yellow* [%]	Black* [%]
128 - 256	0.00	97775	100.00	0.00	0.00	0.00
64 - 128	11671.00	86104	88.06	38.33	39.44	22.22
32 - 64	45269.00	40835	41.76	64.68	24.39	10.93
16 - 32	21063.00	19772	20.22	55.62	23.86	20.52
8 - 16	10349.00	9423	9.64	52.30	18.95	28.74
4 - 8	4642.00	4781	4.89	48.70	19.90	31.40
2 - 4	1938.00	2843	2.91	38.90	21.60	39.60
1 - 2	881.00	1962	2.01	38.20	20.70	41.10
0.5 - 1	480.00	1482	1.52	37.50	16.90	45.70
0.25 - 0.5	614.00	868	0.89	33.10	18.40	48.50
0.125 - 0.25	648.00	220	0.23	30.50	17.80	51.70
0.075 - 0.125	92.00	128	0.13	25.80	16.50	57.70
< 0.075	128.00	0	0.00	25.70	19.60	54.70

* Percentage of colour retained on screen.

PUBLICATION I

Generation of Fines around a Borehole: a Laboratory Study.

Svahn, V., 2002.
Proceedings of the 7th International Symposium on Rock Fragmentation by Blasting, Beijing, China, August 11 – 15, pp 122 - 127.

Generation of Fines around a Borehole: a Laboratory Study

Victoria Svahn
(Chalmers University of Technology, Department of Geology, SE-412 96 Gothenburg, Sweden)

Abstract: Production of fines is a major problem for many quarries in western Sweden. This unwanted aggregate product is both an environmental issue and an economic loss for the producers. Small-scale blasting was done in 2001 to investigate the extent to which fines originate from the crushed zone around a borehole. Coloured concrete cylinders made it possible to trace the origin of each fraction. The resulting distribution curve for each colour indicates that the closer to the borehole, the finer the material. Although this was generally believed, it had not been looked into specifically. Also, by plotting the amount of fines in each layer as a function of the radius shows that another mechanism could be responsible for some part of the fines generation. While these tests were made to study only the specific crushing mechanism, it is worth remembering that there could be greater sources of fines generation than this one. The tests indicated that a reflected tensile wave from the free face, caused by a crack or joint for example, is a likely source of fines as well.
Key Words: Fines; Bench Blasting; Fragmentation; Blasting; Aggregates

1. INTRODUCTION

One of the major concerns in western Swedish quarries is the excess of fines, which is a by-product of blasting and crushing. Fines, < 8 mm, represent up to 20 - 30% of the Swedish aggregate production (Gynnemo 1997); this totals about 8 million tons/year (1998) in Sweden (Bohloli *et al*. 2001). In most quarries this material cannot be used, hence it becomes both an environmental issue and an economic loss for the producers. It has been found that the quantity of fines formed by secondary crushing, approximately 60%, is greater than that produced by detonation, 40% (Glatolenkov *et al.* 1992). Reducing this amount, even by only a few percent, would result in a significant cost reduction for the aggregate industry.

It is critical to understand the mechanism of the formation of fines; there are research projects that have specifically studied this generation of finer material. Hagan (1979) found that decoupled and decked charges reduced the production of fines, which was also true for multiple-primed or continuously side-initiated charges. In general, increases in borehole diameter, burden distance, velocity of detonation, and decreases in stemming length and blasthole spacing all lead to more fines (Hagan 1979, Kristiansen 1995 and Kristiansen 1994). Bench blasts conducted by Bolger *et al.* (1996) showed that a reduced level of energy, as well as fewer blastholes per round, produced less fines. Sheahan *et al.* (1990) discovered, by smaller bench blasts, that different kinds of explosives do not have the same effect on the production of fines, < 16 mm; they also found a correlation between the effective energy and the amount of fines produced. The fines appeared to be generated around the borehole, since their mass remained constant as the borehole pattern was expanded. Although decoupling the charge reduced the mass of fines only slightly, it also reduced significantly the amount of coarser material. Moreover, a decrease in specific charge lowered the amount of fines (Gynnemo 1997).

Together with the detonic and geometric factors, geological conditions also affect the generation of fines. These conditions have not been investigated as much however, since it is harder to control rock properties, which are unique for every bench blast. *In situ*-material present in the rock mass before blasting, for example in cracks, is an important factor that influences the blasting result significantly (Adhikari *et al.* 1990).

Although it has been believed that the crushing of the rock around boreholes causes a major part of the fines (Liu *et al.* 1993 and Glatolenkov *et al*. 1992), this hypothesis had not yet been quantitatively investigated. Therefore, tests were initiated at Chalmers University of Technology to investigate the hypothesis. Results from small-scale blasts performed in 2001 are presented, with the aim of contributing to better understanding of the mechanisms involved when fines are generated. This could mean that quarries, which nowadays destroy a great part of the rock, may eventually be able to produce more valuable aggregate products.

2. METHOD

The test specimen was cylinder-shaped with a height of 600 mm and a diameter of 300 mm. The cylinder needed to have three layers that differed from one another so that they could be separated after a blast, enabling one to trace the origin of each fraction after the test material was sieved. It was decided to differentiate layers by colour, which made the choice of material easy; the only material that could easily be coloured was concrete.

Pigments can be added when mixing the concrete, and they do not affect the properties of the final hardened product. Three test bodies were cast so that the blast could be repeated for a more reliable outcome.

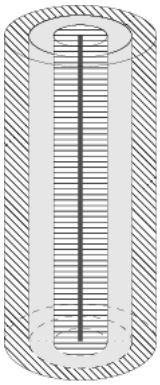

Fig. 1 The test specimen was designed in the form of a cylinder consisting of three layers of coloured concrete: an inner black layer, a middle yellow one and an outer green one.

The concrete specimens were blasted in a container constructed for this purpose, after which all of the fragments were collected. They were sieved and test samples were taken to collect information for constructing size distribution curves.

2.1 Choice of material

Concrete is a multiphase complex material consisting of aggregate particles, of various sizes and irregular shape, which are dispersed and embedded in hardened cement paste, i.e. the matrix of concrete differs from that of rock material. In an attempt to give the concrete a more rock-like matrix, the size of the aggregate particles was limited to 0.5 mm or smaller and consisted of 94.7% quartz. This mix is considered to be closer to mortar than concrete. The recipe was designed to produce a high-strength mortar with low porosity. To achieve this, the water-cement-ratio was set to 0.35 and a superplasticizer was added. The superplasticizer not only decreased the air voids, but also gave the mortar a lower viscosity (an essential property in the casting procedure). The complete recipe can be seen in Table 1. To colour the mortar, two oxides of iron and one of chromium were chosen. The colours were selected after studying their intensity when mixed with white cement and hardened to mortar. Black, yellow and green were chosen because they are easy to distinguish visually. Each pigment was tested, for any colour changes due to high temperature or pressure, by blasting small specimens. Although no changes could be detected, the remains of the explosive blackened the material surrounding the charge. Therefore, it was decided to place the black mortar closest to the charged hole.

Table 1 The mortar mixture

Sand	Industrisand (Askania)
Cement	White Std. Cement (Aalborg, Cementa)
Superplasticizer	1.7% (Cementa SSP20)
Pigment	4% (BKN Byggekemi AB)
Water-cement ratio	0.35
Sand-Cement ratio	1.5:1

2.2 Casting procedure

The test bodies were produced in three stages. The first stage included the inner layer, which was cast in a cylinder formwork with a diameter of 120 mm (height 600 mm). Before the mortar was poured into the formwork, a ∅9 mm stick was placed in the middle of the cylinder to form a hole for the charge. After two days of hardening, the mortar was strong enough to remove the formwork. When testing another casting procedure, some weakness zones resulting from water enclosure were discovered between each coloured layer. To ensure that such zones were not formed, the envelope surface of each coloured cylinder was sand blasted to roughen it and to remove any weaker material. Thereafter, the ∅120 mm cylinder was placed inside a ∅200 mm formwork and the second mixture, yellow mortar, was poured into the remaining space. The same sand blasting procedure followed after another two days and, finally, the green mortar was placed, in a ∅310 mm formwork, outside the yellow. The final three-layered cylinder was left to harden for 28 days at 20°C. This approach produced a cylinder consisting of 15% black mortar, 28% yellow and 57% green.

2.3 Concrete properties

Both fresh and hardened properties were tested at the time of casting, after 28 days and on the day of blasting. Measured properties can be seen in Table 2. The measurements were most important for the last green mortar mixtures, as these were separately mixed for each cylinder. The first two layers, black and yellow, for all three cylinders, were mixed in the same batches; unfortunately this was not possible for the last layer, since the volume of mortar was too large for the existing equipment. The only way to proceed was to accept having three batches of green mortar and carefully repeat the mixing procedure.

Table 2 Mortar properties at the day of blasting

Layer	Fresh density [kg/m^3]	Density [kg/m^3]	Compressive strength [MPa]	Flexural tension strength [MPa]	P-wave velocity [m/s]
Black	2214	2253	76.6	7.8	3922
Yellow	-	2266	98.4	7.8	4143
Green1	2055	2039	62.2	7.2	3803
Green2	2325	2338	85.3	7.6	4078
Green3	2316	2340	86.3	8.7	4178

As can be seen in Table 2, the first green batch showed lower values for all properties. The fresh density indicates that something was different in the mixture from the beginning, despite the use of the same recipe, mixing procedure and equipment. To get an indication of the porosity, the P-wave velocity was measured: it was relatively similar for all five batches of mortar.

2.4 Blasting and sieving

The blasting took place in a container designed and constructed for the purpose. The container, reinforced with 10 mm walls of steel, was lined with a layer of rubber. The rubber was to reduce the risk of further fragmentation of the pieces when they hit the wall after

the blast. A 40 g/m Dyno-cord was placed inside the ∅9 mm hole in the mortar cylinders. This gave a specific charge of 0.53 kg/m^3. A Nonel initializer (U500) initiated the blast and afterwards all fragments of the material were collected.

Concrete material has a tendency to fall apart easily when it is sieved, since it is brittle. To make sure that no more fines were produced, apart from those generated by the blast, the sieving process was changed from the ordinary laboratory method to a gentler one. The first stage of this process consisted of six screen decks, which were shaken by hand; the smallest mesh was 4 mm in size. Although the material smaller than 4 mm was placed in ordinary laboratory sieving equipment, it was sieved by hand for 2 to 3 minutes instead of sieving it for 10 minutes automatically.

2.5 Test sampling

Each of the larger fractions (> 8 mm) was separated by colour. The number of mortar fragments within each colour group was then counted. As there were too many fragments of the material less than 8 mm in size, test samples were taken instead of counting them all. For the fractions of 4 - 8 and 2 - 4 mm, the randomly taken test samples together made up 15% of the entire fraction. For the fractions smaller than 2 mm, even 15% was too much to count: instead, enough samples were taken to obtain confidence limits of 2% or less with a significance level of 0.05. This meant counting a total of approximately 6000 - 11000 fragments per fraction in no fewer than 5 test samples.

3. RESULTS AND DISCUSSION

To find possible trends in the results from the sieved blasted material, the percentage of each colour in every fraction was plotted for the three cylinders (Figures 2, 3 and 4).

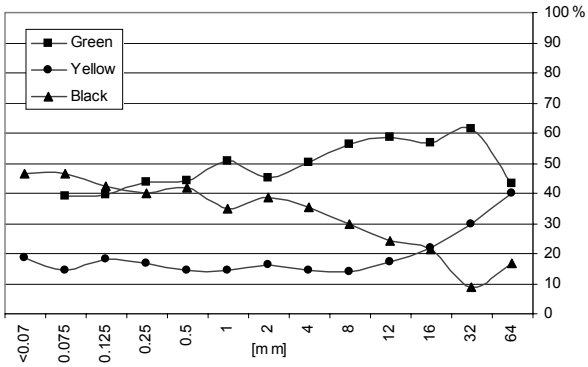

Fig. 2 Percentage of each colour for the fractions in cylinder 1.

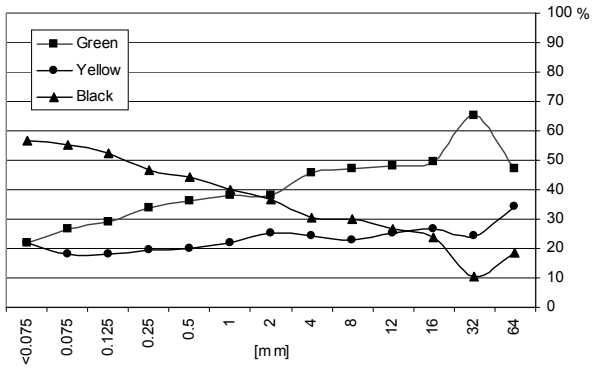

Fig. 3 Percentage of each colour for the fractions in cylinder 2.

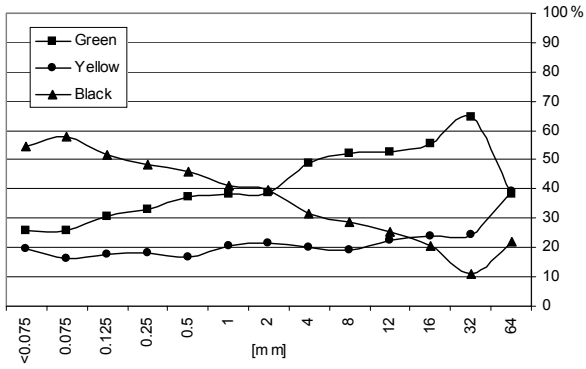

Fig. 4 Percentage of each colour for the fractions in cylinder 3.

Comparing the three cylinders shows that the first one has a slightly different fragmentation. The green layer of cylinder 1 is more finely fragmented than that of the other two cylinders, which could be the result of its weaker mortar properties. The cylinders blasted second and third have very similar curves, which is why these two are discussed further.

Noticeable is that the yellow layers in cylinders 2 and 3 are not represented in the smaller fractions as much as would be expected. This is probably the result of a few very large pieces (64 – 128 mm) that included all three layers. The green and the black, however, had been fragmented, while the yellow was intact and thereby "stole" a great part of the total amount of yellow mortar. The black layer was fragmented by crushing, since it was near the borehole; the fragmentation of the green layer could be the result of the compression wave meeting the free face and being reflected as a tension wave that started to fragment the material at the envelope surface of the cylinder. This would produce more green pieces than if the wave had not been reflected. How far the tension wave extended is hard to say, but it was probably not more than a few centimetres, since the larger pieces start about there. However, this could also be seen as evidence of how compression waves behave when they meet a free face in the form of a fracture or crack in the bench. It may also be a source of fines. Another explanation for the fragmentation of the outer green layer could be that these pieces were thrown against the walls of the container, which caused secondary breakage.

Generally, it can be observed that the finer the fractions are, the more the proportion of fragments from the black layer increases. For the green layer, it is the reverse. All this shows that the finer fractions originate from the vicinity of the charged borehole.

It is of interest to look at the distribution curves for cylinders 2 and 3. These curves give an idea of how much of each colour was present in each fraction. It is important to take this into account because the original amount of each colour was not the same in the cylinders.

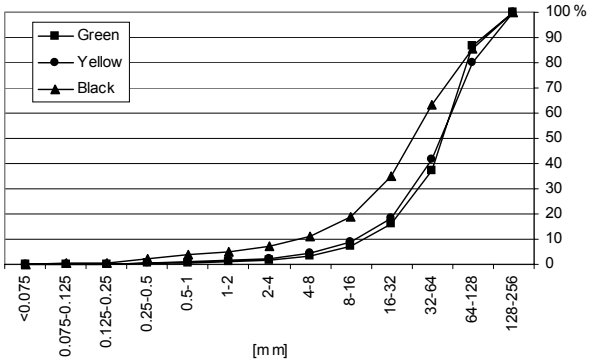

Fig. 5 Distribution curves för each colour of cylinder 2.

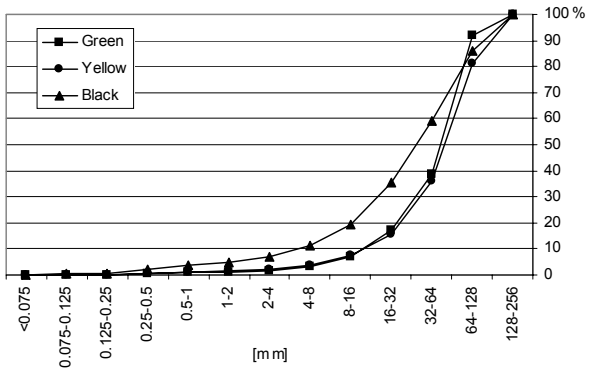

Fig. 6 Distribution curves för each colour of cylinder 3.

For the fraction < 8 mm, approximately 12% of the black mortar is found but only about 4% of the green. When studying finer fractions, such as < 4 mm or < 2 mm, black is still the dominating colour, although the percentages are very small. It should be kept in mind that the test samples all have confidence limits of 2% or less, for example 12% ± 2%, which means that it is hard to draw any solid conclusions if the percentages are too close to one another. However, a clear indication that the black layer is more finely fragmented can be seen in the entire distribution curve.

The results confirm that most of the fines do originate from the area surrounding the borehole. This can also be illustrated by plotting the amount of fines for the volume of each layer. Figures 7, 8 and 9 show the amount of fines as < 8, < 4 and < 2 mm. The values on the x-axis represent the radius, where 0 is the location of the charged borehole and 0.3 is the envelope surface of the cylinder. The values for the layers are given at the radius of the middle point in each layer.

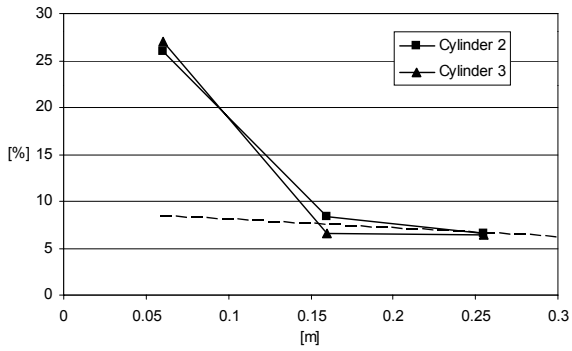

Fig. 7 The percentage of fines, < 8 mm, for each colour as a function of the distance from the charged borehole for cylinders 2 and 3.

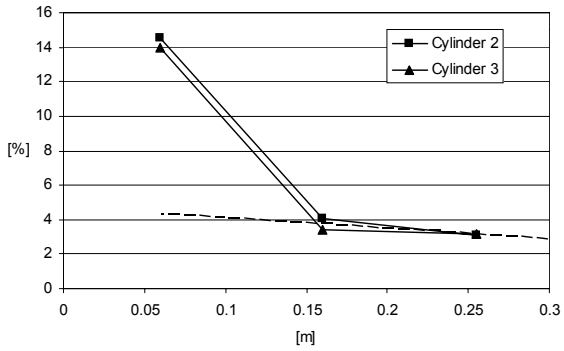

Fig. 8 The percentage of fines, < 4 mm, for each colour as a function of the distance from the charged borehole for cylinders 2 and 3.

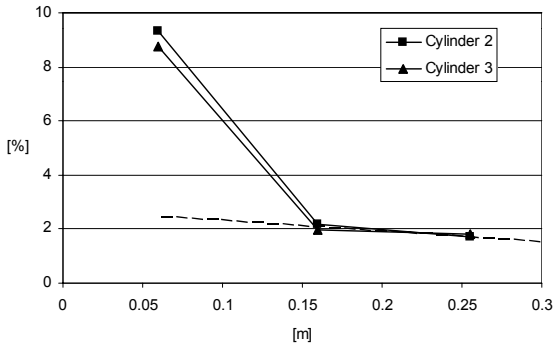

Fig. 9 The percentage of fines, < 2 mm, for each colour as a function of the distance from the charged borehole for cylinders 2 and 3.

The figures reveal an interesting finding: close to the borehole a lot of fines are generated, but further away there is hardly any change in the amount. This suggests another breakage mechanism not connected with the crushing from the borehole. It could mean that the amount of fines between the extended dashed line (drawn between the values for the yellow and green layers and interpolated to the black layer) and the total amount of black fines would represent the fragmentation caused by the crushing mechanism, while the fines below the line are caused by another source.

The tests conducted do have one weakness worth noting, namely the use of a substitute material, mortar, rather than the material to be understood, i.e. rock. Whether the fragmentation process is the same in mortar

and rock is left unsaid; a study of this would be desirable. It would also be of interest to carry out similar tests again using an additional layer, since the outer green layer seemed to be fragmented by the tensile wave returning from the free face. It would be interesting to study a fourth layer to see if the fragmentation would be changed for the green mortar. Such a change may revel whether a crack or joint could also be a source of fines worth looking into.

4. CONCLUSIONS

The data from the test blasts described above confirm that more fines are generated in the close vicinity of a borehole than at a distance from it, as was previously believed (Liu *et al.* 1993 and Glatolenkov *et al*. 1992). The results are given here by distribution curves and by figures plotting the amount of fines as a function of the distance to the charged borehole. These figures reveal an interesting finding. Plotting the amount of fines as a function of the radius indicates that another fragmentation mechanism is involved. That would explain why the amount of fines is so similar in the yellow and green layers.

Although this study deals specifically with the generation of fines close to a borehole, it should be kept in mind that this is only one source; there may be others of equal or greater importance.

ACKNOWLEDGEMENT

This work was supported by Swedish Rock Engineering Research (SveBeFo), the Development Fund of the Swedish Construction Industry (SBUF), Swedish Aggregates Producers Association (GMF), the Swedish National Road Administration (SNRA) and by the Swedish National Railway Administration. The author also acknowledges Professor G. Gustafson for valuable suggestions and comments.

REFERENCES

Adhikari, G.R., Barman, B.K. and Singh, B. (1990): Control of fines through blasting design at a limestone quarry. *Mining and Science Technology*, Vol. 11, p. 173-177.

Bohloli, B., Gustafson, G. and Ronge, B. (2001): A laboratory study on reducing the quantity of rock fines at failure: Application to rock blasting and crushing. *Bulletin of Engineering Geology and the Environment*, Vol. 60:271-276.

Bolger, J.M. and McMaster, K.E. (1996): Fines reduction program at the Canadian Salt Company. *Proceedings 22nd Conference Explosives and Blasting Technique*, Feb. 4-8, Orlando, Florida, p. 282-285.

Glatolenkov, A.I., Ivanov, V.I. (1992): Mechanism of breakdown of rock mass and formation of fines by blasting. *Journal of Mining Science,* Vol. 27:5 Sept.-Oct., p. 444-452.

Gynnemo, M. (1997): *Undersökning av styrande faktorer vid pallsprängning* (in Swedish). Department of Geology, Chalmers University of Technology, Göteborg, Pub. A84.

Kristiansen, J. (1994): Finandelens beroende av håldimensionen (in Norwegian). *Sprängteknisk konferens Nitro Nobel*, Feb. 8-10, Stockholm-Helsingfors.

Kristiansen, J. (1994): Sprengbarhet av berg. Et prosjekt for å optimere kvaliteten av fragmentert berg for Norsk Pukk- og Grusindustri (in Norwegian). *Sprängteknisk konferens Nitro Nobel*, Jan. 18-20, Göteborg-Fredrikshamn.

Liu, Q. and Katsabanis, P.D. (1993): A theoretical approach to the stress waves around a borehole and their effect on rock crushing. *Rock Fragmentation by Blasting*, Balkema, Rotterdam, p. 9-16.

Sheahan, R.M. and Beattie, T.A. (1990): Effect of explosive type on fines generation in blasting. *Proceedings of FRAGBLAST'90*, Brisbane, Australia, p. 413-415.